Field Experiments and Reactive Transport Modeling of Subsurface Arsenic Removal in Bangladesh

Rahman, Mohammad

DOI
10.4233/uuid:5b950e57-3704-43b2-ab03-f0da1dd79cc9

Publication date
2017

Document Version
Final published version

Citation (APA)
Rahman, M. (2017). *Field Experiments and Reactive Transport Modeling of Subsurface Arsenic Removal in Bangladesh*. [Dissertation (TU Delft), Delft University of Technology].
https://doi.org/10.4233/uuid:5b950e57-3704-43b2-ab03-f0da1dd79cc9

Field Experiments and Reactive Transport Modeling of Subsurface Arsenic Removal in Bangladesh

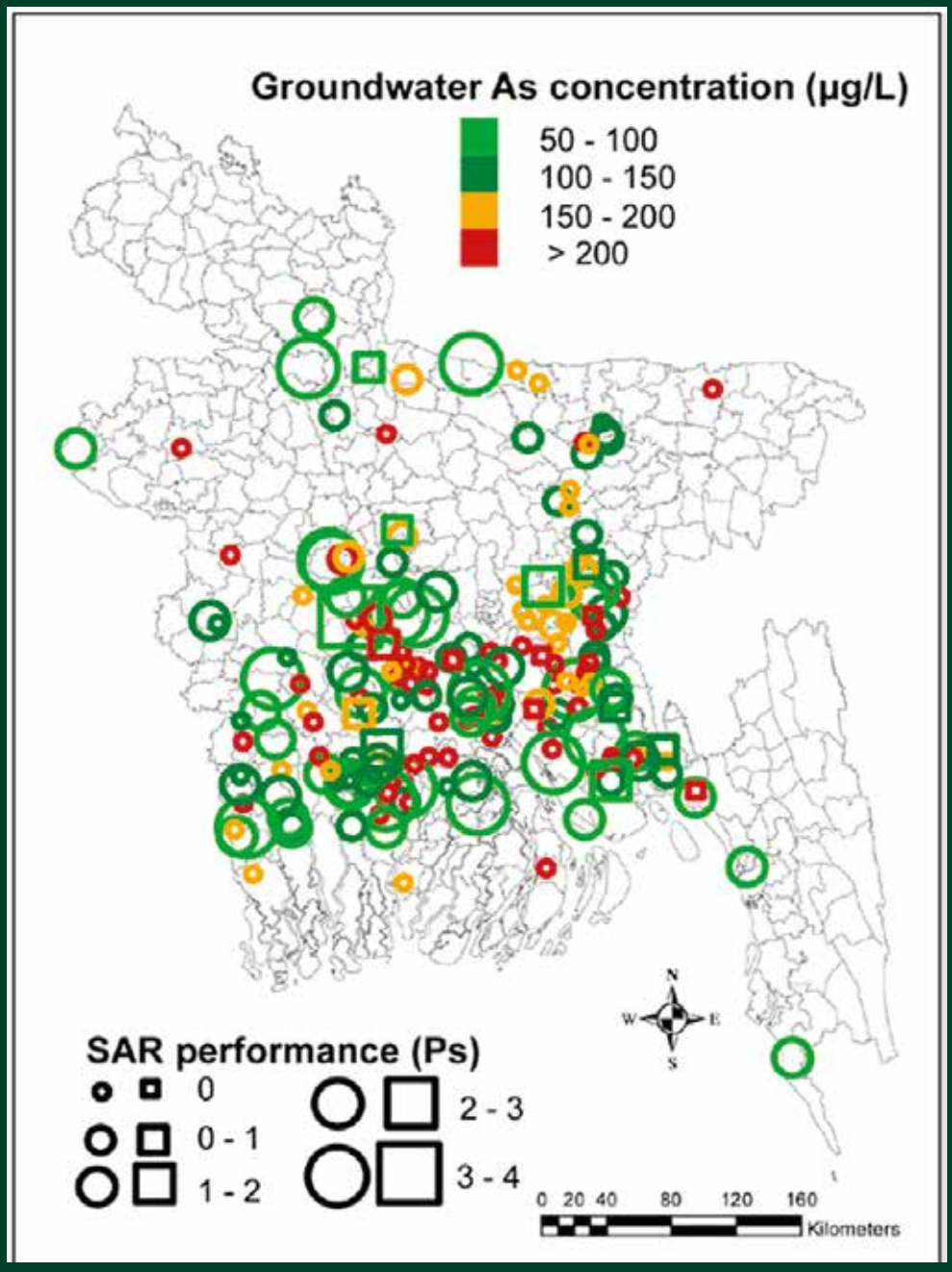

Mohammad Moshiur Rahman

Field Experiments and Reactive Transport Modeling of Subsurface Arsenic Removal in Bangladesh

FIELD EXPERIMENTS AND REACTIVE TRANSPORT MODELING OF SUBSURFACE ARSENIC REMOVAL IN BANGLADESH

Proefschrift

ter verkrijging van de graad van doctor
aan de Technische Universiteit Delft,
op gezag van de Rector Magnificus prof. ir. K. C. A. M. Luyben,
voorzitter van het College voor Promoties,
in het openbaar te verdedigen op donderdag 7 september 2017 om 12:30 uur

door

Mohammad Moshiur RAHMAN

Master of Science in Applied Environmental Geosciences,
Queens College, City University of New York,
New York, USA
geboren te Comilla, Bangladesh.

This dissertation has been approved by the

Promotor: Prof. dr. ir. Mark Bakker

Copromotor: Dr. B. M. van Breukelen

Composition of the doctoral committee:

Rector Magnificus,	Chairman
Prof. dr. ir. Mark Bakker,	Delft University of Technology
Dr. B. M. van Breukelen,	Delft University of Technology

Independent members:

Prof. dr. P. J. Stuyfzand,	Delft University of Technology
Prof. dr. ir. T. J. Heimovaara,	Delft University of Technology
Prof. dr. ir. W. G. J. van der Meer,	University of Twente
Dr. B. J. Mailloux,	Barnard College, New York
Prof. dr. ir. L. C. Rietveld,	Delft University of Technology, reserve member

Other member:

Prof. dr. K. M. U. Ahmed,	University of Dhaka

Keywords: Groundwater, Arsenic, Bangladesh, Reactive transport modeling, Subsurface arsenic removal

Printed by: Ipskamp Printing

Front & Back: Designed by Mohammad Moshiur Rahman

Back cover: Image taken from Freitas et al. [2014]

ISBN 978-94-028-0701-1
An electronic version of this dissertation is available at

http://repository.tudelft.nl/.

To my parents

PREFACE

I was in serious dilemma about whether I should pursue for this PhD project or continue with my new job as a lecturer at the North South University (NSU), Bangladesh. Teaching as a faculty member at an university has been one of my dream jobs. According to the rule of NSU, one need to work for at least 3 years at the university in order to get a leave absence for pursuing higher studies. The situation was that, I had to choose one from the two most important dreams of my life. It was a very tough decision to make. Thanks to my parents and my loving wife, who motivated me for pursuing this PhD project. My parents kept saying that I would be able to get a faculty position at many universities in Bangladesh if I get the PhD degree. Therefore, I decided to quit my faculty position at NSU and continue with the PhD project but fortunately I did not have to quit my job as the NSU authority granted me a leave of absence to conduct my PhD research. Thanks to the NSU authority. It was quite a fascinating ride with ups and downs while conducting my PhD research. I am very fortunate to be able to contribute for the people of Bangladesh through the research work I have conducted during my PhD endeavor. I consider myself lucky as I got the opportunity to learn a lot during my PhD research. I would like to thank my promotor and co-promotor for enlightening me with loads of scientific knowledge and experience. Finally, I am very happy that I could live upto the dreams of my parents and my loving wife by completing this PhD thesis and achieving the degree.

Mohammad Moshiur Rahman
Delft, September 2017

CONTENTS

List of Figures

LIST OF TABLES

SUMMARY

Arsenic (As) in drinking water is a major public health concern in many parts of the world. More than 35 million people in Bangladesh are estimated to consume groundwater containing more than 50 µg/L As (the Bangladesh drinking water standard); an overwhelming 57 million people drink groundwater with more than 10 µg/L As. Available As mitigation options in Bangladesh include the use of As-safe rainwater, surface water, deep groundwater, and a number of As removal filter systems. The overall contribution of the filter systems is insignificant in the As mitigation in Bangladesh. Subsurface As removal (SAR) is a relatively new treatment option that can be operated by modifying existing shallow tube wells. The principle of SAR is to extract anoxic groundwater, aerate it and re-inject it. Oxygen in the injected water reacts with iron in the resident groundwater to form hydrous ferric oxide (HFO). Dissolved As adsorbs onto the HFO, which allows for the extraction of groundwater with lower As concentrations. The performance of SAR is a function of the groundwater composition, which varies from place to place in Bangladesh. The effect of subsurface processes and key hydrogeochemical parameters on SAR performance must be quantified to determine the spatial variability of potential SAR performance in Bangladesh.

The principal objective of this research is to asses the potential of SAR technology in Bangladesh and to determine the processes that control the (im)mobilization of As in the shallow subsurface during SAR operation. The objectives of this research are achieved by conducting field experiments and by developing and applying a reactive transport model.

Two SAR units were built to asses the effect of different operational parameters. SAR operation with a larger injection volume performs better for As and Fe removal in the subsurface than the use of a smaller injection volume. Higher As removal was observed during the extraction phase when a lower pumping rate was used compared to a higher pumping rate. SAR operation with intermittent pumping resulted in higher As removal than cycles with continuous pumping. Repeated injection-extraction cycles of an equal volume resulted in higher As removal compared to regular cycles. All three alternative operations (repeated injection-extraction-injection cycles of an equal volume, lower pumping rates, and intermittent pumping) resulted in better As removal than regular operation. Cycles with intermittent pumping resulted in the highest As removal efficiency and cycles with a lower pumping rate resulted in the lowest As removal efficiency of all

the alternative operations performed in this study. A combination of the three alternative operation is recommended for SAR application in rural Bangladesh.

A one-dimensional radially symmetric reactive transport model was developed with the computer code PHREEQC (version 2.17) to simulate key hydrogeochemical reactions during SAR operation. The model was developed for one of the SAR units. The model gave reasonable results for measured concentrations of various parameters in the extracted water at the SAR well. The pH of the groundwater in the SAR system during injection, storage, and extraction phases significantly influenced the sorption of As. During SAR operation, As(III) oxidizes to As(V) which is preferentially removed from the water and thereby As(III) dominates in the end. These processes increase the overall As sorption. The increased sorption capacity due to gradual buildup of HFO facilitates As removal during SAR operation. The surface complexation modeling suggests that simultaneous sorption of H_4SiO_4 is an important factor limiting As removal during SAR operation. The simulated amounts of freshly precipitated HFO are such that aquifer clogging does not seem to be a problem. The model was applied to two additional SAR sites in Bangladesh to assess its transferability. The model is able to reproduce the observations reasonably well for most of the considered parameters. The modeled SAR performance was generally underestimated compared to the observed performance at the SAR wells. Overall it is concluded that the model may be used to assess potential SAR performance at other locations in Bangladesh with similar aquifer characteristics based on local hydrogeochemical conditions.

The reactive transport model used to simulate the field experiments was coupled to a new aeration model using a Python script to calculate the injection water composition for SAR simulation so that the model can be used at locations where the injection water composition is not measured. The new model was used to quantify the sensitivity of SAR performance to As, Fe, P, Si, pH, alkalinity, HFO, and CEC on SAR performance. Ranges of these parameters were determined from several databases of Bangladesh groundwater where possible. The model was applied at 200 locations with highly variable groundwater composition across Bangladesh. The model was run for a maximum of 500 cycles to determine peak performance and to determine the number of cycles needed to reduce performance to half peak performance. Results indicate that SAR performance is lower for higher background levels of As, P, and Si. SAR performance is higher for higher background levels of Fe, alkalinity, CEC, HFO (except for the highest background HFO), and molar ratio of Fe over As. The effect of background pH on SAR performance varies. A preliminary map of suitable locations for SAR application is generated. 27.5% of the studied locations resulted in SAR performance above 1 which indicates that the potential for SAR application in Bangladesh is substantial. Results show that 93% of the studied locations with background As levels ranging between 50-100μg/L resulted in peak SAR per-

formance above 1 and 38% of the locations with background As concentrations ranging between 100-150μg/L resulted in peak SAR performance above 1. 22% of the locations with background As levels ranging between 150-200μg/L resulted in peak SAR performance above 0 and 5% of the locations with with background As levels above 200μg/L resulted in peak SAR performance above 0. A significant amount of As can be removed from groundwater with very high levels of As even when the drinking water standard is not reached. The lifetime of SAR systems for most of the locations in Bangladesh where SAR performance is above 0.5 can be significant as it takes on average more than 300 cycles to reduce peak SAR performance by 50%.

1

INTRODUCTION

1.1. BACKGROUND

Access to safe drinking water is a basic human right and an essential component of effective policy for health protection [WHO, 2006]. Millions of tube wells have been installed in Bangladesh since the 1970s to provide pathogen-free drinking water instead of the biologically contaminated surface water used before [Yu et al., 2003]. Due to the extensive use of groundwater, Bangladesh has achieved success in the field of access to pathogen-free drinking water and food security through groundwater irrigation. In Bangladesh, about 97% of the total population came under pathogen-free water supply coverage due to the extensive use of groundwater, facilitated by the presence of highly productive aquifers [Yu et al., 2003].

Arsenic (As) in groundwater is a well known human carcinogenic substance which causes cancers of the bladder, liver, and lung [Chowdhury et al., 2000; Chen and Ahsan, 2004]. Consumption of groundwater with As additionally causes cardiovascular disease and hinders the mental growth of children [Chen et al., 1996; Wasserman et al., 2004]. Several parts of the world have elevated concentrations of geogenic As in drinking water derived from groundwater sources. Considering the risk, the World Health Organization (WHO) has set a drinking water standard of 10 μg/L for As [WHO, 2011]. About 200 million people worldwide are exposed to arsenic concentrations above 10 μg/L [WHO, 2011]. Affected countries include Bangladesh (57 million exposed people), India (40 million), China (1.5 million) Argentina (1.2 million), and the United States (2.5 million).

It is estimated that more than 100 million people living in alluvial floodplains formed by sediments derived from the Himalaya are exposed to elevated levels of As by drinking shallow groundwater that has high concentrations of As [Ravenscroft et al., 2009]. The drinking water standard for As in Bangladesh is 50 μg/L, which was also the standard in the USA till 2001 [Koerth-Baker, 2017]. More than 35 million people in Bangladesh, i.e., 27% of the total population, are estimated to consume groundwater containing more than 50 μg/L As; an overwhelming 57 million people drink groundwater with more than 10 μg/L As (WHO guideline; [WHO, 2011]), of which 36% are children younger than 15 years [WRI, 1998; BGS and DPHE, 2001]. Arsenic poisoning has been recognized as the second most important health hazard related to drinking water in the Synthesis report of the United Nations [Johnston et al., 2001].

Globally, aquifers where geogenic As mobilization into groundwater plays an important role can be classified broadly in three groups [Smedley and Kinniburgh, 2002]:

1. Strongly reducing aquifers.

2. Oxidizing aquifers mostly with high alkalinity and pH.

3. Aquifers with high contents of arsenopyrite and other sulfide minerals.

High As aquifers associated with strongly reducing conditions pose the most serious problems from a human health perspective because of its widespread nature. These kinds of aquifers exist in, e.g., Bangladesh, India, Vietnam, Cambodia, and Pakistan [Smedley and Kinniburgh, 2002]. Arsenic in the strongly reducing aquifers of Bangladesh is supplied most likely by the As-containing sulfide minerals in the Himalaya that are weathered, transported by the Ganges, Brahmaputra, and Meghna rivers, and deposited throughout the Bengal Basin. Geochemical analysis of the sediments from the Bengal Basin shows that a major portion of As is strongly associated with secondary Fe oxides, which were formed by the oxidation of primary and secondary sulfide minerals containing As [Islam et al., 2004; Lowers et al., 2007; Kocar et al., 2008].

The most widely accepted mechanism responsible for As release into the resident anoxic groundwater is reductive dissolution of Fe oxides mediated by microbes in the aquifer. The reductive dissolution of Fe oxides reduces the binding sites for As associated with Fe oxides, with an additional contribution due to the reduction of As(V) to As(III) [Nickson et al., 1998; BGS and DPHE, 2001; Akai et al., 2004; McArthur et al., 2004; Islam et al., 2004; Ravenscroft et al., 2005; Meharg et al., 2006; Harvey et al., 2002, 2006; Polizzotto et al., 2006, 2008; Neumann et al., 2010]. The organic carbon in the aquifer serves as the electron donor driving these reduction processes. The sources of organic content in the aquifer include degradation of plant material deposited within the sediments during the process of landform development, dissolved organic matter released by near-surface peat deposits, and dissolved organic matter recharged from the surface and ponds by irrigation pumping [BGS and DPHE, 2001; Harvey et al., 2002; McArthur et al., 2004; Meharg et al., 2006; Neumann et al., 2010].

Dissolved sulfate in the water can also be reduced to form poorly soluble sulfide phases are formed because of the same anoxic aquifer conditions that trigger the release of As in the groundwater of Bangladesh. These secondary sulfide minerals can sorb and thereby sequestrate As from groundwater [Kirk et al., 2004; O'Day et al., 2004; Lowers et al., 2007; Polizzotto et al., 2008]. A continuous supply of high concentrations of sulfate can sustain the sulfide-induced As sequestration [Quicksall et al., 2008; Buschmann and Berg, 2009]. A more likely source of sulfate is water recharged from surface water bodies like ponds and rivers [Aziz, 2010].

Arsenic is also commonly found in oxidizing aquifers with high pH and alkalinity in, e.g., the Chaco-Pampean region of Argentina where groundwater has elevated levels of As primarily mobilized from volcanic ash, dispersed or interbedded within sediments [Bhattacharya et al., 2006]. The main source of dissolved As in oxidizing aquifers is the desorption of As from the metal oxides present in the sediments (especially Fe and Mn oxides and hydroxides) under high pH conditions [Smedley and Kinniburgh, 2002]. Oxidizing aquifers with high levels of dissolved As are not found in Bangladesh.

In Bangladesh irrigated agriculture began in the early 1970s as part of the "Green Revolution" and has resulted in a total irrigated area of 4.2 million ha in 2006, or 30% of the total land area of Bangladesh. Approximately 3.8 million ha, or 90% of the total irrigated area, uses groundwater [Hossain et al., 2008]. Arsenic accumulates in the soil over time due to irrigation with high arsenic water [Khan et al., 2009; Panaullah et al., 2009; van Geen et al., 2006; Norra et al., 2005; Patel et al., 2005; Meharg and Rahman, 2003; Ali et al., 2003; Huq et al., 2003; Alam and Sattar, 2000]. This can lead to soil As concentrations that are toxic to rice plants, which in turn reduce the yield. The negative impact of arsenic from irrigation with groundwater in Bangladesh is emerging and is likely to have long-term consequences for food security and safety [Heikens et al., 2007; Hossain et al., 2008; Panaullah et al., 2009].

1.2. Arsenic mitigation activities in Bangladesh

Available As mitigation options in Bangladesh include the use of As-free rainwater, surface water, deep groundwater, and a number of As removal systems with adsorption media, such as Sono, Alcan, RedF, Sidko, etc. Sutherland et al. [2002] investigated the performance of two household filters (Sono and Alcan) for removal of As and other key elements such as Fe, Mn, and Al. The possible risk of microbial contamination of the treated water, and the long-term efficiency of the filters was also investigated. Potential problems with these filters include sudden As breakthrough, clogging of the filter, and generation of As-rich sludge. The overall contribution of these removal units is insignificant in the As mitigation in Bangladesh [JICA and DPHE, 2009]. It has been found that community acceptance of many of the options is low as people do not find them as convenient as tube wells [Huq et al., 2003; Jakariya et al., 2005, 2007; Johnston et al., 2010]. The concept of drinking water from tube wells has become an integrated part of the daily life of people in Bangladesh. Any additional task to obtain safe drinking water is thus likely to be difficult to manage in the long run, including the handling of filters on the household basis and the management of subsurface arsenic removal [Kundu et al., 2016b] (discussed in the following section). This may be the reason for the failure of several As mitigation options that have been provided in Bangladesh [Kundu et al., 2016a].

Collecting water directly from tube wells is considered the easiest option by the people of Bangladesh. That is why water from deep aquifers (>150 m) offers a possible alternative source for As-safe drinking water; deep aquifers are generally known to have low dissolved concentrations of As [BGS and DPHE, 2001]. However, drilling to depths of 150 m or more is prohibitively costly as it involves mechanized techniques as compared to the locally available hand-percussion technique used for shallow wells. The cost of drilling deep wells costs approximately 2 to 4 times more money depending on

the depth than locally available hand-percussion technique used for shallow wells.

1.3. Subsurface Arsenic Removal

Subsurface arsenic removal (SAR) is a relatively new treatment option that can be operated with negligible waste generation [Sarkar and Rahman, 2001; Rott et al., 2002; Appelo and de Vet, 2003; Van Halem et al., 2009, 2010a,b; Sen Gupta et al., 2009]. The principal idea of SAR is that injection of oxygenated water into an anoxic aquifer creates a subsurface iron oxide filter for As. A similar approach has been used in central Europe for subsurface iron removal (SIR) for many decades [Hallberg and Martinell, 1976; Van Beek, 1985]. SAR has the potential to be a cost-effective option to provide safe drinking water in rural areas of Bangladesh as existing shallow tube wells can be modified to perform SAR [Van Halem et al., 2010a].

SAR technology consists of three steps (e.g., Van Halem et al. [2009]). At the first step, anoxic water containing iron and As is extracted from the aquifer and aerated in an aeration tank. Second, the aerated water is re-injected into the aquifer where the oxygen in the injected water reacts with ferrous iron in the aquifer to form hydrous ferric oxide (HFO), and at the third step, a larger volume of water with low As concentration can be extracted because As sorbs onto the HFO. Arsenic, in many instances, co-occurs in groundwater with significant levels of iron, as reductive dissolution or desorption of As from iron oxides releases both iron and As to the groundwater [Nickson et al., 1998, 2000; McArthur et al., 2001; Dowling et al., 2002; Harvey et al., 2002; Swartz et al., 2004; Postma et al., 2007, 2010]. Availability of iron is essential for As retention in the subsurface by the processes of ferrous iron oxidation, precipitation of iron oxide, co-precipitation and adsorption of As, iron, and other ions on iron oxide surfaces. A cyclic injection of oxygen-rich water creates an oxidation zone in the subsurface and oxidizes adsorbed Fe(II) to Fe(III)-oxide, thereby forming new adsorption sites in the aquifer for Fe(II) and trace elements such as As. A number of injection-extraction cycles may be required to reach maximum removal efficiency [Van Halem et al., 2010a].

SAR has the following advantages over other household and community arsenic removal systems, such as SONO and Alcan [Van Halem, 2011]:

1. No filter media is required.

2. Only minor maintenance is required.

3. All hardware for the modification of an existing hand pump are locally available or repairable.

4. Fe is removed from the water in addition to As (often in larger volume than As), which

improves the taste and color of the water and greatly enhances the potential for social acceptance.

5. SAR can be used on a large scale to provide irrigation water with lower levels of As. The use of irrigation water with lower levels of As will reduce the accumulation of As in crops (rice) and soil As and reduce the crop (rice) production loss.

Previous field studies with small-scale application of SAR have indicated that the subsurface retention of arsenic can be achieved, but results are inconsistent. Rott et al. [2002] and Appelo and de Vet [2003] reported a reduction of As concentrations from 40μg/L to below the WHO guideline in SAR field experiments in Germany and the Netherlands, respectively. In Bangladesh, SAR was tested by Sarkar and Rahman [2001] and Van Halem et al. [2010a]. In the study of Sarkar and Rahman [2001], the background As level was 500-1300 μg/L and the As concentration of the extracted water never dropped below the Bangladesh guideline, while in the study of Van Halem et al. [2010a] the background As concentration was 145 μg/L and the level dropped below the Bangladesh guideline.

The SAR studies performed in Bangladesh Sarkar and Rahman [2001] and Van Halem et al. [2010a] listed a number of possible reasons for insufficient As removal:

1. Insufficient oxygen (below the saturation level) in the injection water [Sarkar and Rahman, 2001]

2. Low Fe to As ratio in the background water [Sarkar and Rahman, 2001]

3. Insufficient contact time between reduced groundwater and the oxidized zone in the subsurface to reach sorption equilibrium during extraction due to high pore water velocity or small injection volumes [Van Halem et al., 2010a]

4. The presence of anions, especially phosphate, competing with As for available sorption sites on iron oxide [Van Halem et al., 2010a]

Insight into the mechanisms controlling SAR is still limited [Appelo and de Vet, 2003; Van Halem et al., 2010b] and it is difficult to estimate SAR performance a priori for a given location. It is important to determine the hydrogeochemical processes that are responsible for the (im)mobilization of As in the shallow subsurface during SAR operation and to develop a tool that can assess the potential SAR performance based on local hydrogeochemical conditions. Reactive transport modeling is a process-based approach to describe the geochemical reactions and mechanisms controlling the (im)mobilization of As in the shallow subsurface during SAR operation and may be used to assess potential SAR performance. The spatial variability of the groundwater composition in Bangladesh

is very high [BGS and DPHE, 2001], which increase the uncertainty whether SAR can be a potential As mitigation option for significant parts of Bangladesh. It must be explored how SAR performance varies under different hydrogeochemical settings and sensitivity of SAR performance to different key hydrogeochemical parameters must be quantified.

1.4. Research Objectives

The principal objective of this research is to determine the potential of subsurface arsenic removal as an effective arsenic mitigation option in rural Bangladesh. The following four specific objectives are considered in this research:

1. To determine the effect of operational parameters (e.g., injection volume, pumping rate, continuous vs. intermittent pumping) on SAR performance through field experiments. Insight in the effect of operational parameters is critical for successful application of SAR under field conditions in rural Bangladesh.

2. To develop a reactive transport model through simulations of the conducted SAR experiments in order to understand the processes that control the (im)mobilization of As during SAR operation in Bangladesh.

3. To determine the sensitivity of subsurface arsenic removal to key hydrogeochemical parameters with a reactive transport model.

4. To quantify and map the potential performance of SAR under different hydrogeochemical settings in Bangladesh with a reactive transport model.

1.5. Thesis outline

The research objectives are achieved by conducting field experiments and by developing and applying a reactive transport model.

In Chapter 2, the basics of a SAR system are described and details of the conducted experiments are presented, including site selection and characterization, well drilling, sediment collection, SAR unit installation, water sampling and analyses, and geochemical analysis of sediment samples collected from different SAR sites.

The focus of Chapter 3 is the effect of operational parameters on SAR performance under field conditions in rural Bangladesh. Four experiments were carried out. Each experiment was designed to investigate the effect of an alternative SAR operation on the performance. Objective 1 and part of the principal objective of this research are addressed in Chapter 3.

In Chapter 4, the development of the reactive transport model is described to quantify the specific processes that are active in the highly reducing shallow Holocene aquifer

in Bangladesh. In this modeling study, the specific focus was to obtain mechanistic insight in the interplay of the hydrogeochemical processes responsible for the (im)mobilization of As during SAR operation. The effects of pH, ion competition for sorption sites, and dominant surface complexation reactions involved during SAR operation are discussed. The transferability of the model to other areas of Bangladesh is assessed at the end of this chapter. Chapter 4 addresses Objective 2 of this research.

The focus of Chapter 5 is the evaluation of SAR performance under strongly reducing condition with different hydrogeochemical settings throughout Bangladesh to develop a preliminary map of suitable locations for SAR application. The effect of background levels of different key hydrogeochemical parameters on SAR performance in Bangladesh is discussed including pH, alkalinity, As, Fe, P, Si, Hydrous ferric oxide (HFO), and cation exchange capacity (CEC). The main objective of this research along with Objectives 3 and 4 are addressed in Chapter 5.

A synthesis of the performed research is provided in Chapter 6 with special emphasis on the mechanisms and parameters (operational and hydrogeochemical) responsible for limiting As im(mobilization) during SAR operation. The implications for process-based SAR performance calculations are highlighted and future research directions are given for SAR application along with subsurface removal of Mn in Bangladesh and other parts of the world.

2

SAR EXPERIMENTAL SETUP, SAMPLING, ANALYSES, AND AND BACKGROUND HYDROGEOCHEMISTRY OF SAR SITES

This chapter is based on:

M.M. Rahman, M. Bakker, S.C.B. Freitas, D. van Halem, B.M. van Breukelen, K.M. Ahmed, A.B.M. Badruzzaman, Exploratory experiments to determine the effect of alternative operations on the efficiency of subsurface arsenic removal in rural Bangladesh (Hydrogeology, 2014) and

M.M. Rahman, M. Bakker, C.H.L. Patty, Z. Hassan, W.F.M. Röling, K.M. Ahmed, B.M. van Breukelen, Reactive transport modeling of subsurface arsenic removal systems in rural Bangladesh., Science of the Total Environment, 2015)

2.1. Description of a SAR unit

Several SAR units were installed at different locations in Bangladesh to perform SAR operation. A SAR unit consists of a well, an aeration tank, and pipelines for injection and extraction of water during SAR operation. The experimental setup of a SAR units is illustrated in Figure 2.1. Separate pipelines with valves were connected to the SAR wells for injection and extraction. Flow meters were connected to the pipes to measure volumes of injected and extracted water. The injection and extraction pipes were connected to an aeration tank. The tanks were placed on a roof top about 5 m above ground level to allow for gravity injection. Shower heads and disc aerators were placed in the aeration tank to achieve high dissolved oxygen levels with the help of an air compressor. Connections for inline monitoring of field parameters were made and sampling taps were attached to the injection and extraction lines for sampling during injection and extraction. Electrical suction pumps were used for extraction of groundwater.

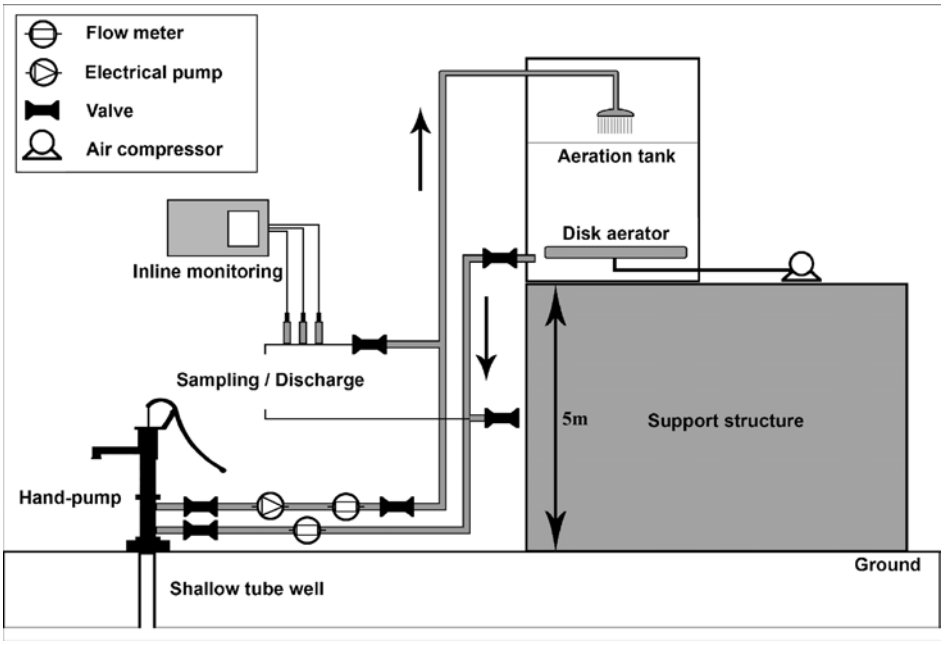

Figure 2.1: Experimental set-up for subsurface As removal at the study site after [Freitas et al., 2014]

2.2. SITE SELECTION FOR SAR UNIT INSTALLATION

The SAR experiments for this study were performed in two phases. The first phase was from September 2012 to December 2013 and the second phase was from March 2014 to June 2015. Selection of suitable locations to perform SAR experiments was necessary for this research in order to determine the As removal efficiency with SAR under different hydrogeochemical conditions. Several sites were selected primarily for the first phase based on hydrochemical parameters favorable for As removal such as low PO_4, SiO_4, and HCO_3, and high Fe, molar ratio [Fe]/[As], and high pH. A number of sites were selected primarily for the second phase based on the same hydrochemical parameters considered during the first phase except the background As concentrations were about half compared to the location used for SAR experiments during the first phase. Several social aspects were also considered during site selection for the second phase. The social criteria are as follows: 1) high percentage of As contamination, 2) low safe water coverage, 3) minimum As mitigation option available, 4) locations unfavorable for deep well installation, 5) location with potential demand for SAR technology. Groundwater samples were collected and on site measurements were taken from the primarily selected locations. Finally based on the laboratory analyses the best location was selected during both phases for SAR experiments. The sites selected for SAR experiments for the first and second phase are in Muradnagar upazila (sub district) of Comilla district and Singair upazila of Manikganj district respectively(see Figure 2.2).

2.3. FIELD SITE DESCRIPTION

Three SAR units were constructed at the Comilla site and are referred to as SAR well A1, SAR well A2 (both 1 m^3 injection capacity) and SAR well A3 (5 m^3injection capacity)(Figure2.3). One well was drilled for each SAR unit using the hand percussion reverse circulation drilling technique, the "sludger" method, commonly used in rural Bangladesh [BGS and DPHE, 2001]. SAR wells A1 and A2 are 1.5 inches (38.1 mm) in diameter and are drilled to depths of 20.5 m and 22.5 m respectively with a 3 m screen section placed at the bottom of each well. SAR well A3 is 2 inches (50.8 mm) in diameter and is drilled to a depth of 22.5 m with a screen section of 5 m placed at the bottom of the well. One SAR unit was constructed at Manikganj site and referred to as SAR well B. Same method was used to drill the well. SAR well B is 1.5 inches (38.1 mm) in diameter and drilled to a depth of 18.5 m with a screen section of 3 m placed at the bottom of the well.

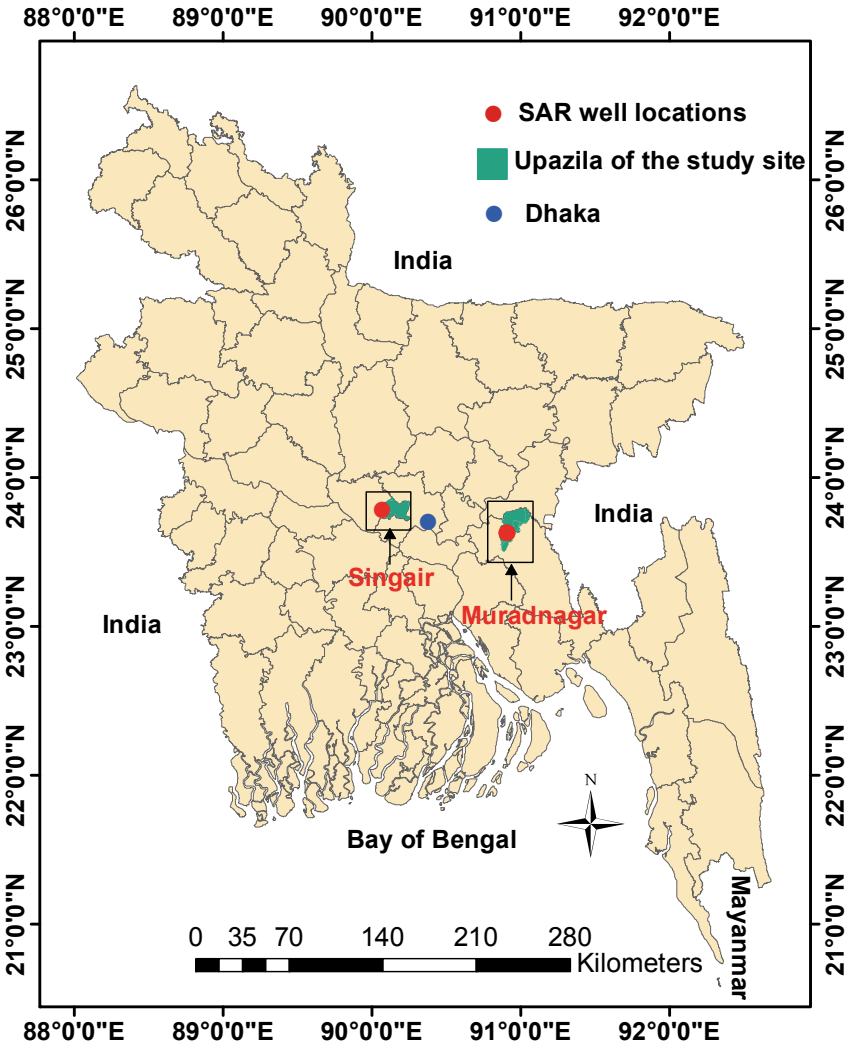

Figure 2.2: Map of SAR wells located in, Muradnagar upazila of Comilla district, and in Singair upazila of Manikganj district, Bangladesh.

2.3.1. Location, geology, and hydrogeology of the site selected for the first phase

The area of the study site for the first phase is about 1900 m^2. The aquifer at this site is composed of unconsolidated alluvial sediments derived from the Himalayan and Indo-Burman Range. These sediments were deposited by the Ganges-Brahmaputra-Meghna (GBM) river systems in the Bengal basin ([Uddin and Lundberg, 1998] and form the most productive aquifer system, being the main source of drinking, household, and irrigation

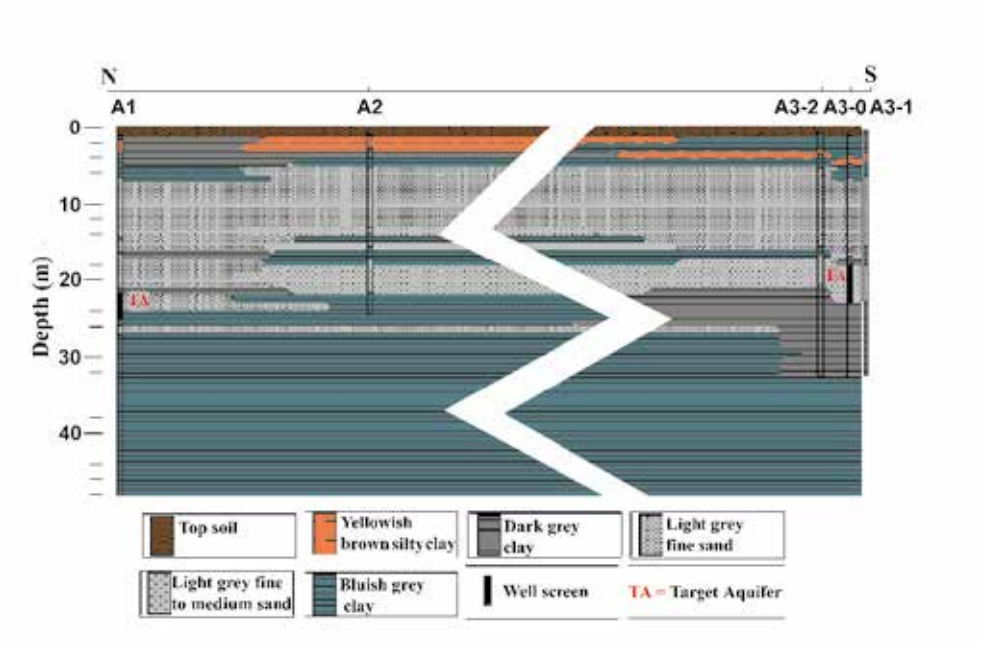

Figure 2.3: Cross section (length 55 m) of the study site constructed from the cutting data of the five boreholes drilled at the study site. Borehole logs are also plotted. Borelogs A1, A2, and A3-0 represent the three SAR wells used in the experiments

water in Bangladesh. The study area is within the geomorphic unit called the Tiperra surface [Morgan and McINTIRE, 1959]. This is a relatively elevated (3–10 m asl) flat land, lying between the Meghna Flood Plain in the west and Tripura Foot Hills in the east. The Tippera surface is made up of recent alluvial deposits of clay, silt, silty loam, and sand. Bakr [1977] subdivided the Tippera Surface into two geomorphic units, viz. the Chandina Deltaic Plain, between Meghna Flood Plain in the west and Lalmai Hills in the east, and the Lalmai Deltaic Plain, between Lalmai Hills and Tripura Foot Hills. The Lalmai Deltaic Plain is an uplifted terrace as evidenced by the surface presence of Madhupur Clay at some places. The surface geology of the study area can be divided into alluvial silt (asl), alluvial silt and clay (asc), alluvial clay (ac), and paludal clay and peat (ppc) [Alam et al., 1990].

The aquifer at the study site is composed predominantly of argillaceous (sand–silt–clay) facies, representing the Holocene alluvial deposits [Hasan et al., 2009]. The borehole logs of Comilla site depict that the aquifer is composed of alternating silty clay and very fine to fine grained sandy material. The upper shallow sandy aquifer is covered by a heterogeneous near-surface silty section. The screened aquifer can be considered as leaky-confined and is bounded by a thin (0.5 m) clay layer on top and a thick (30 m) clay layer

at the bottom. Groundwater in the study area occurs mostly within 5 m below ground level (bgl) and yearly fluctuation of the water level is between 2 and 6 m bgl. Groundwater flow follows the general topography of the area, i.e. from higher elevations in the east to lower elevations in the west. The groundwater flow direction is almost reversed during the dry season due to large scale extraction for irrigation [Hasan et al., 2009]. Hydraulic conductivity (K) of the target aquifer at SAR well A3 is 4.9 m/day as determined with a slug test. The estimated groundwater flow velocity of the study site is about 0.071 m/day.

2.3.2. Location, geology, and hydrogeology of the site selected for the second phase

The study area at Singair upazila of Manikganj district is located approximately 70 km NW of the capital city of Dhaka (Figure 2.2). The study area is limited geographically, within 23.80 to 23.90^0N latitude, and 89.95 to 90.05^0E longitude. The area is covered mostly by recent alluviums deposited by the Ganges–Brahmaputra river system. The surface geology of the area is characterized by alluvial silt and clay, alluvial silt, and marsh peat and clay deposits [Shamsudduha et al., 2008]. The geomorphology of the study area is typically fluvial which is characterized by several active channels, abandoned channels, natural levees, backswamps, and floodplains. The geomorphic features and surface geology of the study area suggests that these landforms were formed mostly during the late Quaternary period [GRG and HG, 2002].

The subsurface geology and the formation of various aquifers in the study area is characterized by several fining-upward sedimentary sequences. The color of the sediment in the study area varies from dark gray to orange-brown [Shamsudduha et al., 2008]. Shallow (10–60 m bgl) sediments are generally gray to dark gray indicating reducing conditions, whereas, deeper (>60 m bgl) sediments are mostly yellowish-brown to orange indicating oxidizing conditions. A detailed description of sedimentary facies and petrography of the study area can be found in Shamsudduha et al. [2008]. Aquifers are broadly classified into two groups: (1) the shallow aquifer system is encountered at ~10 m bgl and extends down to a depth of 90 m bgl, is composed of fine to medium gray to pale-yellowish sand and silt in the upper 50 m bgl and the bottom part of the aquifer is composed of medium to coarse sand with some gravels; and (2) the deep aquifer system occurring at >100 m bgl is composed of fine to medium grained yellowish brown to bright orange-brown sands. The bottom part of the deep aquifer system is composed of medium to coarse grained sands. Sediment characteristics, color, and composition suggest that deep aquifers are composed of sediments equivalent to the Dupi Tila Formation of the Pliocene–Pleistocene age [BGS and DPHE, 2001; Shamsudduha et al., 2008].

2.4. On-site measurements

Temperature, pH, redox potential (Eh), electrical conductivity (EC), and dissolved oxygen (DO) were measured using portable meters in a flow-through cell connected at the sampling point of the SAR unit. Electrical conductivity and temperature were measured using an Aqualytic portable meter (CD 22). A Hanna portable meter (HI 9025) was used to measure groundwater pH. Dissolved oxygen was measured using a Luton meter (DO 5510). Redox potential was measured with a Pt/HgCl electrode and corrected with respect to a standard hydrogen electrode (SHE).

2.5. Groundwater sample collection and analysis

Groundwater samples were collected from the study sites before the start of SAR to determine the background groundwater quality. During the experiments, samples were collected from selected injection and extraction cycles and were preserved in 30 ml polyethylene bottles following the sampling protocol described by Bhattacharya et al. [2002b] and Hasan et al. [2007]. Samples were filtered (using Sartorius 0.45 μm online filters) and subsequently acidified (1:100) with suprapure HNO3 (14 M) to bring the pH below 2 for cation and trace element analyses; samples for anion analyses were stored without acidification. As speciation was done with a field method (Clifford et al., 2004) using anion exchange resin columns (Amberlite IRA400).

Analyses of Cl, SO_4, NO_3 and PO_4 were done with a Dionex DX-120 ion chromatograph equipped with an IonPac As14 column. Dissolved organic carbon (DOC) in the water samples was determined on a Shimadzu 5000 TOC instrument. Alkalinity was determined by standard titration method. Cations (Ca, Mg, Na, and K) and trace elements including total As were analyzed by a Perkin-Elmer Flame AAS 3110, a Perkin-Elmer 4300 ICP-OES, and a Varian 730 ES ICP-OES.

2.6. Sediment sample collection and analysis

Coring operation to collect sediment samples from borehole was accomplished using local geotechnical methods of percussion drilling. Sediment cores were collected from each SAR site. Sediments were collected in PVC tubes and immediately sealed with wax and epoxy to prevent oxidation as much as possible as described by von Brömssen et al. [2008]. Two sediment cores were collected from the depths of 20.7 m and 21.5 m from SAR well A at Comilla district and three sediment cores from the depths of 15.8 m, 16.5 m and 17.1 m were collected from SAR well B at Manikganj district.

The sediment samples were analyzed for mineral constituents and soil organic matter (SOM) contents. Each sediment cores were homogenized and sub-samples were

taken for different analyses. Major mineral constituents of sediment samples were determined by standard methods of powder X-ray diffraction (XRD) by a Bruker D8 Advance diffractometer and Bragg-Brentano geometry with graphite monochromator and Vantec position sensitive detector. Soil organic carbon was determined from acidified sample on a Carlo Erba 1500NA elemental analyzer. Calcium carbonate was determined by calculating the carbonate percentage of sediments by measuring the weight loss as a function of temperature in a controlled environment using the LECO TGA-601. The clay and silt fraction were determined according to Konert and Vandenberghe [1997] by measuring the grain size distribution on a FRITSCH Laser Particle Sizer A22 (Fritsch, Idar Oberstein, Germany).

Sequential extraction was carried out to quantify the reactive Fe content of the sediments. The sediment samples from study site were sequentially leached as described by von Brömssen et al. [2008] using:

1. deionized water (DIW) for quantification of the water soluble fraction of As and other trace elements
2. 0.01 M $NaHCO_3$ for the release of elements under high pH conditions
3. 1 M Na acetate ($C_2H_3NaO_2$, NaAc) for elements bound to carbonate and phosphates phases
4. 0.2 M ammonium oxalate ($NH_4C_2O_4$) for quantification of Fe, Al, and Mn bound to amorphous oxides and hydroxides in the sediments
5. 0.2 M ammonium oxalate ($NH_4C_2O_4$) + 0.1 M ascorbic acid (Oxalate+AA) for residual amount of Fe, Al and Mn bound to oxides and hydroxides including crystalline phases.

Resulting solutions were analyzed by standard methods of ICP-OES as described in section 2.5.

2.7. Background hydrogeochemistry at different SAR wells

2.7.1. Geochemistry of the aquifer at SAR well A3

The geochemical composition of homogenized sediment core samples is shown at the bottom of Table 2.1. Core samples were taken at 20.7 m and 21.5 m below surface level (bsl) at SAR well A3. Core samples were taken at 15.8 m, 16.5 m, and 17.1 m below surface level (bsl) at SAR well B. The sediment samples were analyzed for mineral constituents

and soil organic matter (SOM) content, reactive Fe content (amorphous and crystalline), and for grain size. Sediment iron content determined by oxalate extraction is considered as HFO in this research for simplicity according to Robinson et al. [2011].

The saturation index of the groundwater with respect to calcite was -0.37, near saturation. According to X-ray diffraction analysis, pyrite and siderite were below the detection limit (the detection limit is 2-3%). The aquifer layer contains large amounts of HFO (Table 2.1). The cation exchange capacity (CEC) was high in the aquifer layer (Table 2.1) and was calculated based on the average clay and soil organic matter contents according to Appelo and de Vet [2003]:

$$CEC(mmol/kg) = 7Wc + 35Wc' \tag{2.1}$$

where Wc is weight percentage of clay and Wc' is weight percentage of organic carbon.

Table 2.1: Background hydrogeochemistry of the aquifers at the SAR locations.

Parameters	Units	Detection limit	SAR well A1	SAR well A2	SAR well A3	SAR well B	Bangladesh value (10, 50, 90 percentiles)[a]
Depth	m		21.4	20.7	22.5	18.3	16, 35, 137.2
EC	μS/cm	N/A	580	630	588	495	N/A
Cl	mg/L	0.1	40	28.1	47.81	17.5	N/A
Eh	mV	N/A	-137.0	-130.0	-137.2	N/A	N/A
T	°C	N/A	26.5	26.5	26.47	28.9	N/A
pH		N/A	6.95	6.88	6.97	6.67	N/A
Alkalinity	mg/L	N/A	195	357	292.8	293	N/A
DO	mg/L	N/A	0.1	0.3	0.38	0.3	N/A
NO_3	mg/L	0.05	bdl[b]	bdl[b]	bdl[b]	bdl[b]	N/A
DOC	mg/L	0.06	4.82	5.1	5.1	N/A	N/A
SO_4	mg/L	0.1	bdl[b]	0.06	0.3	0.1	0.3, 1.6, 17.3
Na	mg/L	0.008	25.1	27.7	35.9	49.6	8.3, 25.8, 263
K	mg/L	0.003	7.5	8.1	8.5	2.9	1.2, 2.9, 9.9
Ca	mg/L	0.02	24.4	40.5	63.1	46.1	7.8, 32.8, 119
Mg	mg/L	0.01	40.2	40.6	52.6	17.3	3.4, 15.3, 41.3
PO_4	mg/L	0.1	0.08	0.1	0.14[c]	0.1	N/A
P	mg/L	0.004	N/A	1.9[c]	N/A	1.9[c]	0.2, 1.31, 2.7
Fe	mg/L	0.002	12.59	12.9	8.6	9.1	0.06, 1.1, 9.1
Mn	mg/L	0.0001	0.27	0.24	0.16	0.29	0.03, 0.3, 1.4
Si	mg/L	0.01	29.6	27.6	31.2[d]	25.7	12.2, 20.2, 29.3
As	μg/L	0.007	203	380	201	69	1.1, 21, 248
As(III)	μg/L	0.007	165	304	162[d]	60	N/A
As(V)	μg/L	0.007	38	76	39[d]	9	N/A
HFO[e]	mol/L[f]	N/A	N/A	0.71[g,h]	0.71[h]	1.47	N/A
	g/L	N/A	N/A	12.3	12.3	25.33	N/A
Goethite[e]	mol/L[f]	N/A	N/A	3.2[g,h]	3.2[h]	2.9	N/A
	g/L	N/A	N/A	45.86	45.86	41.56	N/A
CEC[i]	eq/L[f]	N/A	N/A	0.095[g,h]	0.095[h]	0.099	N/A
	meq/kg	N/A	N/A	15.85	15.85	10.54	N/A

[a] Bangladesh values were taken and calculated from the dataset (n=3354) published by BGS and DPHE [2001].

[b] Concentrations were below detection limit.

[c] Used in the model (see Chapter 4).

[d] Measured after 16 cycles.

[e] Amorphous iron oxide.

[f] The conversion from g/kg or eq/kg to mol/L as required in PHREEQC was done assuming a bulk density of 1.855 and 30% porosity (see Chapter 4).

[g] mean concentrations (n= 2 for SAR wells A3 and A2; for SAR well B, n = 3).

[h] Concentrations were measured at SAR well A3;Wells A2 and A3 are only 75 m apart.

[i] Cation exchange capacity.

2.7.2. HYDROCHEMISTRY OF THE AQUIFER AT ALL SAR WELLS

Background groundwater chemistry of all SAR units is presented in Table 2.1. The groundwater pH of the study site is circum-neutral. Groundwater redox potential (Eh) indicates highly reducing aquifer conditions in agreement with low dissolved oxygen (DO) levels and high Fe levels. Ca and HCO_3 (alkalinity) are the dominant ions followed by Cl, Mg, and Na. All major ions at the study site are well above the Bangladesh 10 or 50 percentile values (Table 2.1). The Na and Ca concentrations at SAR Well A1 are slightly lower than the Bangladesh's 50 percentile value. The SO_4 concentration at SAR Well A3 is equal to the 10 percentile value of Bangladesh and the As concentrations at SAR units A1, A2, and A3 are close to the 90 percentile value of Bangladesh (Table 2.1). There is a large difference between Ca and alkalinity levels of the four SAR units. Redox reactions are considered as a driving factor of As mobilization and hence concentrations of redox-sensitive parameters such as Eh, HCO_3, DOC, SO_4, NO_3, Fe, and Mn in the groundwater are important in understanding the redox conditions[Bhattacharya et al., 1997, 2002a; Smedley and Kinniburgh, 2002; Ahmed et al., 2004; Zheng et al., 2004; Bhattacharya et al., 2006; Mukherjee et al., 2009; Hasan et al., 2009; Harvey et al., 2002]. From Table 2.1 it is clear that total As, Fe, and HCO_3 concentrations are high compared to Bangladesh median values; DOC concentrations are also high but national statistics are not available. Mn and SO_4 concentrations are low, as is typical for reducing aquifer conditions. The SO_4 to Cl molar ratio was 0.002 compared to an ocean water ratio of 0.05 reflecting the (past) occurrence of sulfate-reduction. Groundwater phosphate concentration is very low compared to the Bangladesh reference at all SAR well. Si levels are around the 90 percentile values.

3

EFFECT OF ALTERNATIVE OPERATIONS ON THE EFFICIENCY OF SUBSURFACE ARSENIC REMOVAL IN RURAL BANGLADESH

This chapter is based on:

M.M. Rahman, M. Bakker, S.C.B. Freitas, D. van Halem, B.M. van Breukelen, K.M. Ahmed, A.B.M. Badruzzaman, Exploratory experiments to determine the effect of alternative operations on the efficiency of subsurface arsenic removal in rural Bangladesh (Hydrogeology, 2014)

The principle of subsurface arsenic (As) removal (SAR) is to extract anoxic groundwater, aerate it and re-inject it. Oxygen in the injected water reacts with iron in the resident groundwater to form hydrous ferric oxide (HFO). Dissolved As sorbs onto the HFO, which allows for the extraction of groundwater with lower As concentrations. SAR was applied at a rural location in Bangladesh (As in groundwater = 200 μg/L) to study the effect of different operational parameters on SAR performance, including repeated injection and extraction of an equal volume, lower pumping rate, and intermittent pumping. Larger injection volume, lower pumping rate, and intermittent pumping all had positive effects on As removal indicating that As adsorption is kinetically limited. Repeated injection-extraction of an equal volume improved As removal efficiency by providing more HFO for sorption. After injection of 1,000 liters, a maximum of 3,000 liters of 'safe' water, as defined by the Bangladesh national standard for As (<50 μg/L), was extracted, of which 2,000 liters can be used as drinking water and the remainder is used for re-injection. Under this setup, the estimated cost for 1,000 liters of As-safe drinking water is US$2.00, which means that SAR is a viable mitigation option for rural areas.

3.1. INTRODUCTION

Groundwater extracted from shallow alluvial aquifers in Bangladesh and the West Bengal state of India contains As concentrations above the World Health Organization (WHO) guideline (10 μg/L) at many locations [Bhattacharya et al., 1997, 2002b; Nickson et al., 1998; Acharyya et al., 1999; BGS and DPHE, 2001; McArthur et al., 2001; Ahmed et al., 2004; Ravenscroft et al., 2005]. The use of this groundwater for drinking and irrigation purposes has created great concern for public health in this region [Chakraborti et al., 2004]. Available mitigation options include the use of As-safe rainwater, surface water, deep groundwater, and a number of As removal systems with adsorption media, such as Sono, Alcan, RedF, Sidko etc. The overall contribution of these removal units is insignificant in the As mitigation of Bangladesh [JICA and DPHE, 2009]. Subsurface As removal (SAR) is a relatively new treatment option [Sarkar and Rahman, 2001; Rott et al., 2002; Appelo and de Vet, 2003; Van Halem et al., 2010a,b; Sen Gupta et al., 2009]. SAR has the potential to be a cost-effective option to provide safe drinking water in rural areas of Bangladesh as existing shallow tube wells can be modified to perform SAR [Van Halem et al., 2010a].

SAR technology consists of three steps (e.g., [Van Halem et al., 2009]. At the first step, water containing anoxic iron and As is extracted from the aquifer and aerated. Second, the aerated water is re-injected into the aquifer, and at the third step, a larger volume of water with low As concentration can be extracted. As, in many instances, co-occurs in groundwater with significant levels of iron, as reductive dissolution or desorption of As from iron oxides releases both iron and As to the groundwater [Nickson et al., 1998, 2000; McArthur et al., 2001; Dowling et al., 2002; Harvey et al., 2002; Swartz et al., 2004; Postma et al., 2007, 2010]. Availability of iron is essential for As retention in the subsurface by the processes of ferrous iron oxidation, precipitation of iron oxide, co-precipitation and adsorption of As, iron, and other ions on iron oxide surfaces. A cyclic injection of oxygen rich water creates an oxidation zone in the subsurface and oxidizes adsorbed Fe(II) to Fe(III)-oxide, thereby forming new adsorption sites in the aquifer for Fe(II) and trace elements such as As. A number of injection-extraction cycles may be required to reach maximum removal efficiency [Van Halem et al., 2010a].

Rott et al. [2002] and Appelo and de Vet [2003] reported a reduction of As concentrations from 40 μg/L to below the WHO guideline in SAR field experiments in Germany and the Netherlands, respectively. In Bangladesh SAR was tested by Sarkar and Rahman [2001] and more recently by Van Halem et al. [2010a]. In the study of Sarkar and Rahman [2001], the background As level was 500-1300 μg/L and the As concentration of the extracted water never dropped below the Bangladesh guideline, while in the study of Van Halem et al. [2010a] the background As concentration was 145 μg/L and the level

dropped below the Bangladesh guideline.

The performance of SAR systems may be expressed in terms of the extraction efficiency (Q_E).

$$Q_E = \left(\frac{V - V_i}{V_i} \right) \tag{3.1}$$

where V is the volume of extracted water meeting the drinking water standard and V_i is the volume of injected water. When Q_E equals zero, this means that the volume of extracted water meeting the drinking water standard is equal to the injected volume. To calculate Q_E, the Bangladesh drinking water standards of 1 mg/L for Fe and 50 μg/L for As are used. Both Sarkar and Rahman [2001] and Van Halem et al. [2010a] reported extraction efficiencies in the range of 0-0.6. Both studies listed a number of possible reasons for low removal efficiency:

i) insufficient oxygen (below the saturation level) in the injection water,

ii) low Fe to As ratio in the background water [Sarkar and Rahman, 2001],

iii) insufficient contact time between reduced groundwater and the oxidized zone in the subsurface to reach sorption equilibrium during extraction due to high pore water velocity or small injection volumes,

iv) the presence of anions, especially phosphate, competing with As for available sorption sites on iron oxide [Van Halem et al., 2010a].

The objective of the study presented in this chapter is to explore the effects of various alternative operational parameters on SAR performance, as insight on the effect of operational parameters is critical for successful application of SAR under field conditions in rural Bangladesh. Four experiments were carried out. Each experiment investigates a different approach to increase the opportunity for subsurface As immobilization by adsorption on iron hydroxide surfaces.

The first experiment investigates the effect of larger and smaller injection volumes with saturated levels of dissolved oxygen. The hypothesis is that larger injection volumes will result in a larger oxidized zone and better adsorption opportunities for As.

The second experiment investigates the effect of repeated injection-extraction-injection cycles of an equal (extraction=injection) volume (of water) followed by extraction of a larger volume than was injected. The hypothesis here is that the repeated injection-extraction cycles of an equal volume will enrich the oxidized zone and provide more adsorption sites, which will increase performance of the SAR system.

The third experiment investigates the effect of pumping rates on As removal during the extraction phase. The hypothesis is that a lower pumping rate will increase the

adsorption opportunity of As to the available adsorption sites in the oxidized zone and enhance As removal.

The fourth experiment investigates the effect of intermittent extraction rather than continuous pumping on As removal. The hypothesis is that intermittent operation will increase the adsorption opportunity of As on the available adsorption sites in the oxidized zone and enhance As removal. At the end of the chapter, a cost estimate is presented for construction and operation of a SAR unit in rural Bangladesh based on extraction efficiencies observed in the experiments.

3.2. Experimental Design

As stated, four experiments were carried out, each consisting of a number of injection and extraction cycles. The experiments were carried out at SAR well A1 and SAR well A3. In experiment 1, the effect of different injection volumes on SAR performance was assessed with regular operational mode. In experiments 2, 3 and 4 regular operations are compared with different, alternative operational parameters/modes. During regular operation each cycle was performed with a single injection-extraction mode. Extraction during the regular operation was performed continuously and the extraction volume was always larger than the injection volume. In experiments 2, 3 and 4, each cycle with alternative operation is alternated with a cycle of regular operation so that results can be compared. One cycle with regular operation and cycle(s) with alternative operation is referred to as a round. Specific operational parameters of each experiment are presented in Figure 3.1 and discussed in the following.

3.2.1. Experiment 1:- Different injection volumes

The purpose of this experiment is to investigate the effect of a larger injection volume.Two different injection volumes of 1 m^3 at SAR well A1 and 5 m^3 at SAR well A3 were used for this purpose. It is noted that there are other differences between SAR well A1 and SAR well A3 that may cause differences in extraction efficiencies. These will be discussed in detail in the Discussion section. Two different suction pumps were used for extraction with pumping rates of 30 and 50 L/min for SAR well A1 and SAR well A3, respectively, and the procedure flow diagram is shown in Figure 3.1a. First the aeration tank was filled with water extracted from the aquifer and aerated with an air compressor and disc aerator until oxygen concentrations reached the saturation point (8.1-9.9 mg/L depending on the ambient temperature of that day). See section 2.4 for detailed information on on-site measurements. Next, valves were opened to inject aerated water into the aquifer through gravity drainage. On completion of injection, the system was left undisturbed for ~ 15 hours (referred to as the storage period) after which extraction was started and

the concentrations of As and Fe were monitored to assess the removal efficiency (see section 2.5 for detailed information on water sample collection and analyses. About 8-10 m^3 (for SAR well A1) and 20 m^3 (for SAR well A3) of water were extracted for each extraction phase of which the first 1 m^3 (for SAR well A1) and 5 m^3 (for SAR well A3) of water were saved every time in the aeration tank for the next injection phase. This process was repeated eleven times, referred to as cycle-1 through cycle-11. The first extracted water was used to fill the injection tank to avoid sludge formation in the tank. Precipitation of iron in the tank was negligible as the extracted water was almost free of iron at the beginning of extraction, so that the tank needed no cleaning.

3.2.2. Experiment 2:-Repeated injection-extraction of an equal volume

The purpose of experiment 2 is to investigate the effect of repeated injection-extraction of an equal volume on As removal. Experiment 2 is a modification of experiment 1 and was performed at SAR well A1. In this experiment regular operation was alternated with alternative operation. The alternative operation was performed by carrying out three consecutive injection extraction cycles of 1 m^3, followed by a 1 m^3 injection and then 3 m^3 extraction. At the start of the alternative operation, 1 m^3 of water in the tank, left over from the previous cycle, was aerated and injected. Injected water was left in the aquifer for ~ 15 hours after each injection except between cycle 2 and 3. After the fourth injection, ~3 m^3 of water was extracted (Figure 3.1b). Fe and As concentrations were measured during the last cycle of the alternative operation. Six rounds of the above operation were performed.

3.2.3. Experiment 3:-Lower pumping rate

The purpose of experiment 3 is to investigate the effect of lower pumping rate on As removal. Experiment 3 was performed at SAR well A3. Before carrying out this experiment, groundwater was extracted from the aquifer (100 m^3 over a 7 day period) until background conditions were reached to reduce imprints of prior experiments as much as possible. The experimental setup is illustrated in Figure 3.1c. During this experiment, 5 m^3 of water was aerated and injected for each cycle. Extraction of ~5 m^3 of water started after a storage period of ~15 hours in line with prior experiments. Five rounds were performed with alternating high (50 L/min) and low (13 L/min) pumping rates.

3.2.4. Experiment 4:-Intermittent pumping

The purpose of experiment 4 is to investigate the effect of intermittent pumping of groundwater on SAR performance. Shallow tube wells with a suction hand pump are common

at the household levels in rural Bangladesh due to low cost and easy operation [BGS and DPHE, 2001]. In order to simulate a typical hand-pump operation, SAR well A1 was operated intermittently. Three rounds were performed, where each round consisted of 1 cycle with regular extraction and one cycle with intermittent operation. Intermittent operation consisted of the extraction of 100 liters in ~7 minutes of pumping, no pumping for 7 minutes, followed by extraction of another 100 liters, no pumping for 7 minutes, and so on. This intermittent operation was continued until 3000 liters of water were extracted. The experimental setup is illustrated in Figure 3.1d.

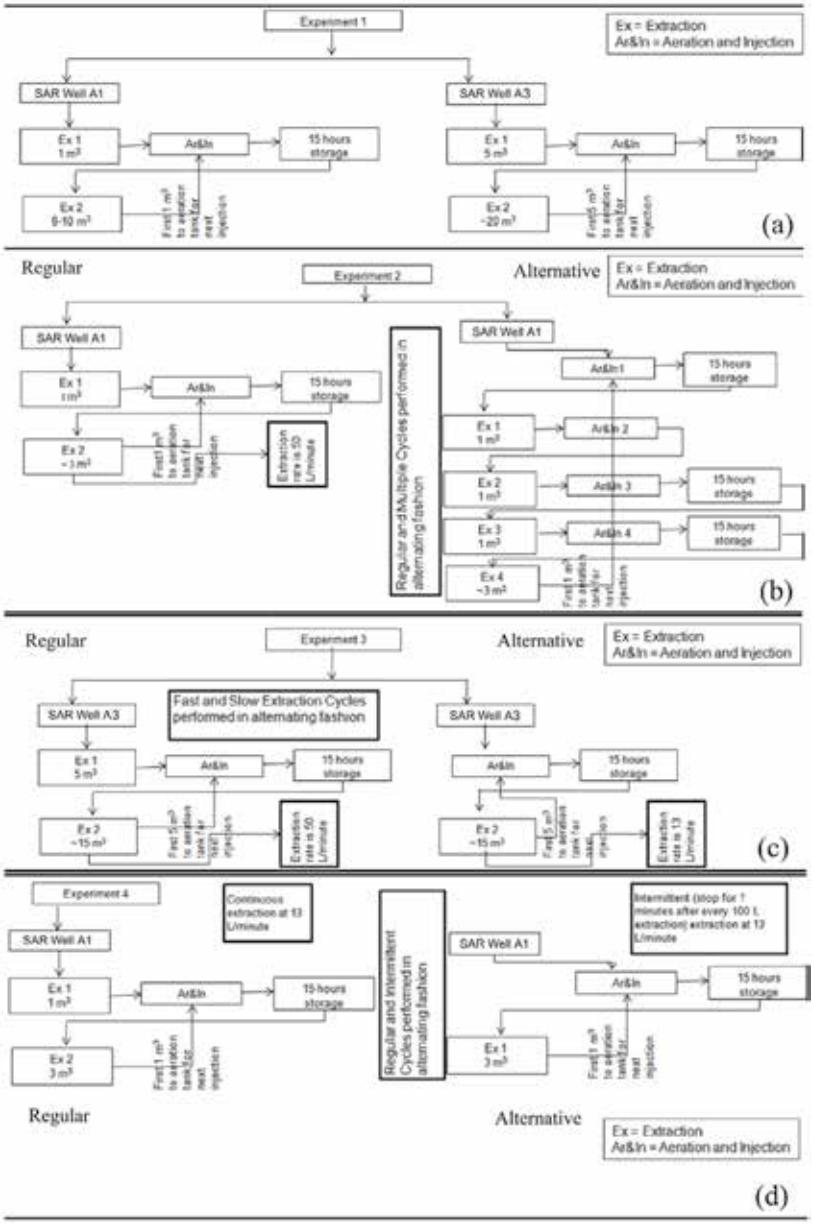

Figure 3.1: Flow charts illustrating the four different experiments performed at the SAR units: experiments 1 to 4 in a to d, respectively. Regular operation on the left (b to d) and alternative operation on the right (b to d).

3.3. Results

3.3.1. Results of experiments

Experiment 1- Different injection volumes

As concentrations of the extracted water for cycles 1, 3, 6, and 11 of SAR well A1, and 1, 3, 8, and 11 of SAR well A3 are shown in Figs. 3.2a and b, respectively. As removal improves with successive cycles for both injection volumes but concentrations never drop below the WHO provisional guideline (10μg/L). Considering the Bangladesh drinking water standard (50 μg/L), As breakthrough occurred at V/V_i = 1.1 at SAR well A1 with 1 m^3 injection volume and at V/V_i = 1.5 for SAR well A3 with 5 m^3 injection volume after cycle 11. The corresponding extraction efficiencies are Q_E = 0.1 for SAR well A1 and Q_E = 0.5 for SAR well A3. The results show that As concentrations never returned to the background concentration for any of the experiments (black dashed line in graphs) even after extraction of five times the injected volume. Results of this experiment show that the extraction efficiency for As is 5 times higher at SAR well A3 than at SAR well A1.

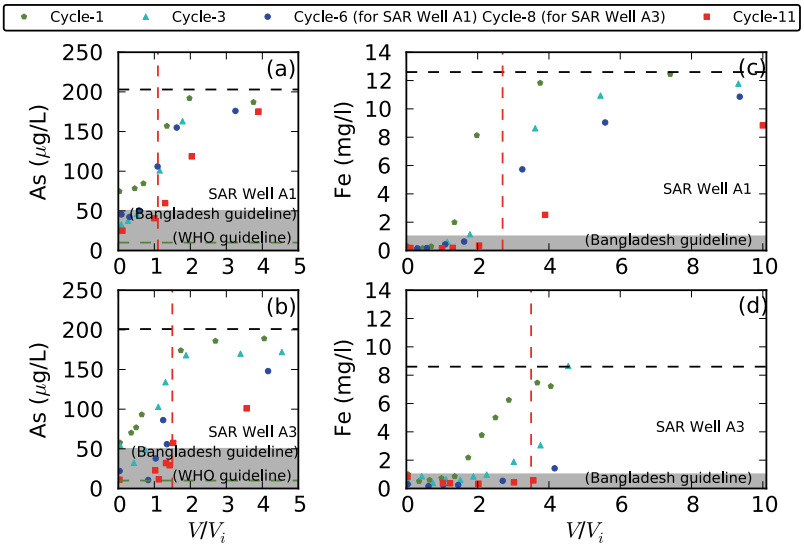

Figure 3.2: Breakthrough curves showing the concentrations of As (a and b) and Fe (c and d) during experiment 1 with different cycles with different injection volumes (injection volume is 1 m^3 for SAR well A1 and injection volume is 5 m^3 for SAR well A3). The black dashed lines represent the background concentrations at the SAR wells. The red dashed lines represent exceedance of the Bangladesh guideline for cycle 11. The grey area represents Bangladesh guideline for As (a and b) and Fe (c and d). The green dashed line represents WHO guideline for As (a and b).

Fe concentrations of the extracted water for cycles 1, 3, 6, and 11 of SAR well A1 and 1, 3, 8, and 11 of SAR well A3 are shown for SAR well A1 and SAR well A3 in Figs. 3.2c and d, respectively. Fe removal improves considerably with successive cycles. Fe removal ef-

ficiency is higher at SAR well A3 with 5 m^3 injection volume, compared to SAR well A1 with 1 m^3 injection volume. Considering the Bangladesh standard (1 mg/L), Fe breakthrough occurred at V/V_i = 2.7 for SAR well A1 and at V/V_i = 3.5 or higher for SAR well A3 (Fe measurements were not continued to levels above 1 mg/L for all cycles). The corresponding extraction efficiencies are Q_E = 1.7 for SAR well A1 and at least Q_E = 2.5 for SAR well A3. The extraction efficiency for Fe at SAR well A3 is about 70% higher than that of SAR well A1 but the background Fe concentration at SAR well A3 is 30% lower than at SAR well A1.

Experiment 2- Repeated injection-extraction of an equal volume

In experiment 2, efficiency of As and Fe removal by SAR was tested using alternating regular cycles and alternative cycles (repeated injection- extraction cycles of an equal volume) at SAR well A1 as detailed in Fig.3.1b. Measured As concentrations and pHs in the extracted water for rounds 3 to 6 are shown in Fig. 3.3. The results show that during each round, alternative cycles performed better than the regular cycles. The difference in Q_E between alternative cycles and regular cycles is always about 0.6. In round 6, As concentrations remained below the Bangladesh standard for $2.6V_i$ for the alternative operation (Q_E = 1.6) compared to the $1.9V_i$ (Q_E = 0.9) for regular operation. It is noted that the performance of regular operation is better than during Experiment 1, because regular operation benefits from the alternating alternative operation.

The pH values of the extraction water are relatively high at the beginning of each cycle and drop back to the background water condition with increasing extraction volume for all cycles. Note that the pH of the injection water was greater than 8 for all cycles. The pH values of the extracted water of alternative cycles are always higher than the regular cycles from the beginning of extraction to ~1.5 V_i. The pH values of both alternative and regular cycles return to the background condition after ~1.5 V_i. The measured concentrations of Si in the extracted water for rounds 3 to 6 are shown in Fig.3.4.

The Si concentrations of the extracted water start with a lower value at the beginning of the extraction phase and approach the background water condition with increasing extraction volume for all cycles. The results show that during each round, the Si concentrations for alternative cycles are lower than for regular cycles.

Experiment 3- Lower pumping rate

In experiment 3, pumping rates of 50 L/min (regular operation) and 13 L/min (alternative operation) were applied at SAR well A3. As concentrations of the extracted water along with As speciation for rounds 3 to 5 are shown in Fig.3.5. The extraction efficiencies are always higher for cycles with a low pumping rate compared to those with a high pumping rate. The Q_E for round 5 with low pumping rate is 0.75 while the Q_E for high

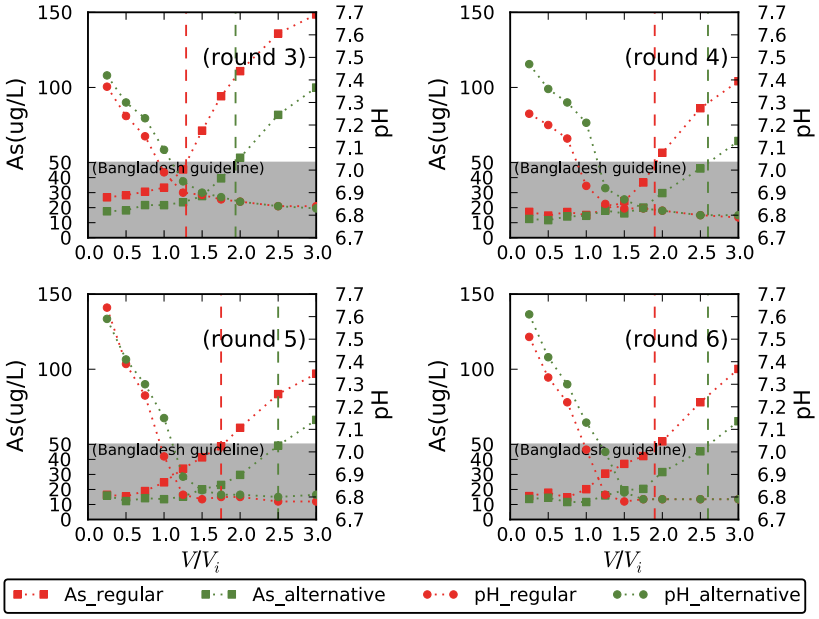

Figure 3.3: Comparison of As concentrations and pH between regular cycles and alternative cycles (repeated injection- extraction cycles of an equal volume) of experiment 2 performed at SAR well A1. The red (regular operation) and green (alternative operation) dashed lines represent the exceedance of the Bangladesh guidelines. The grey area represents Bangladesh guideline for As.

pumping rate is 0.5 (Fig.3.5). Performance of regular operation is again better than during Experiment 1, because regular operation benefits from the alternating alternative operation.

Delayed As breakthrough with the lower pumping rate continues after exceeding the Bangladesh standard. With the higher pumping rate, 50% As breakthrough (100 μg/L) is reached at V/V_i =2.4, while with lower pumping rate, 50% As breakthrough is reached after V/V_i =3. As(III) concentrations show similar behavior for both high and low pumping rates whereas As(V) concentrations show a marked difference between high and low pumping rates (round 5). Initially, As(V) concentrations are similar for both pumping rates, but the difference in As(V) concentrations increases with increasing extraction volume: much lower As(V) is observed with lower pumping rate than with the higher pumping rate for each round (Fig.3.5).

Experiment 4- Intermittent pumping

In experiment 4, regular cycles are alternated with intermittent extraction cycles (Fig.3.6). The results show that during the extraction phases of each intermittent cycle, As concentrations of the extracted water remained below the Bangladesh standard for at least $3V_i$

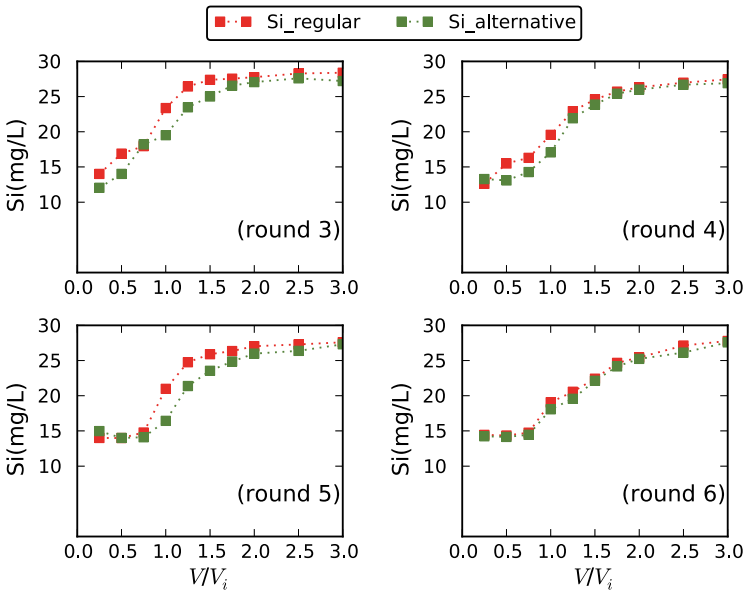

Figure 3.4: Comparison of Si concentrations between regular cycles and alternative cycles (repeated injection-extraction cycles of an equal volume) of experiment 2 performed at SARwell A1.

(only $3V_i$ was extracted). The corresponding Q_E is greater than 2 for every round. On the contrary, As concentrations of the extracted water for regular cycles remained below the Bangladesh guideline for only $\sim 2.4V_i$ corresponding to $Q_E \approx 1.4$ for every round. Performance of regular operation is again better than during Experiment 1, because regular operation benefits from the alternating alternative operation. The pH of the extraction water was high at the beginning of each cycle and returned to the background conditions with increasing extraction volume for all rounds. The pH values of intermittent operation cycles are higher (except for round 1) than regular cycles until $\sim 1V_i$ was extracted and then returned to the background level. Note that the pH of the injection water was greater than 8 for all cycles.

Comparison of extraction efficiencies between regular and alternative operation

Results of experiments 2, 3, and 4 are combined in Fig.3.7. The results of these experiments show that the different alternative operations always performed better than regular operation. Alternative operations in Experiment 4 (intermittent pumping) resulted in the highest extraction efficiency of all the experiments (Fig.3.7).

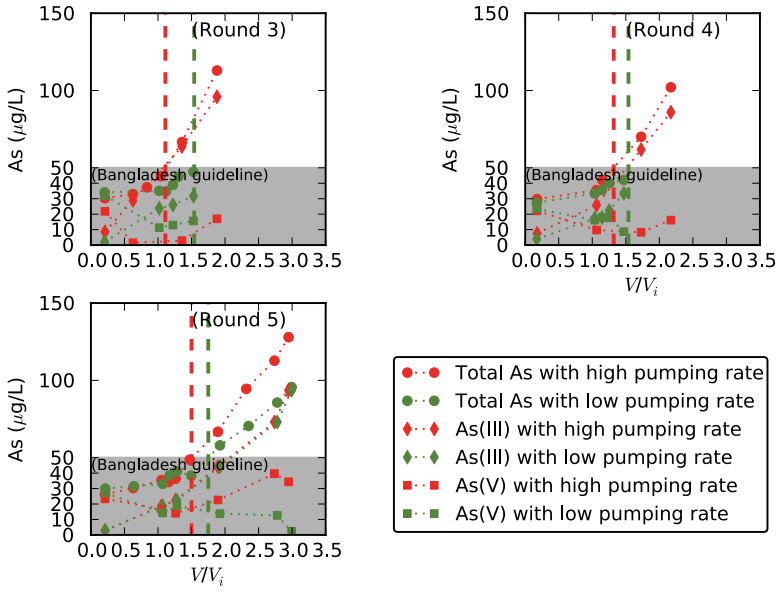

Figure 3.5: Comparison of total As, As(III), and As(V) breakthrough of experiment 3 performed at SAR Well A3 for pumping rates of 50 L/min (red) vs. 13 L/min (green). The red (cycles with high pumping rate) and green (cycles with low pumping rate) dashed lines represent the exceedance of the Bangladesh guidelines. The grey area represents the Bangladesh guideline for As.

3.4. Discussion

3.4.1. Effect of pH on As removal

The pH of the injection water was always greater than 8, but during extraction the pH started with a value lower than 8 (Figs.3.3 and 3.6). This pH difference between injection and extraction water, also between regular and repeated injection-extraction cycles of an equal volume (Fig. 3.3) and regular and intermittent operation (Fig.3.6), might be related to Fe(II) oxidation in the subsurface during injection, which results in the production of H+ following the reaction equation:

$$4Fe^{2+} + O_2 + 10H_2O \rightarrow 4Fe(OH)_3 + 8H^+ \tag{3.2}$$

Consequently, the larger the pH drop, the more Fe(II) must have oxidized. The experiment with repeated injection-extraction cycles of an equal volume showed the smallest reduction in pH, in line with the hypothesis that less Fe(II) is left to be oxidized after three injection/extraction cycles of an equal volume. Also, the Fe concentration decreased

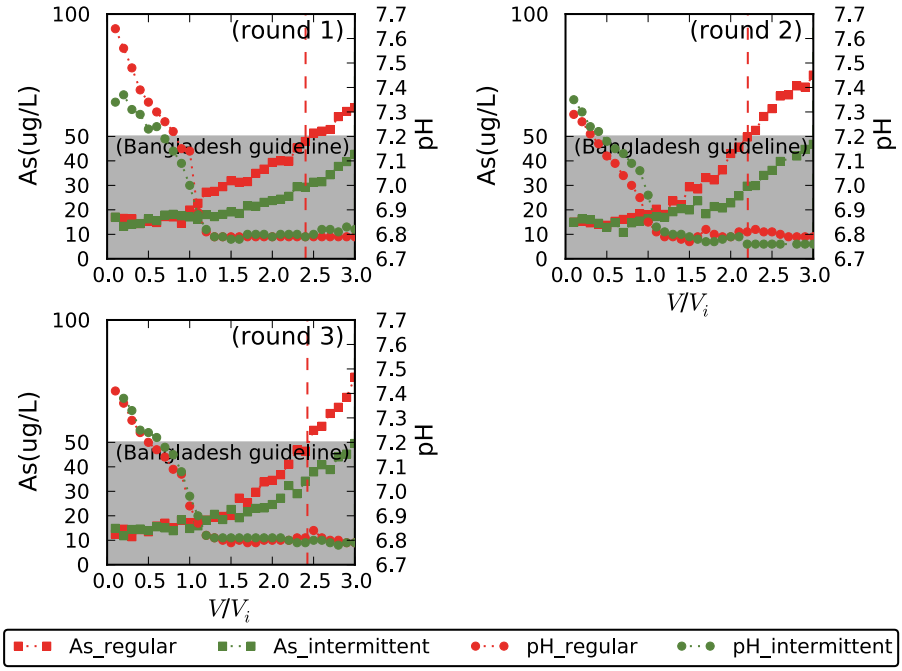

Figure 3.6: Comparison of As concentrations and pH between regular cycles (red) and intermittent extraction cycles (green) of experiment 4 performed at SAR well A1. The red dashed lines represent the exceedance of Bangladesh guideline for regular cycles. Exceedance of the Bangladesh guideline for intermittent cycles was beyond V/V_i =3 and was not observed. The grey area represents Bangladesh guideline for As.

with successive cycles, which means less Fe(II) was oxidized during injection. This might have caused the pH difference between regular cycles and repeated injection-extraction cycles of an equal volume (experiment 2), and between regular cycles and cycles of intermittent operation (experiment 4). The higher pH may also relate to the increased removal of As for the alternative operation in these experiments, because As adsorption is pH sensitive. As adsorption on iron oxides increases with increasing pH till pH values of 8.5, after which adsorption decreases with increasing values of pH [Kartinen Jr. and Martin, 1995].

3.4.2. Surface complexation and effect of ion competition for sorption sites on As removal

The compositions of the sediment surface complexes in equilibrium with the background water (Table 2.1) are shown in Fig.3.8. They were calculated with PHREEQC (v. 2.17) based on the surface complexation model proposed by Dzombak and Morel [1990] using

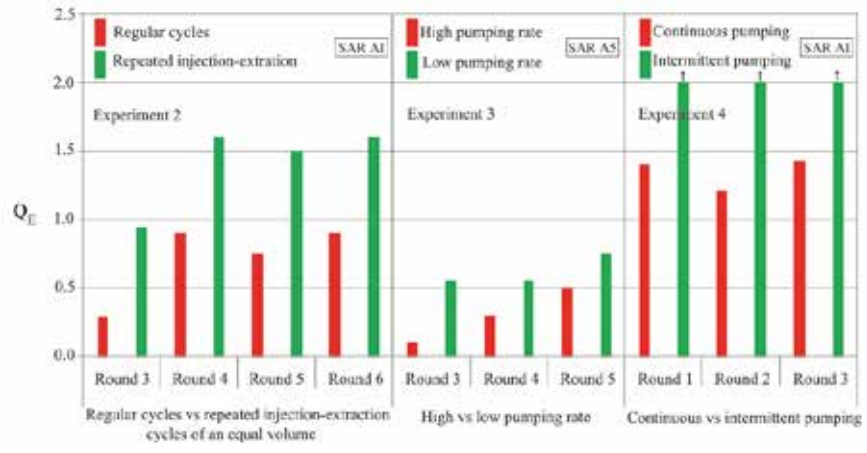

Figure 3.7: Comparison of extraction efficiencies (Q_E) between different operational modes during Experiments 2, 3, and 4. The arrows on the bars of the results of the cycles of intermittent pumping (experiment 4) indicate Q_E values may be higher but were only measured up to this point.

the wateq4f database extended with surface species for carbonate [Appelo and de Vet, 2003], silicate [Swedlund and Webster, 1999] and Fe(II) [Liger et al., 1999; Appelo et al., 2002] as reported by Jessen et al. [2012]. The dominant surface species at both SAR units are silicates and bicarbonates. The results show a higher surface concentration of Fe at SAR well A1 compared to SAR well A3 indicating a stronger relative sorption of Fe at SAR well A1 than at SAR well A3.

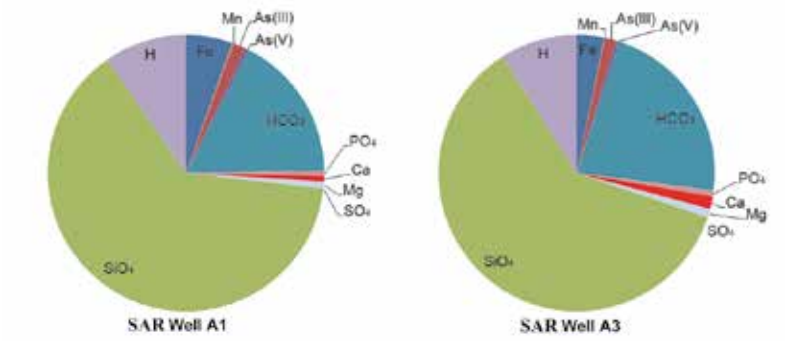

Figure 3.8: The surface speciation at equilibrium with pristine groundwater (Table 2.1), calculated for the sites that are able to adsorb As, with the Dzombak and Morel [1990] model for ferrihydrite. The field for each element in the pie diagram may cover several surface species. The field denoted "H" indicates the sum of all protonated or deprotonated surface sites.

Principal competitors of As for sorption sites are phosphate, bicarbonate, and silicates [Sharma, 2001; Su and Puls, 2001; Meng et al., 2001; Appelo and de Vet, 2003; Stol-

lenwerk et al., 2007; Hug et al., 2008; Guan et al., 2009; Van Halem et al., 2010b; Wallis et al., 2011]. Meng et al. [2001] reported that typically a Fe/As ratio of >40 (mg/mg) or 53 (M/M) is needed to lower As levels to below 50 μg/L by the process of oxidation and co-precipitation of As and Fe. The ratio of iron and phosphate is unfavorable in the most affected districts of Bangladesh [Hug et al., 2008]. As long as there is free phosphate, As removal is minimal because phosphate strongly competes with As for adsorption sites [Meng et al., 2001; Sharma, 2001; Su and Puls, 2001; Stollenwerk et al., 2007; Hug et al., 2008; Guan et al., 2009; Van Halem et al., 2010b].

A molar ratio of 1.5-2.0 Fe per P is needed to remove phosphate at neutral pH by oxidation and co-precipitation. Only the remainder, after phosphate removal, is available to remove As(III) and As(V) [Hug et al., 2008]. The phosphate concentrations at the study site are low compared to the median value of Bangladesh (Table 2.1). The molar Fe to As ratio at the study site is 83 and the molar Fe to PO_4 ratio is 267. Even though the phosphate concentrations at the study site are low, it did not result in As levels below the WHO guideline during SAR operation. This implies that As sorption may be limited due to competitive sorption of other anions present in the groundwater at the study site, as discussed in the following.

The limited extraction efficiencies at the study site during the cycles of all experiments implies that As removal may be limited by competitive sorption of other solutes such as dissolved organic carbon (DOC), silica, and bicarbonate (HCO_3). According to Appelo and de Vet [2003] and Wallis et al. [2011] bicarbonate is the major driving force for As displacement from Hydrous Ferric Oxides (HFO). High concentrations of HCO_3 at the study site may be the principal reason for lower extraction efficiencies than expected. Competitive displacement of As by silica may be another important reason for the release of As during the extraction phase [Hug et al., 2008]. Note that Si concentrations at the site were above the 90th percentile for Bangladesh. The speciation of surface complexation shows silica and HCO_3 as the main surface complex species (Fig.3.8), which is an indication of ion competition for sorption sites. Breakthrough curves of Si from experiment 2 show decreased concentrations of Si during the extraction phase (Fig. 3.4) which is further evidence of the sorption of H_4SiO_4 on HFO. This sorption of silica on HFO is further evidence of ion competition for sorption sites.

Results from experiment 2 (Fig.3.3) demonstrate that repeated injection-extraction cycles of an equal volume has potential for improved As removal. Si concentrations show more sorption during alternative cycles compared to regular cycles (Fig.3.4) in the same round. A possible reason is that the capacity for ion sorption is increased due to additional sorption sites from freshly formed HFO and sites available from HFO from previous cycles.

3.4.3. Influence of injection volume on As and Fe removal

A small improvement in extraction efficiency for As and Fe was observed when a five times larger injection volume was used at SAR Well A3 as compared to SAR Well A1 (experiment 1). The small improvement is more significant when it is taken into account that the background composition of the groundwater differs between SAR Well A1 and SAR Well A3 (Table 2.1) as will be explained later. The improved performance of a larger injection volume seems to imply that the sorption process is kinetically limited.

During the injection phase, the five times larger injection volume resulted in a two times wider oxidation zone and a three times longer residence time in this zone at SAR Well A3 compared to SAR Well A1. The radius R of the oxidation zone and the residence time tr in the oxidation zone are calculated using the following equations.

$$R = \sqrt{\frac{V}{\Pi \times \eta \times b}} \tag{3.3}$$

$$t_r = \frac{V}{Q} \tag{3.4}$$

where V is the injection volume, η is the porosity which is set to 0.3, b is the screen length, and Q is the pumping rate. In case of instantaneous equilibrium sorption, different injection volumes would not make any difference in terms of extraction efficiency. Better extraction efficiency was obtained with the larger injection volumes in this study (Fig. 3.2), which implies that there may be kinetic limitations for the sorption of As and Fe.

Extraction efficiency was larger at SAR Well A3 than at SAR Well A1, while the conditions at SAR Well A1 are more favorable, as is explained in the following. This can only be caused by the larger injection volume at SAR Well A3, which strongly suggests that the sorption of As and Fe is kinetically limited. HCO_3, Si, and PO_4 are higher at SAR Well A3 than at SAR Well A1 (Table 2.1). This means that more competitive displacement of As may be expected at SAR Well A3 than at SAR Well A1. This is clear when the equilibrium concentrations of sorbed As at SAR Well A1 is compared to SAR Well A3. According to the surface complexation model presented in this paper, the equilibrium concentrations of As sorbed to HFO at SAR Well A1 and SAR Well A3 are 0.004 mmol/L and 0.0034 mmol/L, respectively.The calculated distribution coefficients of As and Fe at SAR Well A1 are 1.46 and 9.92 respectively whereas at SAR Well A3 they are 1.28 and 5.41 respectively, which is further evidence that the conditions are more favorable at SAR Well A1 than at SAR Well A3.

3.4.4. Effect of pumping rate and intermittent operation on As removal

The pumping rate during the extraction phase may be an important factor for subsurface As removal because As partitioning to aquifer material decreases with increased pore water velocity [Darland and Inskeep, 1997] and the adsorption of As onto HFO cannot be considered to be in local equilibrium when the pore water velocity is high [Sharma et al., 2011]. Darland and Inskeep [1997] reported 7.2, 35.6, 53.3, and 74.3% recovery of applied As(V) at pore water velocities of 0.048, 0.24, 2.4, and 21.6 m/day, respectively, in column experiments. They proposed that sorption-related nonequilibrium existed even at velocities of less than 0.05 m/day. For this study, velocities are much higher than 0.05 m/day. The calculated pore water velocities at the center of the well and at the edge of the injection zone are 13.6 and 2 m/day, respectively, at a pumping rate of 13 L/min. For a pumping rate of 50 L/min, velocities at the center of the well and at the edge of the injection zone are 52.3 and 7.4 m/day, respectively. As a result, sorption-related non-equilibrium may be expected during the SAR experiments performed at the field site. According to the results of experiment 3, a low pumping rate during the extraction phase shows increased As removal compared to a high pumping rate (Fig.3.5). The average pumping rate of a typical hand-pump used in Bangladesh is about 45 L/min. So, extraction with a hand-pump during SAR operation would decrease As removal compared to the results obtained in this study.

Improved extraction efficiency was observed during intermittent operation. Two processes may explain this improvement. First, intermittent pumping results in increased travel time through the oxidized zone of the aquifer. Second, every time the pump is started, the flow paths are slightly altered [Veling and Maas, 2009]. These new flow paths result in more As sorption opportunity.

3.4.5. Cost estimate

During experiment 4, As concentrations dropped below the Bangladesh standard for at least V/V_i = 3.0 (Q_E = 2.0) at SAR Well A1. This means that 3000 liters of As safe ($\leq$ 50 μg/L) water was extracted from which 2000 liters can be used for drinking purposes and 1000 liters needs to be saved for re-injection. 114 families can be served daily with this amount of water, assuming 5 members per family and 3.5 l/day/capita drinking water [Milton et al., 2006]. At present, the approximate cost for a SAR unit installation with an injection capacity of 1m3 is around US$925.00 or little more than US$8.00 per family. The operation and maintenance costs are estimated as US$1280.00 per year or US$107.00 per month. Different parts of a SAR unit have different costs and life times (see Table 2). In order to simplify the cost calculations for the entire life time of the SAR

unit, costs for replacement parts are estimated as 20% of maintenance costs. In total, it is estimated that the maintenance costs for one SAR unit with a 1 m3 injection capacity are US$1540.00 per year or US$130.00 per month. This breaks down to US$13.00 per year per family or a little more than US$1.00 per month, which is very low for a community-level unit. The estimated cost for 1 m3 of drinking water is approximately US$2.00.

Table 3.1: Estimated costs of installation and operation and maintenance including life times of different parts of a SAR unit with 1 m3 injection capacity. All values are based on presentmarket price.

Items for SAR unit installation (life time in years)	Replacement cost (US$)
Well (50)	350.00
Tank (20)	244.00
Pipes and joints (20)	85.00
Electric suction pump (10)	130.00
Hand pump (10)	30.00
Valves (5)	50.00
Flow meters (5)	37.00
Items for SAR unit operation and maintenance	**Yearly cost (US$)**
Operatior's salary	878.00
Electricity	147.00
Repair	110.00
Miscellaneous	146.00

3.5. Conclusion

Exploratory experiments were carried out to determine the effect of alternative operations on subsurface As removal. It was shown that Fe and As removal in the subsurface during SAR operation was better at SAR Well A3 (larger injection volume) than at SAR Well A1 (smaller injection volume) even though background groundwater conditions were more favorable for Fe and As removal at SAR Well A1 than at SAR Well A3. As the As sorption on iron hydroxides is kinetically limited this explains the better performance with a larger injection volume (and thus a larger oxidized zone). Repeated injection-extraction cycles of an equal volume resulted in higher extraction efficiency. The pH in the subsurface was increased, which benefits As removal. Repeated injection-extraction cycles of an equal volume likely increased the ion sorption capacity in the subsurface due to the precipitation of fresh HFO sorption sites and resulted in better removal of As in the subsurface. Low pumping rates during extraction resulted in better As removal. Similarly, better extraction efficiency was achieved with intermittent pumping. This supports the evidence that As sorption to iron oxides is kinetically limited. A

number of cycles are required to lower the As levels to the drinking water standard of Bangladesh. In this study, more than 5 cycles were needed to lower the As levels to below the Bangladesh guideline (50 μg/L) and more than 10 cycles were needed to increase the Q_E above 1.

In an ideal setting, As concentrations are measured continuously in the extracted water and a new volume of aerated water is injected when the concentration surpasses the drinking water standard. This is not possible in a real-world setting. A more practical scenario is to consume a pre-set volume after which the injection tank is refilled, water is aerated and re-injected. Comparison of extraction efficiencies between the experiments is difficult as extraction with a lower pumping rate was done at SAR Well A3 while experiments with intermittent pumping followed after the experiments with repeated injection-extraction cycles of an equal volume at SAR Well A1, which might have benefited performance of the cycles with intermittent pumping. As all three alternative operations showed improvement, a combination of the three is recommended for application in rural Bangladesh.

4

REACTIVE TRANSPORT MODELING OF SUBSURFACE ARSENIC REMOVAL SYSTEMS IN RURAL BANGLADESH

This chapter is based on:

M.M. Rahman, M. Bakker, C.H.L. Patty, Z. Hassan, W.F.M. Röling, K.M. Ahmed, B.M. van Breukelen, Reactive transport modeling of subsurface arsenic removal systems in rural Bangladesh., Science of the Total Environment, (2015).

Subsurface Arsenic Removal (SAR) is a technique for in-situ removal of arsenic from groundwater. Extracted groundwater is aerated and re-injected into an anoxic aquifer, where the oxygen in the injected water reacts with ferrous iron in the aquifer to form hydrous ferric oxide (HFO). Subsequent extraction of groundwater contains temporarily lower As concentrations, because As sorbs onto the HFO. Injection, storage, and extraction together is called a cycle. A reactive transport model (RTM) was developed in PHREEQC to determine the hydrogeochemical processes responsible for As (im)mobilization during experimental SAR operation performed in Bangladesh. Oxidation of Fe(II) and As(III) were modeled using kinetic-rate expressions. Cation exchange, precipitation of HFO, and surface complexation, were modeled as equilibrium processes. A best set of surface complexation reactions and corresponding equilibrium constants was adopted from previous studies to simulate all 20 cycles of a SAR experiment. The model gives a reasonable match with observed concentrations of different elements in the extracted water (e.g., the r^2 value of As was 0.59 or higher). As concentrations in the extracted water are governed by four major processes. First, As concentration decreases in response to the elevated pH of injection water and likewise increases when native neutral pH groundwater flows in. Second, the sorption capacity for As increases due to the gradual buildup of HFO. Third, As sorption is enhanced by preferential removal of As(V). Fourth, competitive sorption of Si limits the capacity of freshly precipitated HFO for As sorption. Transferability of the developed reactive transport model was demonstrated through successful application of the model, without further calibration, to two additional SAR sites in Bangladesh. This gives confidence that the model could be useful to assess potential SAR performance at locations in Bangladesh based on local hydrogeochemical conditions.

4.1. INTRODUCTION

Elevated levels of arsenic (As) in groundwater of the shallow Holocene alluvial aquifers of Bangladesh and West Bengal in India are a major public health concern [Bhattacharya et al., 1997, 2002a; Nickson et al., 1998; Acharyya et al., 1999; BGS and DPHE, 2001; McArthur et al., 2001; Ahmed et al., 2004; Ravenscroft et al., 2005] . SAR can be a cost-effective way to provide safe drinking water in rural areas provided that the geochemical characteristics of the aquifer are suitable to SAR. When a SAR system works correctly, several times the injected water can be extracted before the As level rises above the drinking water standard (see Chapter 3).

Insight into the mechanisms controlling SAR is still limited [Appelo and de Vet, 2003; Van Halem et al., 2010b; Rahman et al., 2014] and therefore SAR performance is hard to estimate a priori for a given location. For example, Appelo and de Vet [2003] and Van Halem et al. [2010a] reported PO_4 whereas Rahman et al. [2014] (Chapter 3) reported H_4SiO_4 as the main competitor of As for HFO sorption sites. It is important to determine which hydrogeochemical processes are responsible for the (im)mobilization of As in the shallow subsurface during SAR operation and to develop a tool that can assess potential SAR performance based on local hydrogeochemical conditions. Reactive transport modeling represents a process based description of the geochemical reactions and mechanisms controlling the (im)mobilization of As in the shallow subsurface during SAR operation and may be used to assess potential SAR performance.

The only available reactive transport model (RTM) for subsurface As removal prior to this study was reported by Appelo and de Vet [2003] for a location in the Netherlands. They modeled subsurface As removal with an injection volume of approximately 1000 m^3 whereas the injection volumes at the current systems ranges from 0.5 m^3 to 5 m^3. The maximum groundwater As concentration at their site was 14 μg/L which is approximately 15 times lower than at the study sites considered in this study. Kinetic oxidation of Fe(II) and As(III) was not included in their model, whereas the current model simulates kinetic oxidation of both Fe(II) and As(III). Appelo and de Vet [2003] reported a sudden increase in As concentration in the extracted water compared to the background As concentration when the ratio between extracted and injected volume (V/V_i) is approximately 2 due to the competitive displacement of arsenic by PO_4 and HCO_3 present in the native groundwater. After $V/V_i \approx 2$, As concentration in the extracted water again drops below the background level due to better sorption of As(III).

The objectives of this study are (i) to develop a RTM that simulates the SAR experiments reported by Rahman et al. (2014), and (ii) to obtain mechanistic insight into the interplay of the hydrogeochemical processes responsible for the (im)mobilization of As during SAR operation, and (iii) to determine whether the developed RTM is transferable

to other locations in Bangladesh. The latter was assessed through model application to two other SAR sites in Bangladesh with different hydrogeochemical conditions.

4.2. Experimental conditions at SAR well A3

A reactive transport model was developed for SAR Well A3 Fig. 2.1. The reactive transport model was subsequently applied to SAR wells A2 and B without further calibration as discussed in section 4.5. The conditions at SAR well A3 are discussed here in detail.

A SAR experiment was conducted at SAR well A3 from December 2011 to February 2012. The volume of the tank was 5 m^3. Twenty cycles of injection, storage, and extraction were carried out. Each cycle consisted of three steps. First, water previously extracted from the aquifer was aerated and injected into the reduced aquifer. Second, the water was stored in the aquifer for 15-18 hours. Third, groundwater was extracted. The first 5 m^3 were used to fill the tank for the next injection phase (except for cycle 19 where the second 5 m^3 of extracted water was used to fill the tank) after which different amounts of water were extracted depending on the cycle (see Fig. 4.1).

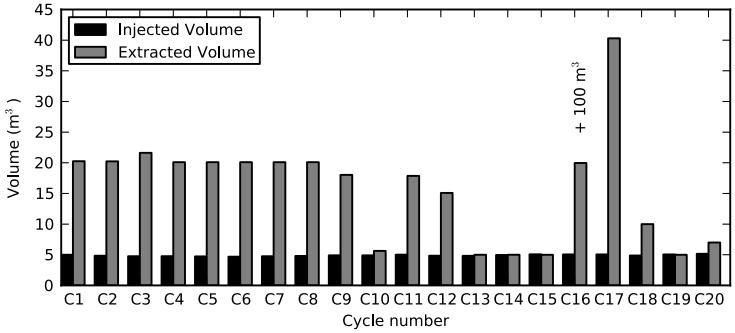

Figure 4.1: Volumes of injected and extracted water for cycles 1 to 20.

Concentrations of Na, K, Ca, Mg, Fe, Mn, As, and Si were measured during the extraction phases of cycle 1, 3, 8, 11, 16, 17, and 20. Injection of 5 m^3 of water took ~3.3 hours, while the extraction rate ranged from 0.77-2.6 m^3/hr. The first 5 m^3 of extracted water was used to fill the injection tank for the next injection phase to avoid sludge formation in the tank. After cycle 16, a large amount of groundwater was extracted from the aquifer (100 m^3 over a 7 day period) to reduce imprints of cycles 1 - 16 as much as possible. Precipitation of iron in the tank was negligible as the extracted water was almost free of iron at the beginning of each extraction (except for the first cycle), so that the tank needed no cleaning.

4.3. REACTIVE TRANSPORT MODEL SETUP

4.3.1. CONCEPTUAL MODEL

The conceptual process model of SAR is based on the processes published by Van Halem et al. [2010a], Wallis et al. [2010], Wallis et al. [2011], and Appelo and de Vet [2003]. The following processes are included in the model for the injection, storage, and extraction phases (the modeling of these processes will be explained later).

Processes during injection and storage phase

a) *Oxidation processes:* during injection, oxidation of dissolved Fe(II) creates a HFO filter or 'curtain' in the subsurface [Van Halem et al., 2010a]. Simultaneously, oxidation of As(III) to As(V), and of soil organic matter forming alkalinity (not included in the model) may occur.

b) *Iron desorption:* during injection, Fe(II) desorbs from clay and SOM surfaces via cation-exchange reactions and via surface complexation reactions on HFO, further driving process 1 [Wallis et al., 2010].

c) *Sorption reactions:* during the storage phase, As(III), As(V), Fe, HCO_3, PO_4, Si, and to a lesser degree other ions, sorb via surface complexation reactions to initially present and newly formed HFO [Wallis et al., 2010, 2011].

Processes during extraction phase

a) *Sorption reactions:* The HFO curtain filters out As and other ions until the capacity is reached and arsenic breakthrough occurs [Appelo and de Vet, 2003].

b) *Competitive sorption processes:* Other ions such as Fe(II), HCO_3, PO_4, and Si sorb simultaneously with As(III) and As(V) during the extraction phases when native groundwater flows towards the SAR well. This simultaneous sorption of Fe(II), HCO_3, PO_4, and Si limits the removal of As. During extraction, Fe(II) also sorbs to the cation exchanger (clay minerals and organic matter) via cation exchange reactions.

4.3.2. MODELING FRAMEWORK

The PHREEQC code (v. 2.17, [Parkhurst et al., 1999]) was used to develop a one-dimensional axisymmetric reactive transport model of the SAR operation. Regional groundwater flow was neglected as it is small (0.071 m/day) compared to the maximum radius and life time of the injection water bubble (1.06 m and ~15 hours, respectively).

A one dimensional PHREEQC model consists of a series of cells. The length of the cells is chosen such that the residence time is equal for each cell. The cell lengths were

calculated according to Appelo and Postma [2005]. The length L1 of the first cell is

$$L_1 = \frac{L_{tot}}{\sqrt{N_{tot}}} \tag{4.1}$$

where N_{tot} is total number of cells (52) and L_{tot} is the total model length (1.08 m). The length L_n of cell n is computed as

$$L_n = L_1\left(\sqrt{n} - \sqrt{n-1}\right) \tag{4.2}$$

Note that a cylinder of aquifer with radius L_{tot} and aquifer thickness b can store a volume

$$V = \theta \Pi b L_{tot}^2 \tag{4.3}$$

where θ is the porosity of the aquifer. The volume of the model is V = 5.36 m^3 based on a radius L_{tot} = 1.08 m, porosity θ = 0.3 and aquifer thickness b = 4.87 m which is more than the maximum injection volume (5.16 m^3) used in the SAR experiment. The volume of each cell is

$$V_{cell} = \frac{V}{N_{tot}} = 0.103 m^3 \tag{4.4}$$

During each advective time step called a shift in PHREEQC, the solution in each cell moves to its neighboring cell in the direction of flow. During the injection phase, water from the storage tank enters the first cell, and the water of the final cell leaves the model.

The number of shifts for each injection and extraction phase was calculated by dividing the volume of injected or extracted water by the cell volume (0.103 m^3). Time steps, reflecting the residence time in each cell, were calculated by dividing the total time of each stress period (injection or extraction) by the number of shifts. The storage phase during SAR cycles was modeled as one time step equal to its duration.

Diffusion and longitudinal dispersion were not modeled, as the simulation period is only a few days. This considerably decreased the model run time without any noticeable influence on the model output.

The initial distribution of mineral and soil organic matter content was approximated as homogeneous and contents were determined from the sediment samples collected from the aquifer (Table 2.1). The initial distribution of solutes in the water was also taken as homogenous and based on the groundwater sample collected from SAR well A3 prior to SAR operation (Table 2.1). Since the maximum number of shifts never exceeded the total cell number and hydrodynamic dispersion was excluded, the composition of the outer two model cells kept invariant and equal to the initial values during the simulation, such that they always represented native groundwater.

4.3.3. Simulation of Hydrogeochemical processes

Kinetic oxidation of dissolved Fe(II) to HFO

Kinetic oxidation of dissolved Fe(II) to Fe(III) as HFO required a modification of the PHREEQC database in order to decouple the two valence states of iron and to calculate the kinetic oxidation of Fe(II) to Fe(III) in water [Antoniou et al., 2013; Parkhurst et al., 1999]. The oxidation rate is given by Singer and Stumm [1970]:

$$r_{Fe^{2+}} = -\left(k\,[OH^-]^2\,P_{O_2}\right) m_{Fe^{2+}} \tag{4.5}$$

where PO_2 [atm] is the partial pressure of oxygen, $m_{Fe^{2+}}$ [mol L^{-1}] is the total molality of ferrous iron in solution, and k is a rate constant with a value of 1.33 x 10^{12} [L^2 mol^{-2} atm^{-1} s^{-1}] at 25° C. This constant was allowed to adjust to a value of 1.41 x 10^{12} [L^2 mol^{-2} atm^{-1} s^{-1}] at the in-situ groundwater temperature of 26.5° C (Table 2) since, according to Stumm and Lee [1961], the rate increases about ten-fold for a 15° C temperature increase. Dissolved ferric iron was modeled in thermodynamic equilibrium with Ferrihydrite (log K = 4.891).

Kinetic oxidation of dissolved As(III) to dissolved As(V)

As(III) in the native groundwater at the study site is ~80 % of total As[Rahman et al., 2014] (Chapter 3). Introduction of oxygen in the groundwater may lead to oxidation of As(III) to As(V) but the rate of oxidation in groundwater is usually slow and deviation from redox equilibrium controlled arsenic speciation is common in nature [Smedley and Kinniburgh, 2002]. A large number of studies [Oscarson et al., 1981; De Vitre et al., 1991; Manning et al., 2002b,a; Hug and Leupin, 2003; Amirbahman et al., 2006] proposed that arsenic speciation in natural groundwater is controlled by abiotic oxidation processes and has been attributed to the presence of MnO2 [Manning et al., 2002b; Amirbahman et al., 2006; Oscarson et al., 1981], iron oxides, and oxygen [De Vitre et al., 1991; Manning et al., 2002a; Hug and Leupin, 2003]. However, biological oxidation may also occur and can be conducted by several microbial respiratory and nonrespiratory enzymatic systems[Hassan et al., 2015]. Oxygen and nitrate are important electron acceptors in aquifers for biologically mediated oxidation[Oremland and Stolz, 2003]. Arsenic speciation data of the extracted water suggests that there may be some oxidation of As(III) to As(V) in the aquifer [Rahman et al., 2014] (Chapter 3).

A kinetic rate expression was used to describe the transition from As(III) to As(V). The As(V)/As(III) redox speciation was disconnected from the overall redox equilibrium and all equilibrium controlled redox reactions of As(III) to As(V) were deactivated according to Wallis et al. [2010]. Albeit the presence of microbial As oxidizers are widespread in Bangladesh [Hassan et al., 2015], only abiotic oxidation of As(III) by oxygen was in-

cluded in the model as the observed extents of As(III) oxidation at SAR well A3 [Rahman et al., 2014] (Chapter 3) and SAR well B were very low. Abiotic As(III) oxidation by Fe-and Mn-oxides has been shown to dramatically increases the As(III) oxidation rate [Driehaus et al., 1995; Oscarson et al., 1981, 1983a,b; Sun and Doner, 1998]. Initial model results with the latter process included produced poor model data agreements (results not shown). Therefore, the As(III) oxidation by iron- and Mn-oxides was not further included in the model. The rate expression for As(III) to As(V) oxidation was taken from Wallis et al. [2010]:

$$r_{As(III)} = -kC_{As(III)}C_{oxidant} \tag{4.6}$$

where CAs(III) and Coxidant are the As(III) and oxidant concentrations [mol-L^{-1}] and k is the second order rate constant with a value of 3.0 x 10-3 [mol-$L^{-1}s^{-1}$] with O2 as oxidant (Table 4.2).

Minor relevance of other oxidation processes

Organic matter oxidation was not included in the model despite the presence of minor amounts of soil organic matter in the aquifer (0.1 % d.w.) because the measured alkalinity in the extracted water did not show a considerable increase and variation with respect to the native groundwater. Furthermore, a simulation including SOM oxidation using representative literature values for the rate parameters following Antoniou et al. [2013] demonstrated negligible differences in modeled outcome (results not shown).

Pyrite oxidation was also excluded from the model because X-ray diffraction analysis did not identify pyrite in the aquifer material and there was only a negligible increase of sulfate compared to the native groundwater (from 0.3 mg/L native to max 1.4 mg/L in the extracted water) suggesting the presence of pyrite in agreement with the low SO_4:Cl ratio of the groundwater. If the sulfate increase would relate to pyrite oxidation it would be equivalent to a consumption of O_2 of only 0.45 mg/L (5.6% of the injected O_2 level of $\approx$ 8 mg/L).

The native groundwater was supersaturated with respect to $FeCO_3$ (saturation index = 1.37) but X-ray diffraction analysis, albeit having a high detection limit, could not identify $FeCO_3$ in the aquifer material. Moreover, Antoniou et al. [2013] showed that $FeCO_3$ is a minor oxygen consumer. Potential $FeCO_3$ oxidation was therefore not included.

Carbonate mineral interaction

The calculated saturation index (SI) of calcite of the extracted water ranges from -0.74 to -0.32, which indicates that the small amount of calcite found in the aquifer (0.39 moles/L or 6.33 g/kg)) is not in equilibrium. Therefore, calcite was allowed to dissolve/precipitate

Table 4.1: Parameters used in the PHREEQC model.

Parameter	Model values	Units	Literature values	References
kFe(II)Ox	1.41×10^{12}	$L^2\ mol^{-2}\ atm^{-1}\ s^{-1}$	1.41×10^{12} [a]	[a] [Singer and Stumm, 1970]
k As(III)ox	3×10^{-3}	$mol\text{-}l^{-1}\ s^{-1}$	3×10^{-3} [b]	[b] calculated from Clifford et al. [1983]
Weak site densities for HFO	0.2	mol/mol	0.2 [c]	[c] [Dzombak and Morel, 1990]
Strong site densities for HFO	0.005	mol/mol	0.005 [c]	
Weak site densities for goethite	5.12×10^{-5}	mol/mol	1.02×10^{-4} [d]	[d] [Stollenwerk et al., 2007]
Strong site densities for goethite	1.28×10^{-4}	mol/mol	2.55×10^{-6} [d]	
Surface area for HFO	6.41×10^{4}	m^2/mol	6.41×10^{4} [c]	
Surface area for Goethite	257.21	m^2/mol	257.21 [d]	
$\mathbf{A_{Calcite}/V}$	2.98×10^{-4} [e]	m^2/L^{-1}	Sand: $(0.4\text{-}1.8)\times10^{-1}$ [f]	[e] [Antoniou et al., 2013]
			Silt: $(1.1\text{-}7.7)\times10^{-2}$ [f]	[f] [Descourvieres et al., 2010]
			Clay: $(3\text{-}4)\times10^{-4}$ [f]	

kinetically according to Plummer et al. [1978]:

$$r_{cal} = \left(k_1\left[H^+\right] + k_2\left[CO_2\right] + k_3\left[H_2O\right]\right)\left(\frac{A_{cal}}{V}\right)\left(\frac{m}{m_0}\right)^{0.67}_{cal} \tag{4.7}$$

where brackets indicate activities, k1, k2, k3 are temperature dependent constants ($cm^{-2}\ s^{-1}$), $\frac{A_{calcite}}{V}$ is the ratio of initial calcite surface area to solution volume ($m^2\ L^{-1}$), and m0 is the initial content of calcite (Table 4.2). The simulation without the calcite interaction shows that the effect of this process is only minor due to short periods of reaction during SAR cycles (discussed later).

Cation-exchange

The following solutes participated in cation-exchange reactions: Na, K, Ca, Mg, Fe(II), and Mn(II). The cation-exchange coefficients from the PHREEQC database were used unchanged. Cation-exchange was included in the model, as a main part of Fe(II) in the aquifer was initially sorbed to clay minerals and organic matter (both sorbents are typically lumped as the cation exchanger) and can be released to the groundwater by means of cation-exchange when dissolved Fe(II) decreases in concentration, for example, when it oxidizes to HFO. Furthermore, during extraction phases, dissolved Fe(II) from native water enters the HFO enriched and Fe(II)X2 (i.e., cation-exchangeable Fe(II)) depleted zone around the SAR well and resorbs to both HFO and the cation exchanger. This results in subsurface iron removal and in the case of HFO also in desorption of As, since Fe(II) competes with As for HFO surface sites.

Surface complexation modeling

The adsorption of As and other compounds such as HCO_3, Fe(II), PO_4, and Si was modeled as surface complexation reactions on freshly formed HFO surfaces, on initially present reactive amorphous iron oxide surfaces, and on initially present less reactive goethite surfaces. The initial reactive amorphous iron oxide content was also considered as HFO

surface for model simplicity. HFO and goethite were considered as different surfaces in the model (Table 4.1). The combination of goethite and initial reactive amorphous iron oxide surface assemblages improved the model results compared to the simulations that assumed the initial iron oxide surfaces to be only goethite (results not shown).

A large number of different combinations of surface complexation reactions and corresponding equilibrium constants for HFO were evaluated until a set was found that gave reasonable results for measured concentrations of Fe, Mn, As, HCO_3, and Si in the extracted water of the first cycle (Table 4.2). Quantification of goodness of fit between modeled and observed data is given in section 4.6.1.For goethite the surface complexation reactions and corresponding equilibrium constants were taken from Stollenwerk et al. [2007]. The modeled results for different combinations of surface complexation reactions are presented in Fig. 4.2. Unfortunately, PO4 was not measured at SAR well A3,

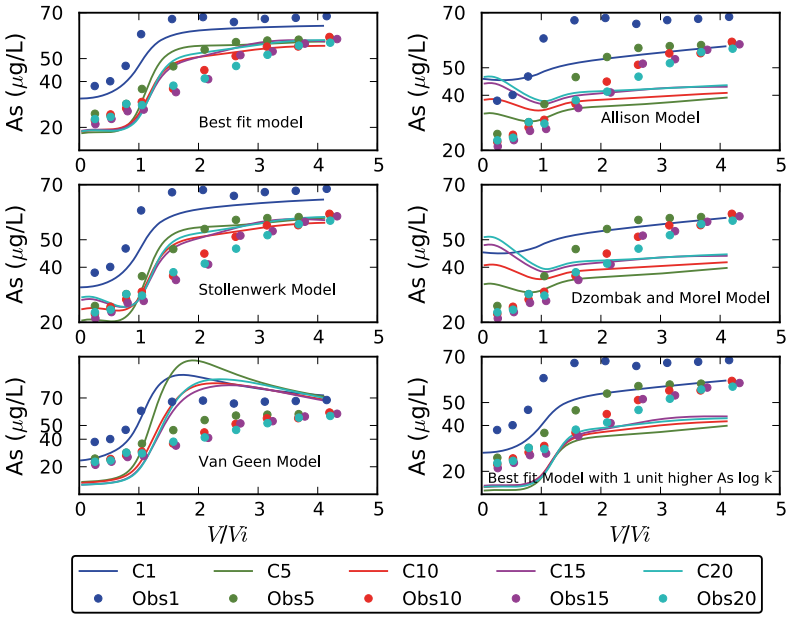

Figure 4.2: Observations and model simulations of As breakthrough during the extraction phases of cycles 1, 5, 10, 15, and 20 at SAR well B for different surface complexation models for As sorption. Change in As breakthrough pattern is also shown for best fit model with one unit higher As log k value.

however, it was measured at SAR well A2 and B. For HFO, the double layer surface complexation model by Dzombak and Morel [1990] was modified and extended with surface species for carbonate [Stollenwerk et al., 2007], silicate [Stollenwerk et al., 2007; Swedlund and Webster, 1999], Fe(II) [Appelo and de Vet, 2003; Liger et al., 1999], As(III) and As(V)[Dixit and Hering, 2003; Wallis et al., 2010], PO4, and protons [Stollenwerk et al.,

2007]. A similar kind of modification and combination was used before by e.g.,Dixit and Hering [2003], Wallis et al. [2010], Robinson et al. [2011], and Jessen et al. [2012].

The sorption behaviors of species strongly depend on the surface complexation models used [Jessen et al., 2012]. It is therefore important to use the surface complexation parameters that can closely reproduce the measured data. Therefore, we need to assess whether it is reasonable to apply the set of surface complexation parameters used by others as obtained for their sites to the data from our site. The surface complexation reactions and equilibrium constants for Fe(II), Si, PO4, and protons used in the current model were previously used by Stollenwerk et al. [2007] for Pleistocene oxidized sediments in Bangladesh. Jessen et al. [2012] showed that the adsorption data for As(III) on Holocene sediments measured by Itai et al. [2010] plot close to the As(III) adsorption data for Pleistocene sediments reported by Stollenwerk et al. [2007]. Therefore Jessen et al. [2012] used the Stollenwerk et al. [2007] surface complexation model for their Holocene reduced aquifer system. The same constants are used here as the study site also represents a Holocene reduced aquifer system. Surface complexation parameters for As(III) and As(V) used in the current model were not taken from Stollenwerk et al. [2007] but adopted from other studies (see Table 4.2) to enable a better reproduction of our observations.

The adsorption of species to both iron oxides was described by equilibrium mass action equations using the surface complexation approach. The Dzombak and Morel [1990] model includes both strong and weak binding sites on HFO. The adsorption of different species depends strongly on the reactions and thermodynamic constants used, and on the adopted surface assemblage (number of strong and weak adsorption sites and HFO surface area). Dzombak and Morel [1990] proposed a surface area of 6.41x 10^4 m^2/mol of HFO, site densities of 0.2 mol weak sites/mol of HFO, and 0.005 mol strong sites/mol of HFO. The numbers of weak and strong sites for HFO adopted in this model were therefore 0.2 and 0.005, respectively (Table 4.2). We adopted those values without further change (Table 4.2).

As mentioned earlier (see section 2.7.1) the amount of crystalline iron oxides initially present in the aquifer was considered as goethite surfaces for surface complexation reactions. In order to include the goethite surface in the model, the wateq4f database was modified according to the model for adsorption on Pleistocene aquifer sediment from Bangladesh [Stollenwerk et al., 2007] to simulate surface complexation to goethite. The number of weak and strong sites for goethite was optimized by maintaining the proportion between site densities and goethite content reported by Stollenwerk et al. [2007] and the values are 5.12 x 10^{-4} and 1.28 x 10^{-5}, respectively, roughly five times higher than applied by Stollenwerk et al. [2007] (Table 4.2). Note a similar kind of optimization was done by Jessen et al. [2012].

Table 4.2: The surface complexation reactions and equilibrium constants for HFO evaluated and used in this model.

Adsorption reaction	Log k[a] Allison	Log k[b] D&M	Log k[c] S&W	Log k[d] D&H	Log k[e] VG	Log k[f] Stoll	Log k[g] Wallis	Log k[h] Model
Hfo_sOH + H^+ = Hfo_sOH_2^+	7.29					7.29		Allison
Hfo_sOH + H^+ = Hfo_sO^-+H^+	-8.9					-7.03		
Hfo_wOH + H^+ = Hfo_wOH_2^+	7.29					7.29		
Hfo_wOH + H^+ = Hfo_wO^-+H^+	-8.9					-7.03		
Arsenate								
Hfo_wOH + As(V)O_4^{-3} + 3H^+ = Hfo_wH_2As(V)O_4+H_2O		29.31		29.88		30.66		D&H
Hfo_wOH + As(V)O_4^{-3} + 2H^+ = Hfo_wHAs(V)O_4^-+H_2O		23.51		24.43		22.34		
Hfo_wOH + As(V)O_4^{-3} + 2H^+ = Hfo_wOHAs(V)O_4^{-3}		10.58				10.54	11.88	Wallis
Hfo_wOH + As(V)O_4^{-3} + 2H^+ +H^+ = Hfo_wAs(V)O_4^{-2}				18.1		8.7		D&H
Hfo_sOH + H_3As(V)O_4= Hfo_sH_2As(V)O_4+ H_2O	8.61							NM[i]
Hfo_wOH + H_3As(V)O_4= Hfo_wH_2As(V)O_4+ H_2O	8.61							
Hfo_sOH + H_3As(V)O_4 = Hfo_sHAs(V)O_4^- + H^+	2.81							
Hfo_wOH + H_3As(V)O_4 = Hfo_wHAs(V)O_4^- + H^+	2.81							
Hfo_sOH + H_3As(V)O_4 = Hfo_sHAs(V)O_4^{-3} + 3H^+	-10.12							
Hfo_wOH + H_3As(V)O_4 = Hfo_wHAs(V)O_4^{-3} + 3H^+	-10.12							
Arsenite								
Hfo_wOH + As(III)OH_3^{-3} + 3H^+ = Hfo_wH_2As(III)O_3+H_2O				38.76		37.5		D&H
Hfo_wOH + As(III)OH_3^{-3} + 2H^+ = Hfo_wHAs(III)O_3^-+H_2O				31.87		32.1		
Hfo_wOH + As(III)OH_3^{-3} + H^+ = Hfo_wAs(III)O_3^{2-}+H_2O						30.01		Stoll
Hfo_wOH + H_3As(III)OH_3 = Hfo_wH_2As(III)O_3+H_2O	5.41							NM[i]
Carbonate								
Hfo_wOH + CO_3^{-2} + H^+ = Hfo_wCO_3^-+H_2O					12.56	10.56		Stoll
Hfo_wOH + CO_3^{-2} + 2H^+ = Hfo_wCO_3+H_2O					20.62	15.62		Stoll
Silica								
Hfo_wOH + H_4SiO_4 = Hfo_wH_3SiO_4+H_2O			4.28			3.78		Stoll
Hfo_wOH + H_4SiO_4 = Hfo_w$H_2SiO_4^-$+H^++H_2O			-3.22			-6.71		
Hfo_wOH + H_4SiO_4 = Hfo_w$HSiO_4^{2-}$+2H^++H_2O			-11.69					NM[i]
Phosphate								
Hfo_wOH + PO_4^{-3} + 3H^+ = Hfo_wH_2PO_4+H_2O	31.29					32.8		Stoll
Hfo_wOH + PO_4^{-3} + 2H^+ = Hfo_wHPO_4^-+H_2O	25.39					24.89		
Hfo_wOH + PO_4^{-3} + H^+ = Hfo_wHPO_4^{-2}+H_2O	17.72					13.56		
Iron (II)								
Hfo_sOH + Fe^{+2} = Hfo_sFe^++H^+		-0.95						D&M
Hfo_wOH + Fe^{+2} = Hfo_wFe^++H^+		-2.98						
Hfo_wOH + Fe^{+2}+H_2O = Hfo_wOFeOH +2H^+		-11.55						
Manganese (II)								
Hfo_sOH + Mn^{+2} = Hfo_sOMn^++H^+		-0.4						D&M
Hfo_wOH + Mn^{+2} = Hfo_wOMn^++H^+		-3.5						

[a] [Allison, J.D. et al., 1990]
[b] [Dzombak and Morel, 1990]
[c] [Swedlund and Webster, 1999]
[d] [Dixit and Hering, 2003]
[e] [van Geen et al., 2004]
[f] [Stollenwerk et al., 2007]
[g] [Wallis et al., 2010]
[h] Used in this study
[i] Not Modeled

4.3.4. Composition of the injection water

In the model, the measured chemical composition (except Si) of the injection water was used, which differed slightly for each injection phase (see Figure 4.3). The pO_2 values of the dissolved oxygen levels in the injection water are higher than the saturation values, as the water in the tank was thoroughly aerated with disk aerators and an air compressor. The tank remained clean of suspended iron particles after cycle 2, therefore the concentration of suspended iron injected into the aquifer was not included in the model. This means that the input of iron into the aquifer was at most underestimated for the first two cycles. Fe measured in the injection water was assumed to be Fe(III) since the water in the tank was aerated for at least 4-5 hours before injection while the half life of Fe(II) under oxic conditions is only a few seconds at pH above 8 (Eq. 4.5). In the PHREEQC model, injected Fe(III) instantaneously precipitates to HFO in the first model cell and consequently lowers the pH in cell 1 somewhat, which is not quite correct as Fe(III) actually occurs as suspended HFO in the injection water. This error is only relevant for the first cycle, after which Fe levels drop to less than 1 mg/L (Bangladesh standard). Arsenic redox speciation for each cycle was calculated with Equation 4.6 and the rate constant presented in Table 4.2, and used as input concentration in the model. These calculations corroborate the findings of Rahman et al. [2014] (Chapter 3). Note the elevated pH levels of the injection water. The pH levels were elevated due to the degassing of CO_2 in the groundwater during the aeration process in the tank.

Si concentrations of the injection water were not measured but speciation of surface complexation suggested that Si is one of the dominant surface species (see section 4.5). So the average modeled Si concentration of the first extracted volume (5 m^3) was used for each cycle since the first extracted volume (5 m^3) was always saved in the aeration tank for the next injection phase (Fig. 4.3).

4.4. Results and Discussion

4.4.1. General model results and performance

The measured and modeled concentrations of eight elements (Fe, As, Mn, Si, Ca, Mg, Na, and K) in the extracted water are presented in Fig. 4.2 for cycle 1. The horizontal axis represents the extracted volume (V) normalized by the injected volume (V_i). The redox sensitive elements are presented in the first row whereas the major cations are presented in the second row. Note that the pH, Alkalinity, and P values of the extracted water were not measured during the experiments at SAR well A3, but the values were measured and modeled at SAR wells A2 and B (to be reported later in section 4.5).

The model-data comparison in Fig. 4.4 illustrates that the model provides a reasonable representation of the key processes that influence the major ion and redox chem-

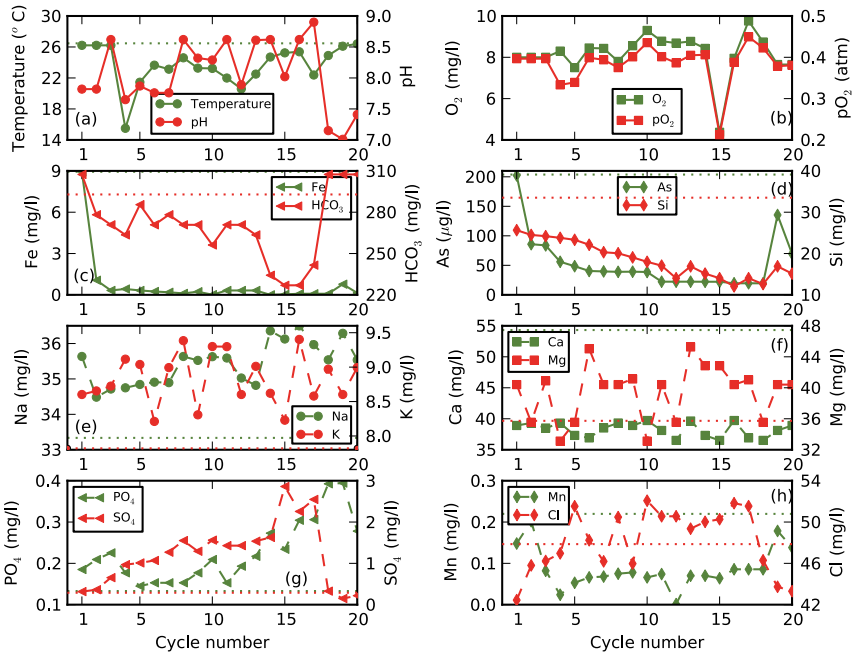

Figure 4.3: Measured composition of injection water used for each cycle at SAR well A3. (a) temperature and pH (secondary y axis), (b) dissolved oxygen concentrations and calculated pO_2 (secondary *y* axis), (c) Fe(III) and HCO_3(secondary *y* axis) concentrations, (d) total As and Si (average calculated from the modeled results) concentrations (secondary y axis), (e) Na and K (secondary *y* axis) concentration, (f) Ca and Mg (secondary *y* axis) concentrations, (g) PO_4 and SO_4 (secondary *y* axis) concentrations, and (h) Mn and Cl (secondary *y* axis) concentrations during each cycle. Groundwater background levels (dotted lines) are shown with dotted lines when they are of the same order else they are off the graph.

istry during SAR operation. Fe(II) and Mn(II) concentrations start with a low value due to their sorption to newly formed iron oxides and present clay minerals, and gradually increase as native groundwater reaches the well. The same pattern is seen for As and Si which sorb to newly formed iron oxides. The model fit for Mg, Na, and K is reasonable, which indicates that the cation exchange process was modeled correctly in the model.

The model was run for all 20 cycles in order to evaluate its performance. Results are shown in Fig. 4.5 for the cycles during which measurements were made. The breakthrough of Fe(II), As, and partly Mn(II) for different cycles was modeled reasonably well. The observed and modeled breakthrough curves of Fe(II), As, and Mn(II) show significantly larger removal for cycle 16 compared to cycles 1, 3, 8, 11, 17, and 20. This is a direct consequence of the experimental setup. Cycles 13-16 were performed differently in an attempt to improve SAR performance (Fig. 4.1; section 4.2). The injection and ex-

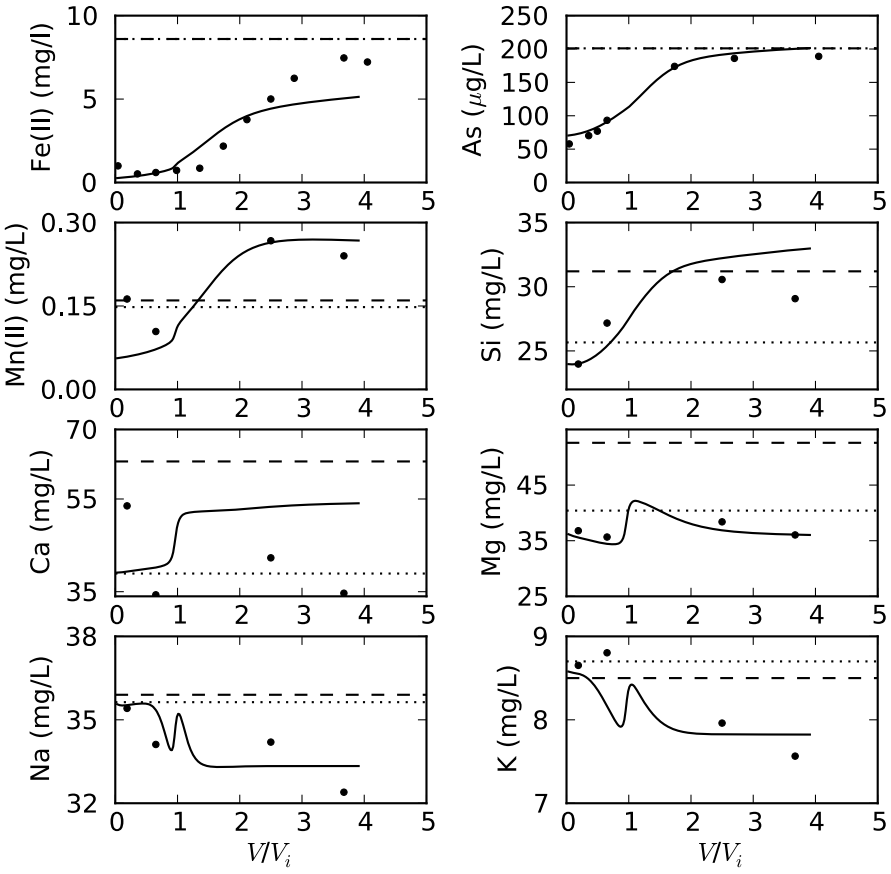

Figure 4.4: Observations and model results for various elements during the extraction phase of cycle 1 of SAR well A3. The dots represent observed values and the solid lines represent modeled results. The dashed lines represent background concentrations and the dotted lines represent injected concentrations.

traction volumes were equal during cycles 13-15 (Fig. 4.1) which resulted in decreased Fe(II), As, Mn(II), and Si concentrations during cycle 16. The increased removal of these elements is due to the increased sorption capacity as sorption sites were produced when HFO precipitated and additional sites were also available from cycles 13-15. The model simulates the performance of cycle 16 quite well (Fig. 4.5). Removal of As, Mn(II), and Si was somewhat less in cycle 17 as compared to cycle 16 (Fig. 4.5), because the aquifer was flushed before performing cycle 17 to reduce the imprints of cycles 1- 16 as much as possible (Fig. 4.1). This is the reason why the model breakthrough curves for As, Mn(II), and Si also show a sudden decrease in the removal as compared to cycle 16 during extrac-

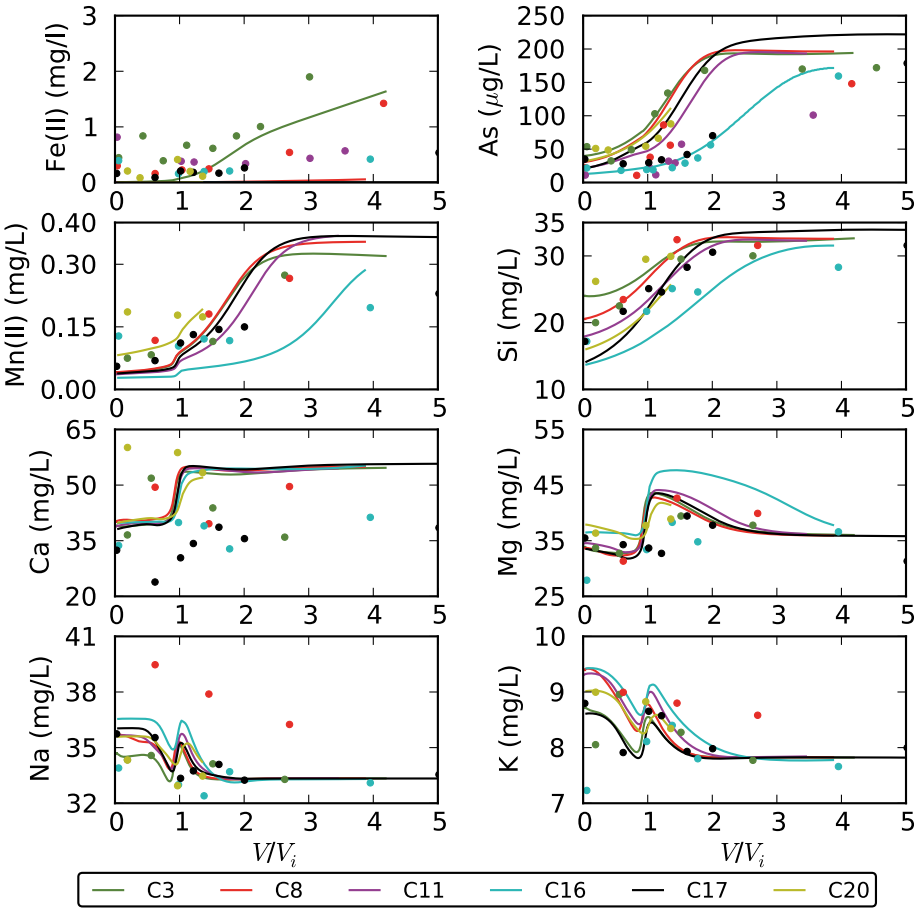

Figure 4.5: Observations and model output for various elements during the extraction phases of cycles 3, 8, 11, 16, 17, and 20 for SAR well A3. The dots represent observed values and the solid lines represent modeled results.

tion phase. The observed decrease of SAR performance was less than simulated by the model. The observed removal of As, Mn(II), and Si during cycle 20 is also smaller than the previous cycles because the second extracted volume with much higher As concentration was used during the injection phase of cycle 19 compared to cycles 16-18 (see Fig. 4.3) and that still had impact on the subsurface removal during cycle 20. The model also predicted this effect reasonably well. The overall agreement between the observed and modeled results for different experimental conditions at SAR well A3 indicates that the reactive transport model is applicable to various SAR experimental conditions.

The model simulated negligible Fe(II) concentrations during the extraction phases

after cycle 3, whereas Fe(II) is still observed in low concentration (< 0.5 mg/L) during the extraction phases of all SAR cycles. This small discrepancy between observed and modeled results might relate to iron-reduction occurring after oxygen has depleted but it is more likely that the measured total Fe includes some Fe(III). This dissolved Fe(III) in the water samples may have come from colloidal Fe-oxyhydroxide particles formed during oxidation, but was too small to be removed by filtration over 0.45 µm before analysis. Interference of colloidal Fe-oxyhydroxide particles in filtered water samples was reported by Appelo and de Vet (2003) and Rott et al. (1996). Colorimetric measurements at SAR well A2 of Fe(II), Fe(III), and Fe(total), according to Viollier et al. (2000), also support the mechanism discussed above (see Fig. 4.6). The model assumes all Fe(III) precipitates to HFO and colloids are not formed.

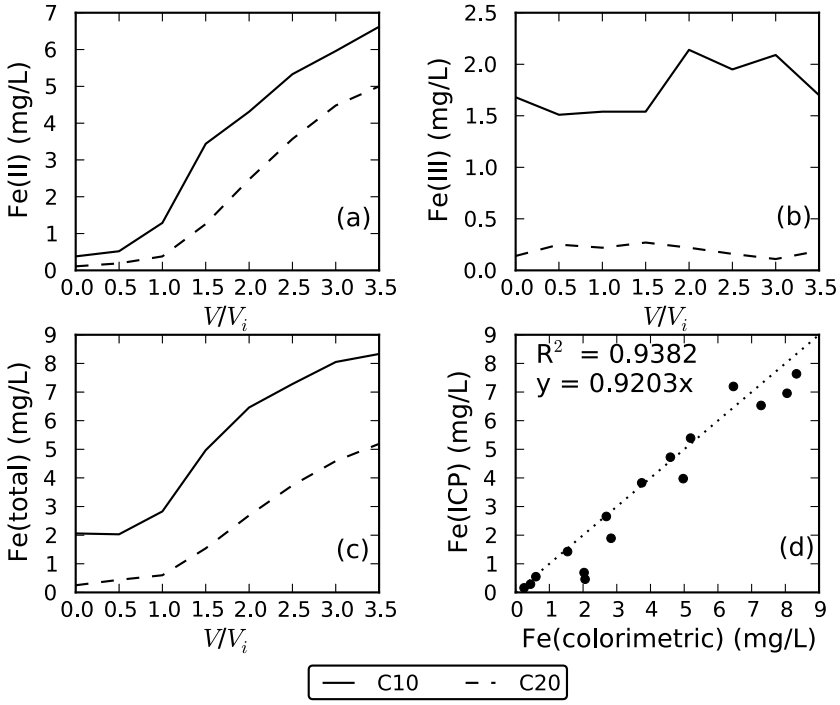

Figure 4.6: Colorimetric measurements, showing Fe(II) concentrations (a), Fe(III) concentrations (b) and Fe(total) concentrations (c) for cycle 10 (solid black line) and 20 (dashed black line. The regression between the colorimetric (Fe(II)) and the ICP determination (Fe(total)) is shown in panel d including the 1:1 line.

4.4.2. Behavior or iron: development of HFO and sorption of iron

The development of HFO precipitates progressively extends away from the well (Fig. 4.7) because the originally sorbed ferrous iron near the well has been oxidized already and the inflowing ferrous iron is effectively sorbed to HFO that forms at the outskirts of the SAR influence zone. The sorption of ferrous iron on HFO is crucial for the removal of

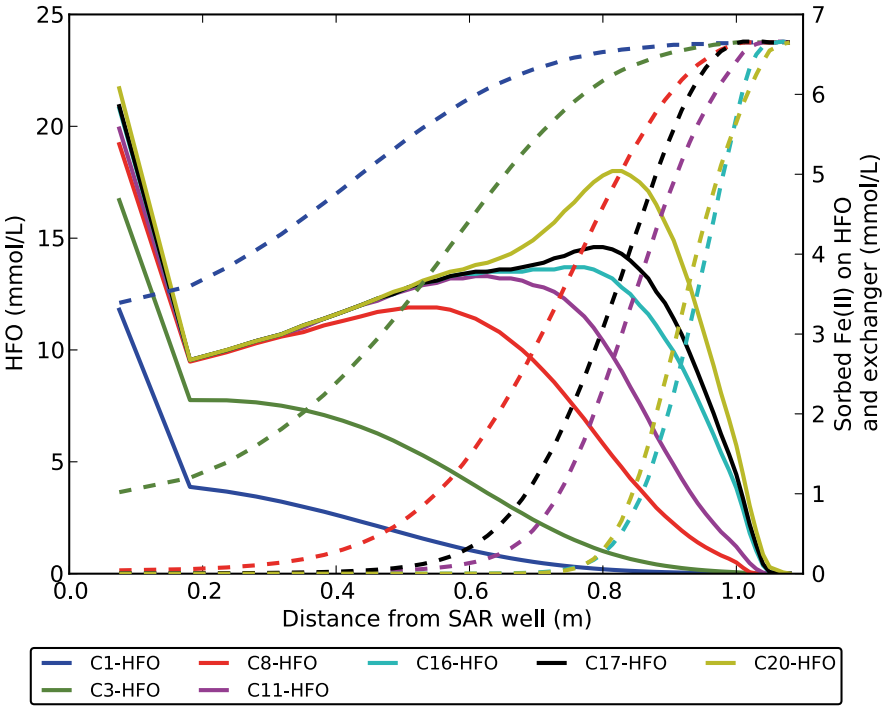

Figure 4.7: Modeled contents of newly formed HFO precipitates (solid lines, primary *y* axis) and of sorbed Fe(II) content (dashed lines, secondary *y* axis) versus distance away from the SAR well A3 at the end of cycles 1, 3, 8, 11, 16, 17, and 20.

trace elements such as As and Mn(II) during SAR operation. Sorbed Fe(II) oxidizes during the injection phase and precipitates as HFO. Freshly precipitated HFO increases the opportunity for As, Fe(II), and Mn(II) to sorb on HFO. The modeled concentration of sorbed Fe(II) on the exchanger and HFO at SAR well A3 is shown for the first four cycles in Fig. 4.8. Sorption of Fe(II) on HFO and the exchanger decreases during the injection and storage phases (Fig. 4.8) as the oxic injection water, deprived of Fe(II), triggers Fe(II) desorption and its subsequent oxidation. During subsequent extraction, the surface sites on HFO and the exchange complex get replenished with Fe(II) from the native groundwater. From Fig. 4.8 it is clear that the concentration of sorbed Fe(II) on the exchanger

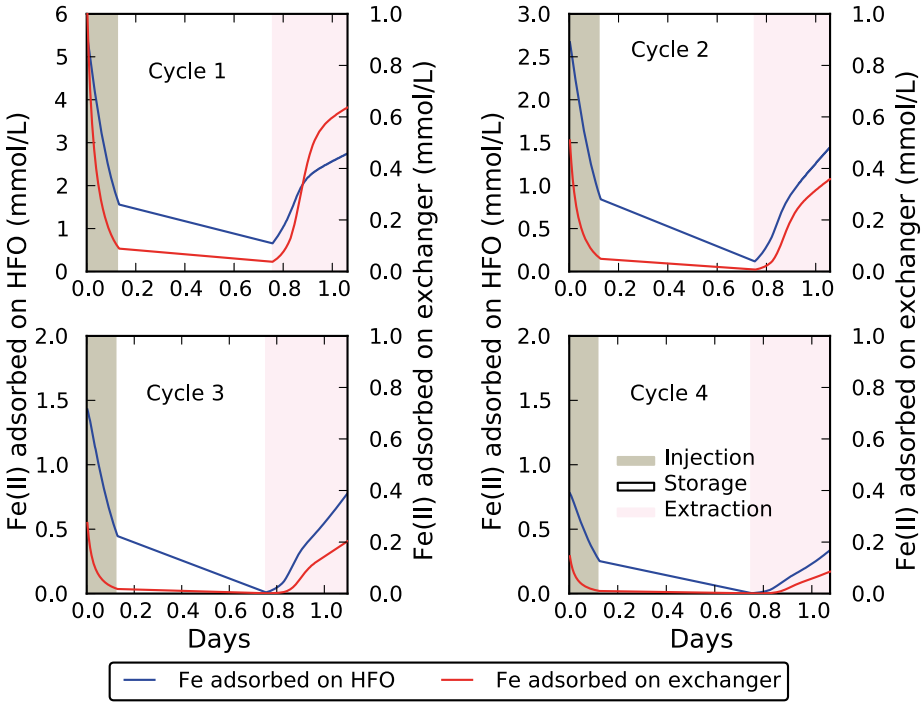

Figure 4.8: Modeled adsorbed concentrations of Fe(II) at SAR well A3 on the HFO (primary *y* axis) and on the exchanger (secondary y axis).

and HFO at SAR well A3 decreases with successive cycles. The lower concentration of exchanged and adsorbed Fe(II) at SAR well A3 is due to the lateral expansion of the HFO filter zone away from the SAR well with successive cycles (Fig. 4.7).

4.4.3. Behavior of arsenic

Effect of surface complexation model parameters on As sorption

SAR experimental results reported by Rahman et al. [2014] (Chapter 3) show that SAR performance increases with larger injection volume and with lower extraction rate, which indicates As sorption is kinetically limited. In this study, a reasonable model fit is obtained by simulating the sorption reactions to be in equilibrium with a set of surface complexation parameters adopted from literature (see section 4.3.3). Note that the model tends to underestimate the removal of As even though equilibrium sorption was simulated. Kinetic sorption with the same set of surface complexation parameters may be expected to result in even less As removal simulated by the model. This means that constants for sorption reactions of As(III) and As(V) need to be increased beyond values

reported in the literature in order to produce a reasonable model fit when kinetic sorption is modeled. Simulation with increased sorption reaction constants of As(III) and As(V) results in increased As removal during SAR operation, but the agreement with the observations is much worse (Fig. 4.2). For the sake of model simplicity, it was therefore decided not to simulate surface complexation reactions as kinetically-controlled but in thermodynamic equilibrium.

Effect of ion competition for sorption sites on As removal

Phosphate and silicates are the main competitors of As for sorption sites (e. g. [Meng et al., 2001; Su and Puls, 2001]. Identification of HCO_3 as a major driving force for As displacement from HFO was reported by Appelo and de Vet [2003] and Wallis et al. [2011], whereas a minimal effect of HCO_3 on As(V) adsorption by HFO was reported by Wilkie and Hering [1996], Meng et al. [2000], Radu et al. [2005], and Stollenwerk et al. [2007] . Meng et al. [2002] reported small effects of bicarbonate on As(III) sorption. The initial composition of the sediment surface complexes in equilibrium with the native water are shown for SAR well A3 in Fig. 4.9. The dominant surface species is silicate. According to the current model setup HCO_3 sorption is too low (not shown in Fig. 4.9) and is not important at the study site. The sorption of PO_4 at the study site is also very low (about 5%) (Fig. 4.9), because the background PO_4 concentrations at SAR well A3 are very low (Table 2.1). The distribution of different ions on sorption sites at the SAR well during SAR operation is presented in Fig. 4.10. Results indicate that the distribution of ions on sorption sites remains largely similar to the initial conditions and is unaffected during SAR operation with the exception of Si (Fig. 4.10).

During the SAR operation at SAR well A3, As concentrations in the extracted water never dropped below the WHO guideline of 10 μg/L even though the native P concentration is low compared to the P concentration of Bangladesh groundwater (see Table 2.1). This implies that As removal may be limited by competitive sorption of other solutes such as silica and bicarbonate as mentioned earlier. According to the model results, HCO_3 is not responsible for the limited As removal since HCO_3 occupies only a very small percentage of sorption sites even though the native HCO_3 is high at SAR well A3 (Table 2.1). As mentioned earlier, the current model uses surface complexation constants for HCO_3 from Stollenwerk et al. [2007] and the use of these constants gives a reasonable model fit. When surface complexation constants published by van Geen et al. [2004] were used they resulted in stronger carbonate sorption and the fit for As, HCO_3, and other species decline (Fig. 4.2). Competition between As and silicate for sorption sites is another reason that makes it difficult to remove As from Bangladesh groundwater [Hug et al., 2008; Stollenwerk et al., 2007]. Silica has been shown to decrease adsorption of As on HFO [Waltham and Eick, 2002]. Note that Si concentrations at SAR

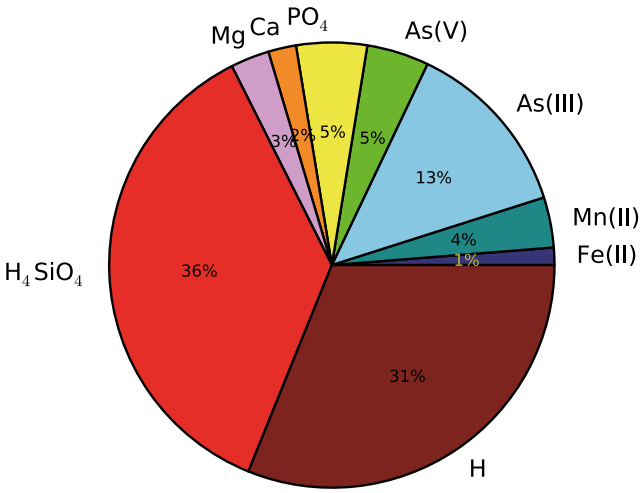

Figure 4.9: The surface speciation at equilibrium with native groundwater at SAR well A3 (Table 2.1), calculated for the sites that are able to adsorb arsenic, with the surface complexation model for HFO with the current surface complexation model settings. The field for each element in the pie diagram may cover several surface species. The field denoted "H" indicates the sum of all protonated or deprotonated surface sites.

well A3 were above the 90 percentile for Bangladesh (Table 2.1. The distribution of surface complexation shows silica as the main surface complex species (Figs. 4.9 and 4.10), which confirms ion competition for sorption sites between As and Si. Modeled breakthrough curves of Si show decreased concentrations of Si during the extraction phase (Figs. 4.4 and 4.5) which is further evidence of the sorption of H4SiO4 on HFO. Similar breakthrough curves for Si were obtained in another SAR pilot in Bangladesh [Rahman et al., 2014] (Chapter 3).

Effect of pH on As sorption

The modeled dissolved As concentrations (total As, As(III) and As(V)) and pH at SAR well A3 (first model cell) during injection, storage, and extraction phases for cycles 1, 5, 10, and 15 are shown in Fig. 4.11. The total As, As(III) and As(V) concentrations decrease with increasing values of pH. pH values are higher than the pH of the native groundwater (6.97) at the beginning of each extraction phase because of the high pH of the injection water. Dissolved As concentrations are low at the beginning of each extraction phase

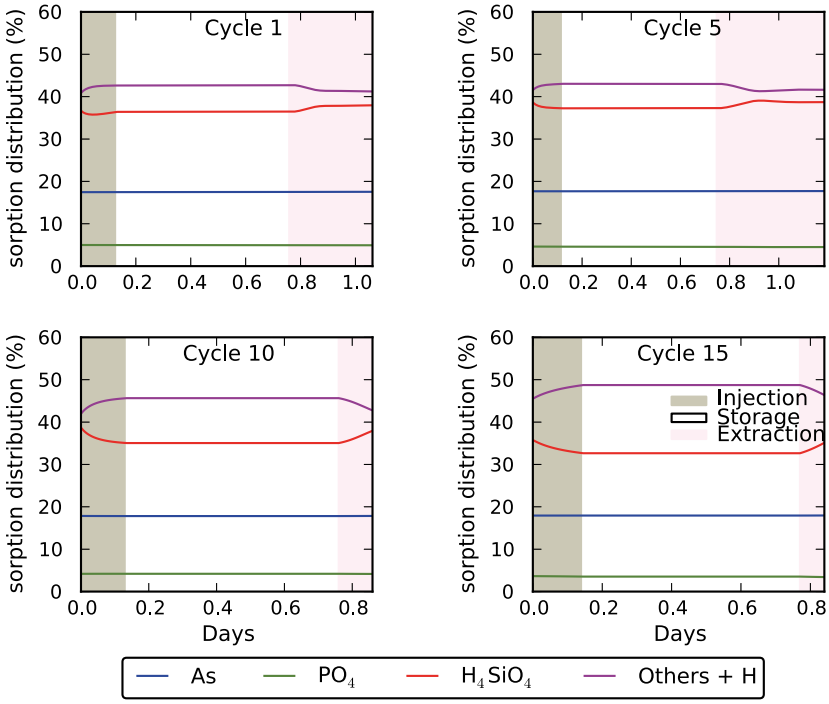

Figure 4.10: Modeled distribution of different surface species on sorption sites of newly formed HFO for cycles 1, 5, 10, and 15 at SAR well A3.

compared to As concentrations of the injection water even when higher levels of As were injected (during the first cycle). Dissolved As concentrations increase with decreasing pH values.

Lower values of As at the beginning of each extraction phase may be related to the higher pH during SAR operation, because arsenic adsorption is pH sensitive [Dixit and Hering, 2003; Kartinen Jr. and Martin, 1995; Stollenwerk et al., 2007] . The mixing of high pH and low As injection water with the neutral pH and high As background water during the injection phase after cycle 1 also plays a role for the low As concentrations during injection, storage and extraction phase at SAR well A3.

The effect of pH on As mobilization from HFO is modeled for the native groundwater composition and is presented in Fig. 4.12. Figure 4.12 clearly illustrates that with higher pH dissolved As concentrations dramatically decrease due to enhanced sorption. The surface complexation reaction equations listed in Table 4.2 suggest that As sorption decreases with higher pH. However, because of much stronger desorption of P at higher pH (Fig. 4.12) the net extent of sorption increases with higher pH over the relevant pH

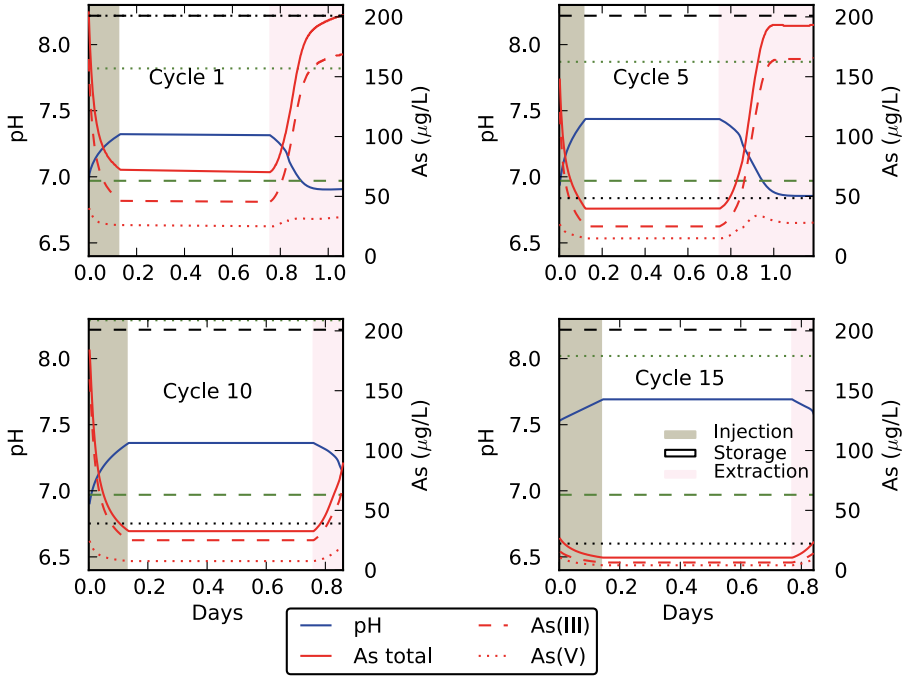

Figure 4.11: Modeled pH (primary *y* axis) and dissolved concentrations of As (secondary *y* axis) at SAR well A3. The solid red lines represents total As, dashed red lines represents As(III) and dotted red lines represents As(V). The dashed and dotted black lines represent background and injection water As concentrations respectively. The dashed and dotted green lines represent background and injection water pH respectively.

range. These results indicate that As sorption to HFO together with the elevated pH of the injection water exert strong control on As levels of the extracted water.

4.4.4. Evaluation of potential impact of HFO precipitates on clogging

After 20 cycles the modeled amount of newly formed HFO at SAR well A3 is ~22 mmol $Fe(OH)_3$/L (Figure 4.7). The newly precipitated HFO after 20 cycles occupies 0.07% of the porosity, assuming a density of 3.0 kg/dm^3 for the precipitate according to Appelo and de Vet [2003]. The portion of the porosity that is occupied by the precipitates is small which indicates that clogging of the aquifer is negligible. This is corroborated by measurements at the study site, where clogging was not observed during the SAR experiments as the rate of infiltration was the same for all cycles performed at the SAR well. Considering a linear increase in the development of HFO with successive cycles, only 4% of the porosity would be occupied if the SAR system was extended for 1000 cycles. These

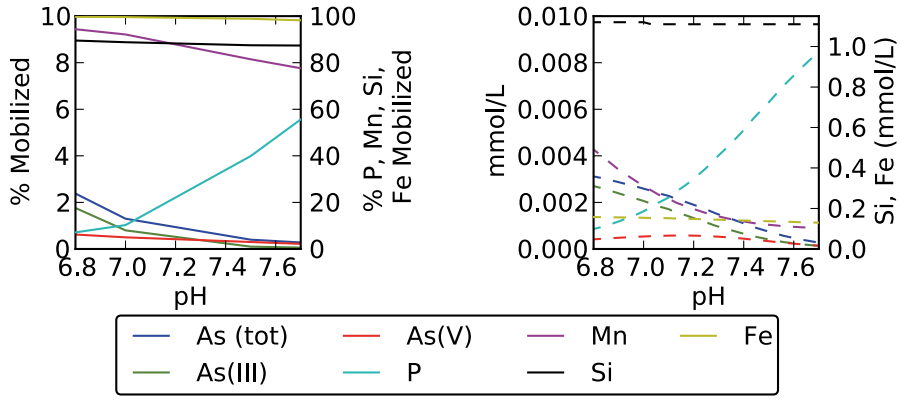

Figure 4.12: Effect of pH on total As, As(III), As(V), P, Mn, Fe, and Si mobilization from HFO (solid line) and corresponding dissolved total As, As(III), As(V), P, Mn, Fe, and Si concentrations (dashed line) due to pH dependent mobilization. Mobilization is defined here as the aqueous concentration over the total (sorbed and aqueous) concentration. Native groundwater composition of SAR well A3 (see Table 2.1) was used to calculate the effect of pH on total As, As(III), As(V), P, Mn, and Si mobilization. Only the relevant pH interval observed during the SAR operation is shown.

calculations indicate that aquifer clogging will not be an issue for SAR systems that run for a longer period of time. Similarly, clogging has not been observed in the subsurface iron removal systems in the Netherlands which have been operating for over 20 years [Meyerhoff, 1996]. Appelo and de Vet [2003] hypothesized that injected water may flow around pores that are closing due to the precipitation of HFO, which may ensure more uniform reactions in space.

4.5. Transferability of the reactive transport model to other areas in Bangladesh

The transferability of the current reactive transport model has been assessed through comparison with two additional SAR experiments referred to as SAR wells A2 and B. Note that the model for SAR well A3 was not calibrated on P, alkalinity, and pH as these were not measured at SAR well A3. These quantities were measured at SAR wells A2 and B, which allows for an independent check of the performance of the model for these quantities.

4.5.1. SAR wells A2 and B

SAR well A2 is located approximately 75 m from SAR well A3 and SAR well B is located in Singair upazila in Manikganj (23.78095E, 90.06831N) district in Bangladesh (Fig. 2.2). The native hydrogeochemistry of all three SAR sites are significantly different from each

other (Table 2.1). The native As concentration at SAR well A2 is about 2 and 5 times higher than at SAR wells A3 and B, respectively. Alkalinity at SAR well A2 is also higher compared to the other SAR wells. The pH is lowest at SAR well B (6.67 compared to 6.95 at SAR well A2). HFO content is higher and the cation exchange capacity is also slightly higher at SAR well B compared to the other SAR wells. Silica levels at all three sites are at the high end but somewhat lower for well B compared to well A3.

The reactive transport model described in the previous is applied with only minor modifications related to the operational aspects of the SAR pilots. The injection volume for SAR well A2 was 0.5 m^3 so that the model length was reduced to 0.43 m. The injection volume for SAR well B was 1 m^3 which corresponds to a model length of 0.6 m. The number of cells for both SAR wells A2 and B were the same as for SAR well A3. For SAR well B, the last volume of extracted water was used for injection rather than the first volume since the first extracted volume contains water with the lowest As concentrations which is better for the consumers. The rate constant for Fe oxidation at SAR well B was adjusted to 1.54 x 10^{12} [L^2 mol^{-2} atm^{-1} s^{-1}] as the native groundwater temperature is 28.9^0 C which is slightly higher than SAR well A3 (Table 2.1). The HFO and goethite contents and cation exchange capacity for SAR well B are also adjusted according to the background values given in Table 2.1.

4.5.2. Model results for SAR wells A2 and B

The observed and modeled concentrations of pH, alkalinity, As, Fe(II), Si, P, Ca, and Mg in the extracted water at SAR wells A2 and B are presented in Figs. 4.13 and 4.14 respectively. The results show that the general trends of the observed values for different parameters are produced reasonably well by the model, except for P for $V/V_i < 1$ at both sites (discussed later); quantification of model fit is discussed in section 6.1.

The model underestimates arsenic removal. The observed and modeled breakthrough curves for As reach a lower plateau (i.e., the more or less constant As levels at higher V/V_i) at $V/V_i > 2$ for both SAR wells A2 and B than the respective background levels 4.13 and 4.14. With successive cycles the observed and modeled level of this plateau declines until it becomes approximately stable. A possible explanation of the successive decline of the plateau level is the progressive increase of the sorption capacity due to the gradual buildup of HFO directly around the well (see Figs. 4.15 and 4.16). A further lowering of the plateau requires the availability of iron in the injection water. This is shown at SAR well A2 where iron levels remained high in the extracted water and the As plateau decreased for many subsequent cycles. Hence, suboptimal subsurface iron removal (SIR) is beneficial for SAR. Note that for SAR well B, cycles 15 and 20 reach a slightly higher plateau level compared to cycle 10. This is likely due to the slow buildup of HFO directly around the well after cycle 5 (Figure 4.16). The ratio between As(III) and

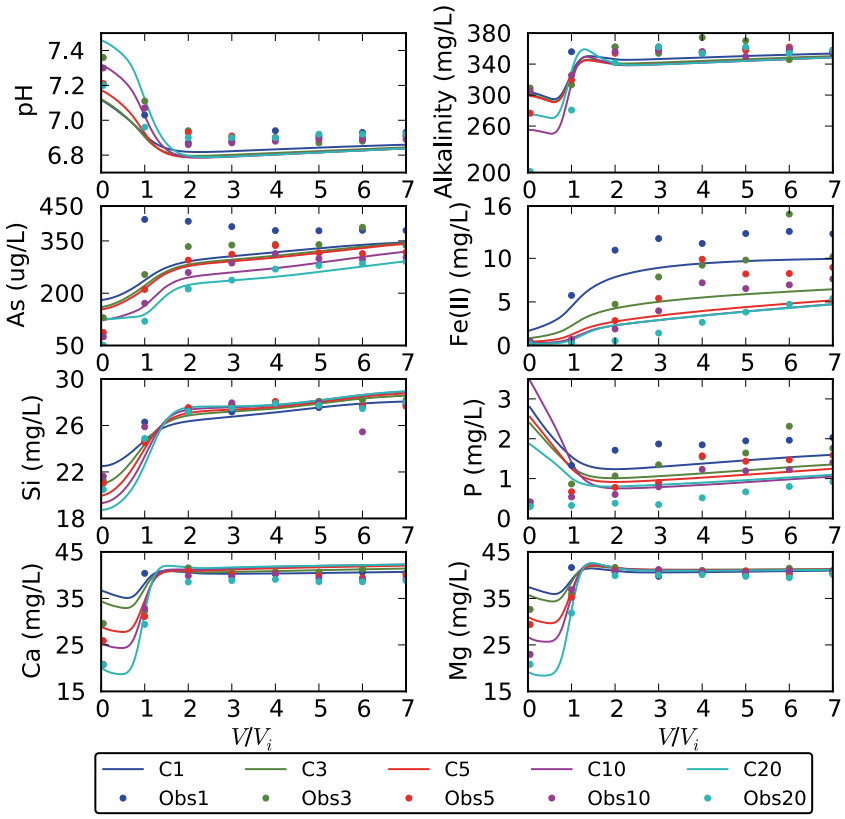

Figure 4.13: Observations and model simulations for various parameters during cycles 1, 3, 5, 10, and 20 for the SAR experiment at SAR well A2. The dots represent the observed values and the solid lines represent the modeled results.

total As of the modeled cycles at SAR wells A2 and B shows that As(III) oxidizes to As(V), which is preferentially removed from the water (as it sorbs less) and thereby As(III) dominates in the end (Fig. 4.17). The overall As sorption increases due to this process. This is an additional explanation for both lower As levels for $V/V_i < 1$ and for the plateau at $V/V_i > 2$ for SAR wells A2 and B. Similar ratios were also obtained for the modeled cycles at SAR well A3 (Fig. 4.17).

The model nicely predicts the gradually increasing iron removal with successive cycles at well A2. At SAR well A2 the modeled iron removal shows a gradual improvement, whereas for the other SAR wells the modeled iron shows near zero concentrations from cycle 3 onward while low Fe(II) concentrations are still observed during the extraction phases of all SAR cycles. As mentioned earlier for SAR well A3, this may be caused by

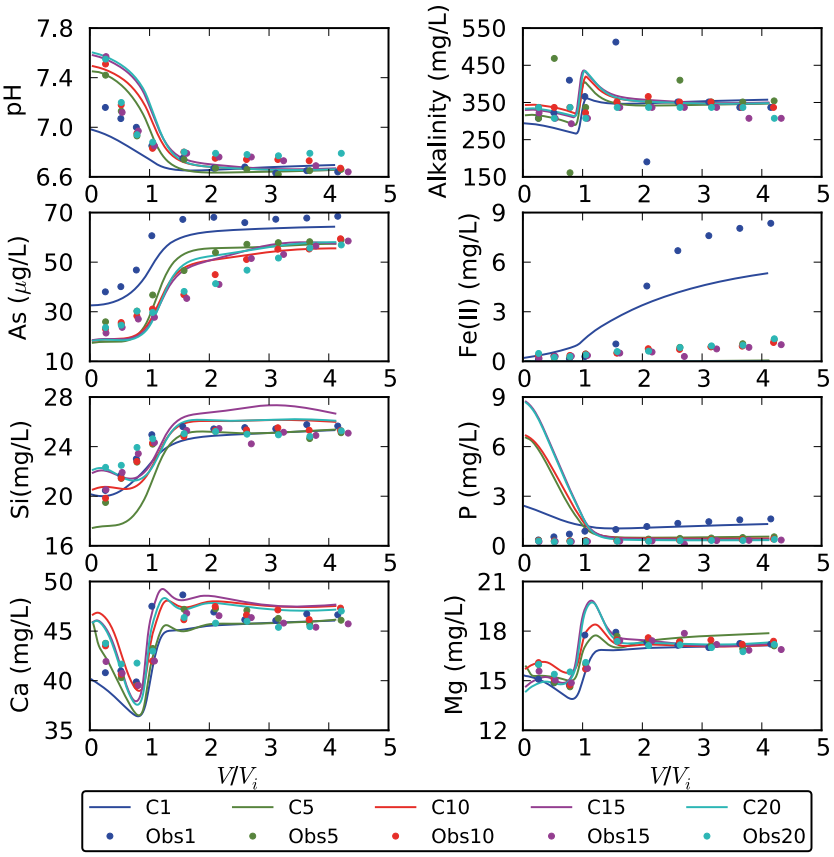

Figure 4.14: Observations and model simulations for various parameters during cycles 1, 5, 10, 15, and 20 for the SAR experiment at SAR well B. The dots represent the observed values and the solid lines represent the modeled results. Modeled results for Fe(II) for subsequent cycles are so small that they are not visible.

the presence of colloidal Fe(III) that passed the 0.45 μm filter, whereas the model assumed all Fe(III) precipitates to HFO. Note that the model nicely predicts the gradually increasing iron removal with successive cycles at well A2. At SAR well A2 the modeled iron removal shows a gradual improvement, whereas for the other SAR wells the modeled iron shows near zero concentrations from cycle 3 onward. This is because at SAR well A2, the background Fe concentration is highest. Also the ratio between the extracted and injected volumes (V/V_i) at SAR well B is 7 whereas at SAR well A3 and B V/V_i is 5 and 4 respectively. At SAR well A2 the extraction volume was $7V_i$ in an attempt to increase the inflow of Fe(II) and subsequent oxidation to provide more sorption sites for As.

The observed and modeled pH starts with high values (as injection water has ele-

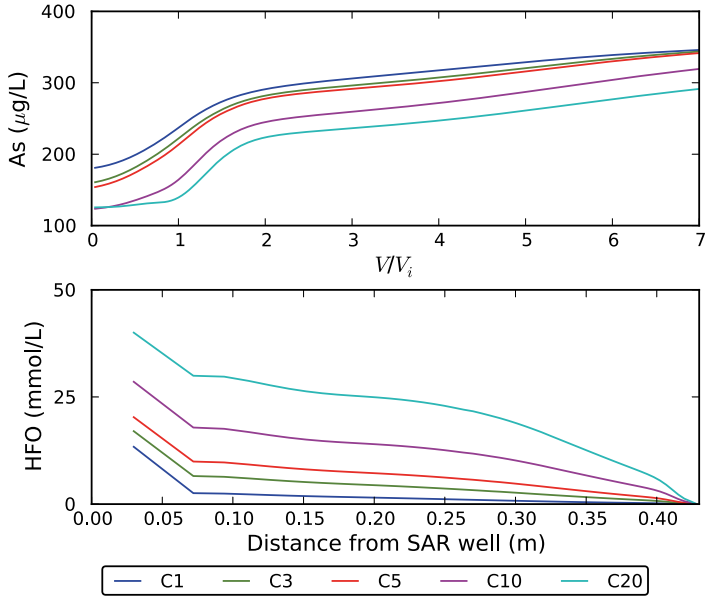

Figure 4.15: Model simulations of As breakthrough during the extraction phases at SAR well A2 and the modeled development of HFO along the flow path at SAR well A2. Results are shown for cycle 1, 3, 5, 10, and 20.

vated pH) and then returns to the background condition for both SAR wells A2 and B; the pH increases with increasing cycle number for $V/V_i < 1$.

The general trend of the observed and modeled alkalinity is similar for both SAR wells A2 and B. The model predicts a slight decrease in alkalinity at the beginning of the extraction till V/Vi ≈1. After V/V_i ≈1 modeled alkalinity starts to increase and eventually returns to the background condition for both SAR wells B and.

The modeled P concentrations in the extracted water at SAR wells A2 and B deviate from the observed P values for V/V_i <1. The observed P breakthrough curves start with a low value and show a gradual increase with increasing extraction, whereas at the beginning of the extraction phase the modeled P concentrations are very high and remain too high till V/V_i ≈1. The high pH of the injection water has clearly lead to P desorption in the model. After V/V_i ≈1, P sorbs again on HFO because lower pH water is extracted. After V/V_i ≈1 the modeled P concentrations plot close to the observed P values (Figs. 4.13 and 4.14). It was not possible to improve the P fit for V/V_i <1 by adjusting the equilibrium constants of the surface complexation reactions within reasonable limits (see Fig. 4.18).

The model fit is very good for Ca and Mg at SAR wells A2 and B considering the kinetic dissolution/precipitation of calcite during SAR operation. However, the simulation

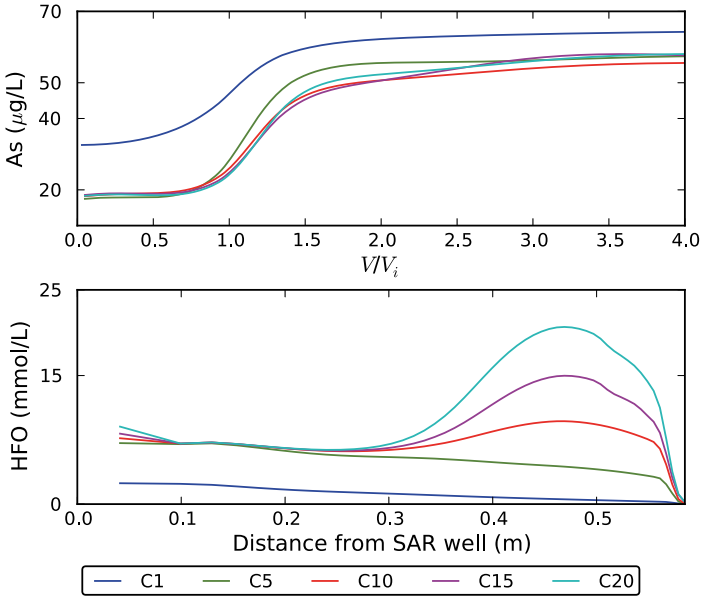

Figure 4.16: Model simulations of As breakthrough during the extraction phases at the well B and the modeled development of HFO along the flow path at SAR well B. Results are shown for cycle 1, 5, 10, 15, and 20.

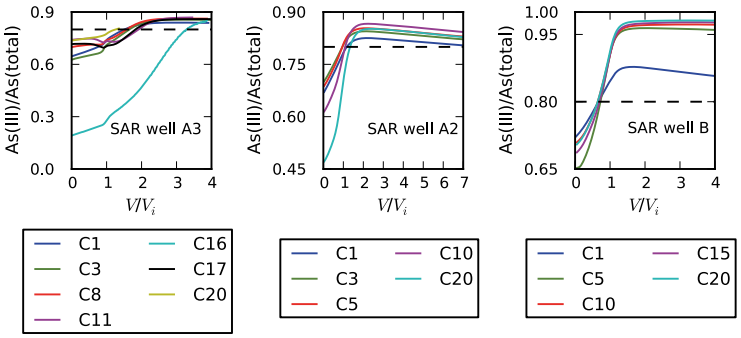

Figure 4.17: Ratio between As(III) and total As during the extraction phases at SAR well A3, A2, and B. Results are shown for cycle 1, 3, 8, 11, 16, 17, and 20 at SAR well A3. Results are shown for cycle 1, 3, 5, 10, and 20 at SAR well A2. Results are shown for cycle 1, 5, 10, 15, and 20 at SAR well B. The black dashed lines represent the initial ratio between As(III) and total As in the Background groundwater.

without the calcite interaction shows negligible change in the model results (Fig. 4.19). This means that the effect of this process is only minor due to the short reaction periods during SAR cycles and could have been excluded from the model.

The model-data comparisons in Figs.4.13 and 4.13 illustrate that the model provides

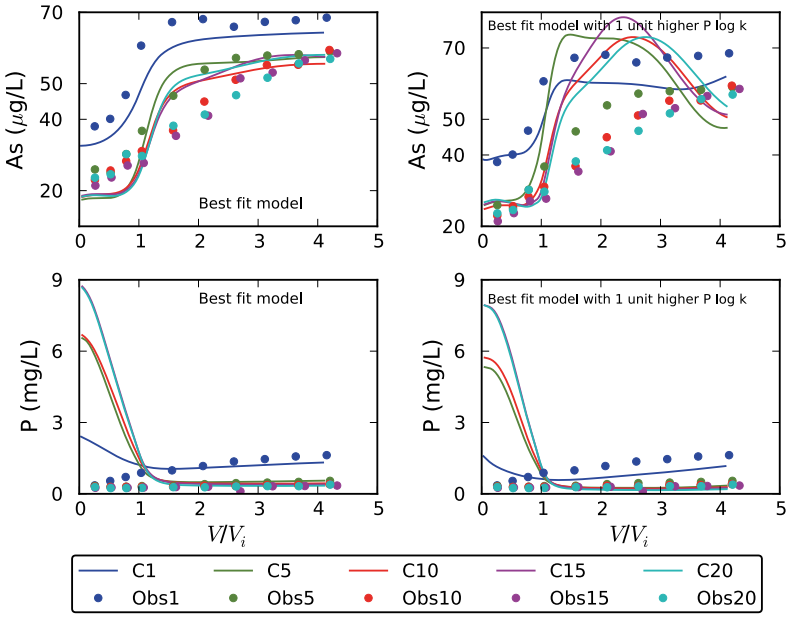

Figure 4.18: Observations and model simulations of As and P breakthrough during the extraction phases of cycles 1, 5, 10, 15, and 20 at SAR well B for best fit model and for best fit model with one unit higher P log k value.

a reasonable representation of the key processes that influence the major ion and redox chemistry during SAR operation and notably the As and Fe removal. The simulation of SAR wells A2 and B based on the model for SAR well A3 indicates that the developed reactive transport model is transferable to other areas of Bangladesh where aquifer sediments have similar chemical and physical properties.

4.6. Model Performance

4.6.1. Goodness of fit

The goodness of fit between modeled and observed data for Alkalinity, pH, As, Fe, Si, and P was evaluated by calculating the root mean squared error percentage (RMSEP) and the coefficient of determination (r^2). The RMSEP is the root mean squared error divided by the observed data range. The RMSEP was calculated as follows:

$$RMSEP = \frac{\sqrt{\sum_{i=1}^{n_{obs}} (Obs_i - Mod_i)^2}}{Obs_{max} - Obs_{min}} \quad (4.8)$$

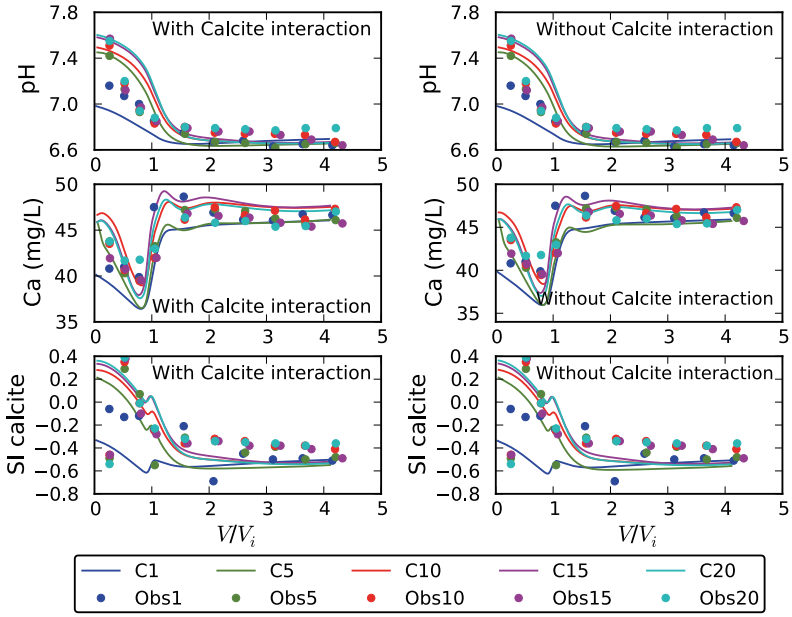

Figure 4.19: Observations and model simulations of different parameters during the extraction phases of cycles 1, 5, 10, 15, and 20 at SAR well B. Results are shown for models with and without calcite interaction.

where Obs_i, and Mod_i are the observed, and modeled values of observation i respectively, and n_{obs} is the number of observations. The coefficient of determination (r^2) was calculated for each individual species following Karlsen et al. (2012)

$$r^2 = 1 - \frac{\sum_{i=1}^{n_{obs}} (Obs_i - Mod_i)^2}{\sum_{i=1}^{n_{obs}} (Obs_i - \overline{Obs})^2} \tag{4.9}$$

where $\overline{Obs}$ is the average of the observations of the specific species. Table 4 summarizes the goodness of fit between modeled and observed data. The RMSEP values in Table 4 shows that model prediction for alkalinity, pH, As, Fe, and Si at all three SAR wells is within 25% for all species. The RMSEP for P at SAR wells A2 and B is very high compared to the other species. The correlation (r^2) between observed and modeled data is larger than 0.5 for most of the species at all three SAR wells. The r^2 for pH at SAR well A2 is lower compared to the other species. The r^2 for alkalinity and Si at SAR well B is low compared to the other species among all SAR wells. The r^2 for P at SAR wells A2 and B is very low compared to other species. The variation in r^2 values for different species

Table 4.3: Statistics of model goodness of fit for SAR wells A3, A2, and B. RMSEP denotes root mean squared error percentage compared to the data range for each parameter.

Parameter	RMSEP(%)			r^2		
	SAR well A3	SAR well A2	SAR well B	SAR well A3	SAR well A2	SAR well B
Alkalinity	N/A	12	17	N/A	0.57	-.44
pH	N/A	22	18	N/A	0.28	0.53
As	20	15	14	0.59	0.65	0.81
Fe	15	19	13	0.62	0.60	0.72
Si	24	14	24	0.33	0.78	0.17
P	N/A	58	148	N/A	-3.31	-38.5

among SAR wells is likely due to the difference in background hydrochemistry. The low r^2 value obtained for alkalinity at SAR well B compared to SAR well A2 is likely due to some outliers in the observed values. The goodness of fit for P at SAR wells A2 and B is poor compared to the other species because the model predicts elevated levels of P for V/Vi ≤ 1, whereas measurements showed decreased P levels for V/Vi ≤ 1 (see Figs. 4.13 and 4.14 and section 4.5.2). The RMSEP and r^2 values are consistent for all species at all three SAR wells except for Si where RMSEP values for SAR wells A3 and B are the same but r^2 at SAR well B is lower than SAR well A3. Most importantly, r^2 values for As and Fe at all three SAR wells were higher than (almost) all other species. The r^2 value for As is even larger at SAR wells A2 and B than at SAR well A3.

4.6.2. Comparison between observed and modeled SAR performance

The performance of SAR systems is defined as the volume of water extracted (V) with As concentrations below the Bangladesh standard (<50 µg/L) divided by the volume of injected water (V_i). The observed SAR performance at SAR wells A3 and B is compared with the corresponding modeled SAR performance at the respective locations (Fig. 4.20). The performance of SAR systems (V/V_i) is defined as the volume of water extracted (V) with As concentrations below the Bangladesh standard (<50 μg/L) as compared to the volume of injected water (V_i). For SAR well A2 both observed and modeled SAR performance is zero for all cycles and was not added to Fig. 4.20. The model was able to reproduce the observed SAR performances reasonably well for both SAR wells A3 and B (Fig. 4.20). The change in SAR performance with successive cycles depends on variations in injection water composition and experimental conditions. The model tends to underestimate SAR performance which is useful from a practical perspective as prognoses are generally conservative estimates. The observed and modeled SAR performance is higher at SAR well B than at SAR well A3 because at SAR well B the background As concentration is about 65% lower than at SAR well A3 (Table 2.1). In practice the model is expected to be useful to give minimum estimates of SAR performance for specific locations and to identify locations where SAR performance may be feasible.

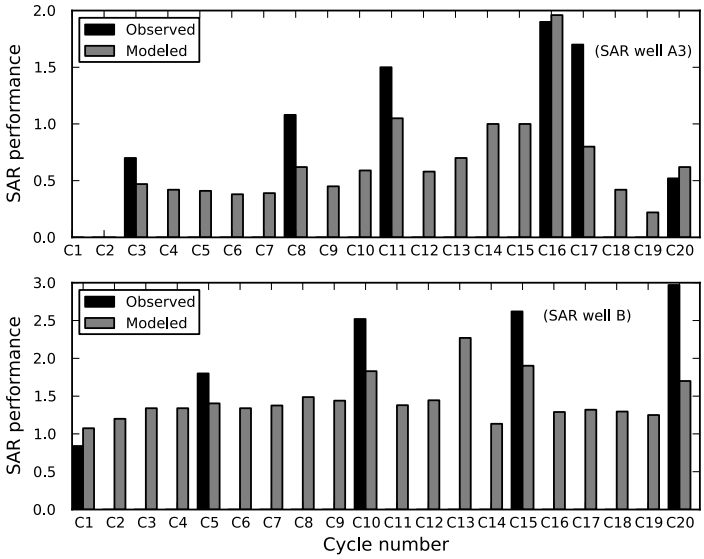

Figure 4.20: Comparison between observed and modeled SAR performances at SAR wells A3 and B.

4.7. CONCLUSIONS

A one-dimensional radially symmetric reactive transport model was developed to model key hydrogeochemical reactions during SAR operation. Oxidation of Fe(II) and As(III) was modeled using kinetic-rate expressions. Cation exchange, precipitation of HFO, and surface complexation, were modeled as equilibrium processes. The model gave reasonable results for measured concentrations of As, Fe(II), Mn(II), Si, Mg, Na, and K in the extracted water at SAR well A3. This indicates that the key processes taking place in the subsurface during SAR operations were modeled correctly by the model. Modeled breakthrough curves of Fe(II), Mn(II), and As indicate that the variations among cycles in subsurface removal depends on the injection water compositions and experimental conditions. High pH and Fe levels in the injection water and multiple injection extraction cycles of an equal volume facilitates As removal during SAR operation. The overall agreement between the observed and modeled results for different experimental conditions indicates that the reactive transport model is applicable to various SAR experimental conditions. The pH of the groundwater in the SAR system during injection, storage, and extraction had significant impact on As sorption in the subsurface. Particularly, the high pH of injection water (as a result of CO_2 degassing during aeration) promoted As sorption. During SAR operation As(III) oxidizes to As(V) which is preferentially removed

from the water and thereby As(III) dominates in the end. These processes increase the overall As sorption. The gradual development of HFO and the increased sorption capacity of precipitated HFO facilitates better As removal during SAR operation. A set of surface complexation reactions and corresponding equilibrium constants was compiled from earlier studies. The chosen set of surface complexation parameters was found to be most suitable in describing observed concentration trends of three SAR systems placed in Holocene reduced aquifer systems in Bangladesh. The results of surface complexation modeling suggest that simultaneous sorption of H_4SiO_2 is an important factor for limiting As removal during SAR operation. The simulated amounts of freshly precipitated HFO are such that aquifer clogging does not seem to be an issue. The model was applied to simulate subsurface As removal at two other SAR sites in Bangladesh resulting in r^2 values for As that were larger than for the original model. The model is able to reproduce the observations reasonably well for most of the parameters discussed in this paper and performed best for As and Fe; As removal was generally underestimated by the model. The model can be used to assess potential SAR performance at other locations in Bangladesh with similar aquifer characteristics based on local hydrogeochemical conditions.

5

Assessment of the potential for subsurface arsenic removal technology in Bangladesh using a reactive transport model

Subsurface Arsenic Removal (SAR) involves injection of aerated groundwater into an anoxic aquifer, where oxygen in the injected water reacts with iron in the groundwater to form hydrous ferric oxide (HFO). Groundwater with lower arsenic (As) can be extracted because As sorbs onto the HFO. The performance of a SAR system is defined here as the volume of water that can be extracted with As concentrations below the Bangladesh standard (<50 µg/L) relative to the volume of injected water. A previously developed reactive transport model was coupled to a new aeration model using a Python script to quantify the sensitivity of SAR performance to As, Fe, P, Si, pH, alkalinity, HFO, and CEC. The SAR performances at 200 locations in Bangladesh is calculated with the same model and a preliminary map of suitable locations for SAR application is generated. SAR performance in Bangladesh ranges from 0 to above 4. The results suggest that SAR performance is lower for higher background levels of As, P, and Si. SAR performance is higher for higher background levels of Fe, alkalinity, CEC, HFO (except for the highest background HFO), and molar ratio of Fe over As. The effect of background pH on SAR performance varies. SAR performance is highest for the base case model background pH (6.85) and lowest for the maximum background pH (7.66). For the minimum background pH value (5.85), SAR performance is slightly lower compared to the base case model background pH. The nationwide SAR performance calculations show that SAR technology may be useful for locations with background groundwater As concentrations ranging from 50 to 150 µg/L. 27.5% of the studied locations resulted in SAR performance above 1, which indicates that the potential for SAR application in Bangladesh is substantial. The results also indicate that a significant amount of As can be removed from groundwater with very high levels of As using SAR even if the targeted drinking water standard cannot be achieved. SAR performance drops after peak performance has been reached. The results of this modeling study show that it takes on average more than 300 cycles for performance to drop below 50% of peak performance for most of the locations in Bangladesh when peak SAR performance is above 0.5.

5.1. INTRODUCTION

Arsenic contaminated shallow groundwater is a major public health and environmental concern in many parts of the world especially when the groundwater is used as a source of drinking water [Nordstrom, 2002; Nriagu et al., 2007]. Subsurface Arsenic Removal (SAR) can be a cost-effective way to provide safe drinking water in rural areas, provided that the geochemical characteristics of the aquifer are suitable for SAR. SAR experiments were carried out at several locations in Bangladesh and a reactive transport model was developed to determine the dominant reactions and parameters that influence As removal in the subsurface (see Chapters 3 and 4).

The dominant mechanisms limiting As removal during SAR operation at the study sites were:

1 The effect of pH (see Chapter 4; section 4.4.3)

2 Oxidation of As(III) to As(V) (see Chapter 4; section 4.4.3)

3 Sorption capacity increase due to gradual development of HFO (see Chapter 4; section 4.5.2)

4 Simultaneous sorption of H_4SiO_4 along with As and other elements. (see Chapter 4; section 4.4.3)

The results of the reactive transport model (RTM) discussed in Chapter 4 demonstrated that the model was able to asses SAR performance for a given set of hydrogeochemical parameters at three different sites.

An important remaining question is whether SAR can be a potential As mitigation option for Bangladesh as the spatial variability of Bangladesh groundwater quality is very high [BGS and DPHE, 2001]. To answer this question, it is explored how the performance of SAR systems varies under different hydrogeochemical settings. The SAR systems are simulated with the previously developed RTMs and performance P_s is defined as:

$$P_s = \left(\frac{V}{V_i}\right) \tag{5.1}$$

where V is the volume of extracted water meeting the drinking water standard and V_i is the volume of injected water. The Bangladesh drinking water standard of 50 μg/L for As is used to calculate P_s. Note that SAR performance in Chapter 3 is expressed in terms of the extraction efficiency (Q_E) (see Equation 3.1). The volume of injected water is subtracted in the definition of Q_E because the first extracted volume of water with low As was injected into the aquifer during the next cycle, so what mattered was how much additional low As water could be withdrawn during the extraction phase. In this chapter,

the volume of injected water was not subtracted in the definition of P_s because the last extracted volume of water (with higher As) was injected during the next cycle.

The objectives of this chapter are:

1. To extend the RTM developed in Chapter 4 with a separate model to simulate the aeration phase resulting in the composition of the injection water.
2. To quantify the potential SAR performance under different hydrogeochemical settings in Bangladesh with a RTM.
3. To quantify the effect of key water quality parameters on SAR performance.
4. To determine the spatial variability of SAR performance across Bangladesh by developing a preliminary map of potential SAR application.

5.2. Modification of RTM to Simulate Injection Water Composition

SAR operation for this chapter was simulated with the RTM as described in Rahman et al. [2015] (Chapter 4) with one important modification. In Chapter 4, measured values of different water quality parameters were used for the injection water composition in the model. In this Chapter the composition of injection water is simulated using a separate PHREEQC model to enable prediction based on background groundwater composition only. In this section, the process of computing the injection water composition is described and results of the modified RTM are compared to results of the RTM of Chapter 4 (with measured injection water composition).

5.2.1. Development of Python script to couple the PHREEQC aeration model and the PHREEQC RTM

The simulations of SAR operation, aeration, and calculation of injection water composition were carried out with a Python script coupled to PHREEQC version 3.0. The RTM discussed in Chapter 4 and a new PHREEQC model to simulate aeration and injection water composition were coupled using the Python script. The new PHREEQC model used to simulate aeration and injection water composition is referred to as the aeration model. Different steps of the Python script that runs the aeration model and the RTM is presented in Fig. 5.1 and discussed in the following. The Python script first generates an input file for the aeration model for the first SAR cycle based on the background groundwater composition and then runs the aeration model to calculate the injection water composition. The Python script then uses the calculated injection water composition and writes input for the RTM to simulate one SAR cycle. The input for the RTM includes

the injection water composition, the background hydrogeochemical settings, the background conditions and definition of the flow path, the rates of the kinetic reactions, and the transport steps. The simulated injection volume is 5 m^3 and the simulated extraction volume is 20 m^3. Note, that the last 5 m^3 of the extracted volume was used for injection after the first cycle onward. The RTM is run by the script to generate the output for the SAR performance calculation and the input file for the aeration model for the next SAR cycle. The script performs a maximum of 500 cycles but automatically stops when the SAR performance reduces to 50% of the peak performance. The script reads the model output after each injection and extraction phase using the new DUMP and INCLUDE$ functions introduced in PHREEQC v.3.0.

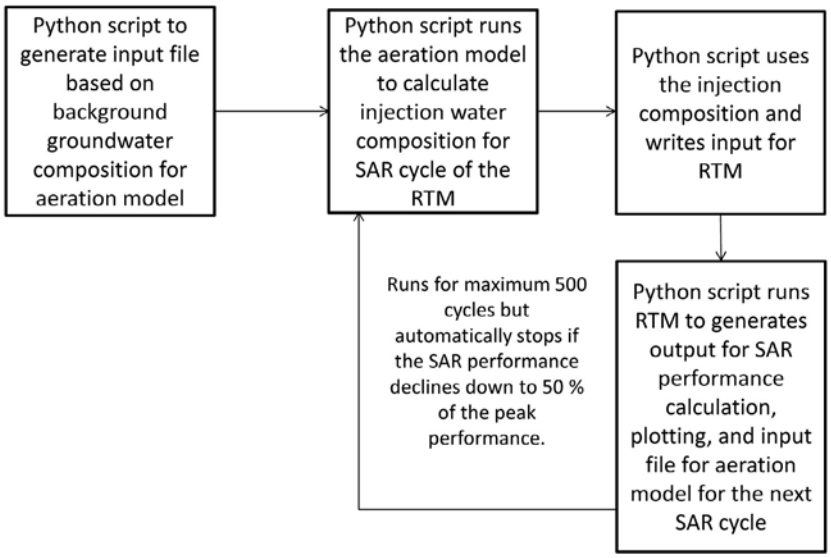

Figure 5.1: Flow chart illustrating the coupling between the Python script and the PHREEQC models.

5.2.2. Simulation of aeration and injection water composition

For the first cycle, the background groundwater composition was used to simulate aeration and subsequent injection water composition (solution 0). During aeration, kinetically-controlled oxidation reactions of Fe(II) to Fe(III), and of As(III) to As(V) were simulated as described in Rahman et al. [2015] (Chapter 4). The precipitation of iron oxide and thereby removal of Fe(III) from the aqueous phase during aeration was not simulated since the iron flocks remained in the water as suspended matter due to the physical mixing induced by aeration. The formed Fe(III) was assumed to be injected into the aquifer and the actual precipitation reaction (to form $Fe(OH)_3$) was allowed to take place there.

Note that formation of iron hydroxide during aeration of water decreases pH (see Equation 3.2). Therefore, the simulated pH values in the injection water may exceed the observed values. This effect can only be seen during the first few cycles as ferrous iron was only present in relevant concentrations during those first cycles. The CO_2 in the groundwater is stripped during the aeration process in the tank, which increases the pH of the injection water as the following equation:

$$H^+ + HCO_3^- \rightarrow H_2O + CO_2(g) \tag{5.2}$$

The aeration and CO_2 degassing processes were simulated as equilibrium processes, i.e., it was assumed that the water in the tank was at complete oxygenated conditions from the start of the aeration process. During aeration the water in the tank was therefore equilibrated with atmospheric O_2. CO_2 requires a longer aeration/stripping time to achieve atmospheric equilibrium due to its higher solubility compared to O_2. Clearly, CO_2 did not reach saturation with the atmosphere within the period of aeration/stripping (Fig. 5.2). Therefore, during aeration the water in the tank was not equilibrated with atmospheric but higher CO_2 pressure. The log pCO_2 levels of the injection water for all observed cycles of experiment SAR well B of Chapter 4 were calculated with PHREEQC (see Fig. 5.2). The simulation of aeration process not only saturated the water with oxygen and oxidized most of the reduced compounds, but also induced degassing of CO_2 from the water, which increased the pH of the injection water. The calculated CO_2 level in the injection water did not drop for the cycles where the pH level was high (Figs. 5.2a and 5.3a). This could be due to some uncertainties in the alkalinity measurements. The accuracy of the alkalinity measurements was ±10 mg/L and this translates in uncertainty of calculated dissolved CO_2 levels.

The observed values at SAR well B show that pCO_2 is initially high but after a few cycles fluctuates around an average value (Fig. 5.2b). The minimum, maximum, and average log pCO_2 levels for all observed injection water compositions for SAR well B were calculated. These values were used as target CO_2 partial pressures to calculate the injection water compositions for SAR simulation. Injection water composition for each cycle was also calculated with pCO_2 levels calculated from the observed injection water composition (referred to as the calculated pCO_2 value). The pCO_2 value is difficult to predict or simulate. So, four different pCO_2 values were considered to calculate the composition of injection water for SAR simulation. The results obtained with these four pCO_2 values were compared with the measured injection water composition to determine the best fit model parameters for further calculations (see the following sections). The time for aeration was not always constant during experiment SAR well B of Chapter 4. Notably, aeration times for monitored cycles were much longer compared to the

other cycles in order to ensure thorough aeration of the water in the tank. On average the aeration time was around 2 hours for general cycles and around 4 hours for monitored cycles. Therefore, two hours of aeration for general cycles and 4 hours for monitored cycles were simulated before injection into the aquifer. Aeration time for the simulations of SAR performance calculations was also 4 hours. The calculated injection water composition was then used. The average composition of the last 5 m^3 of the extracted water from each cycle was used to simulate the aeration and calculate injection water composition for the next cycle. Note that the simulated extraction volume for each cycle is 20 m^3.

5.2.3. COMPARISON OF SIMULATED AND MEASURED RESULTS

Injection water composition for the four different pCO_2 values were compared with the measured values of water quality parameters (Fig. 5.3) for SAR well B of Chapter 4. For comparison, the simulations were using the same approach as in SAR well B in Chapter 4. The CO_2 equilibrium constant for the green dots was -1.61 (maximum value), the equilibrium constant for the blue dots was -3.28 (minimum value), the equilibrium constant for the magenta dots was -2.61 (average value), and pCO_2 values calculated from the observed injection water composition was used for the cyan dots (see Fig. 5.3). The results show that there are large discrepancies between measured and simulated values for pH, HCO_3, and As. The simulated pH values for pCO_2 = -3.28 indicate that CO_2 degassing was higher compared to the degassing during the field experiment whereas the degassing was lowest with pCO_2 = -1.61. The pH value of the observed extraction cycles (5, 10, 15, and 20) are considerably higher compared to the other cycles as aeration time for those cycles were much higher than the others. The pH value for the calculated pCO_2 value compares well to the measured pH values for all cycles whereas the pH value for the average pCO_2 value is more or less comparable with measured pH values for most of the cycles (Fig. 5.3). Overall, the average log pCO_2 level gave the most reasonable results for all four quantities and will be used on the remainder of this chapter.

There is a discrepancy between the observed and modeled concentrations of As in the injection water (Fig.5.3). The measured concentrations of As were used in the model discussed in Chapter 4. The concentrations of As were measured in filtered samples and therefore the sorbed concentrations of As to the suspended Fe-oxides in the injection water were not measured. The model discussed in this chapter does not simulate the formation of suspended Fe-oxide but keeps all elements in solution. The model therefore predicts higher dissolved concentrations in the injection water than observed.

The measured and modeled levels of different parameters (pH, alkalinity, As, Fe, Si, P, Ca, and Mg) in the extracted water are compared for the model of Chapter 4 (solid lines Fig. 5.4) and the model used in this chapter (dotted lines Fig. 5.4). The horizontal axis

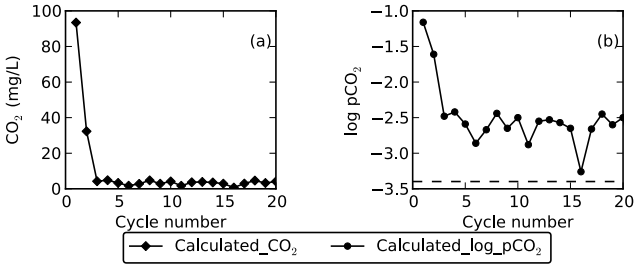

Figure 5.2: Calculated dissolved CO_2 concentrations (a) and calculated log pCO_2 levels (b) from observations at SAR well B (see Chapter 4 for description about SAR well B). The dashed line in panel b represents the atmospheric log pCO_2 value.

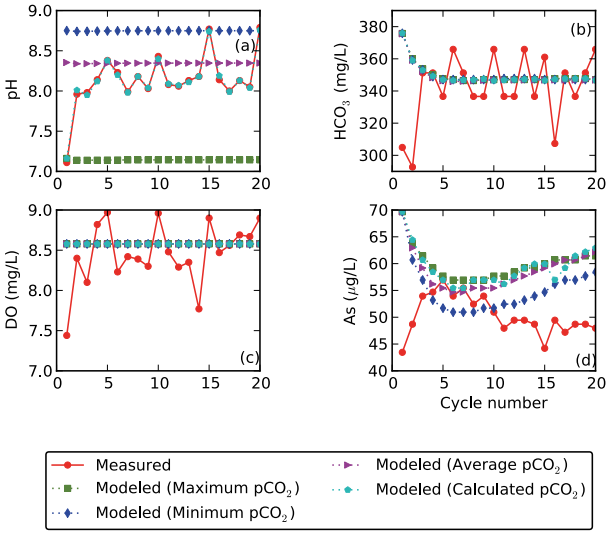

Figure 5.3: Comparison between measured and simulated injection water composition for four different log pCO2 values at SAR well B.

represents the extracted volume (V) normalized by the injected volume (V_i). The model used in this chapter compares reasonably well with the model of Chapter 4.

The observed SAR performance at SAR well B is compared with the SAR performance calculated with the RTM of Chapter 4 and this chapter (based on the average log pCO_2 value) in Fig. 5.5. The results show that SAR performance of the modified RTM with average log pCO_2 value is similar to the SAR performance simulated in Chapter 4 (Fig. 5.5). The SAR performance for Cycles 10, 15, and 20 calculated by the RTM of Chapter 4 are higher than the SAR performance for the same cycles calculated by the RTM discussed in this chapter. This discrepancy is due to longer aeration times and thus lower

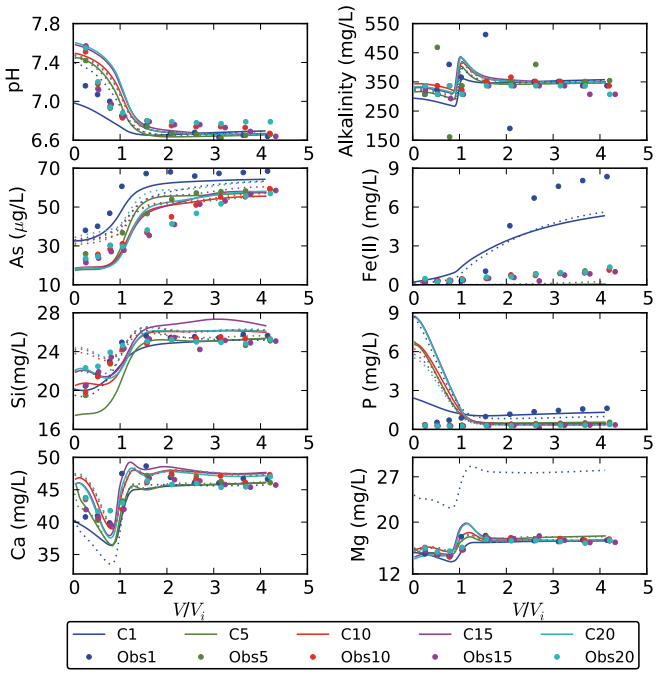

Figure 5.4: Observations and model (Chapter 4 and 5) simulations for various parameters during cycles 1, 5, 10, 15, and 20 for the SAR experiment at SAR well B. The dots represent the observed values and the solid lines represent the results of Chapter 4 model. The dotted lines represent results of modified RTM of this chapter with average log pCO_2 levels as the equilibrium constant for CO_2.

pCO_2 values for the RTM of Chapter 4 than the average log pCO_2 value used in the model used in this chapter. Note that the simulated performance is smaller than the measured performance (as in Chapter 4) so that assessment of the performance is conservative.

5.3. Hydrogeochemical Data Requirement for SAR Simulation

The key hydrogeochemical parameters required for SAR RTM simulation include: background groundwater pH, alkalinity of the background groundwater, background concentration of total As, As speciation (As(III) and As(V)) of background groundwater, background concentrations of Fe^{2+}, PO_4, and Si, HFO content, and cation exchange capacity (CEC). Other minor hydrogeochemical parameters (which have negligible effect on SAR performance) include: background concentrations of Ca, Mg, Na, K, Mn, SO_4, and Cl, Goethite content, soil organic matter (SOM) content, $CaCO_3$ content, and $FeCO_3$ content. All parameters are summarized in Table 5.1, including the literature source used

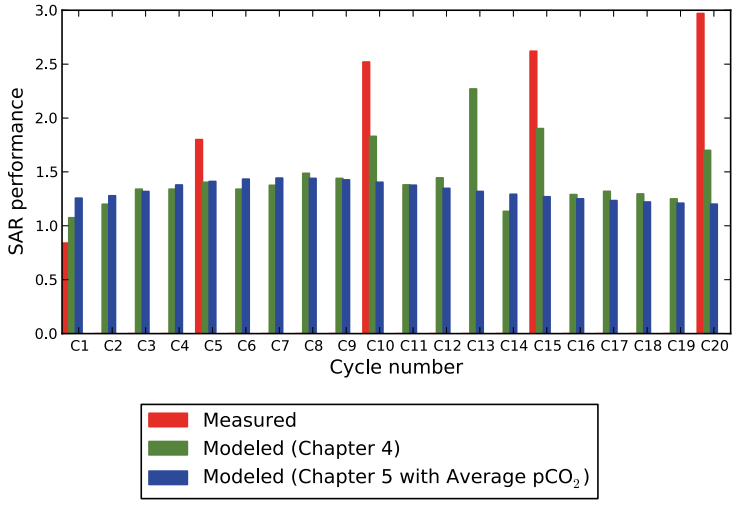

Figure 5.5: Comparison between observed and simulated SAR performances (Chapter 4 and 5). The red bars represent the observed SAR performances. The green bars represent the SAR performances calculated with Chapter 4 model. The blue bars represent SAR performance calculated with Chapter 5 model for simulation with injection water composition calculated with the average of observed log pCO_2 values as the equilibrium constant for CO_2.

for their values (to be discussed in the following).

5.3.1. Databases used for hydrochemical parameters

Arsenic in groundwater along with 19 other parameters were measured during a hydrogeochemical survey performed by the British Geological Survey (BGS) and Department of Public Health and Engineering (DPHE) [BGS and DPHE, 2001]. This data set is referred to as the BGS/DPHE data set. The BGS/DPHE data set consists of 3,354 wells from 433 of the 496 upazilas (sub districts) with coordinates of the wells. The well locations were selected to have an even spatial coverage with a sampling density of 1 per 37 km^2. The BGS/DPHE data set include 1884 location with As concentration less than 10 μg/L, 1470 locations with As concentration greater than 10 μg/L, and, 876 locations with As concentration greater than 50 μg/L. This is the only data set that provides hydrochemical information for the entire country of Bangladesh. However, the BGS/DPHE data set does not include information on pH, alkalinity, and Cl. The BGS and DPHE [2001] database includes a separate data set generated by the Bangladesh Water Development Board (BWDB) which is referred to as the BWDB data set. The BWDB data set includes alkalinity and Cl information at 113 locations across Bangladesh but only 16 of those locations have As concentrations larger than the Bangladesh guideline. Therefore, 184

Table 5.1: Hydrogeochemical parameters required for SAR simulation and corresponding sources.

Key Hydrogeochemical Parameters	Source
pH	[Aziz Hasan et al., 2009]
Alkalinity	[Aziz Hasan et al., 2009]
As(Total)	[BGS and DPHE, 2001]
As(III)	80% of the total As [Rahman et al., 2015]
As(V)	20% of the total As [Rahman et al., 2015]
Fe	[BGS and DPHE, 2001]
P	[BGS and DPHE, 2001]
Si	[BGS and DPHE, 2001]
HFO	0.71 mol/L [Rahman et al., 2015]
CEC	0.095 mol/L [Rahman et al., 2015]
Other Hydrogeochemical Parameters	
Ca	[BGS and DPHE, 2001]
Mg	[BGS and DPHE, 2001]
Na	[BGS and DPHE, 2001]
K	[BGS and DPHE, 2001]
Mn	[BGS and DPHE, 2001]
SO4	[BGS and DPHE, 2001]
Goethite	3.2 mol/L [Rahman et al., 2015]
SOM	N/A
$CaCO_3$	0.39 mol/L [Rahman et al., 2015]
$FeCO_3$	N/A

Note: Chapter 4 is based on Rahman et al. [2015]

locations with As concentration greater than 50 μg/L from the BGS/DPHE data set (see section 5.5 for details) and these 16 locations from the BWDB data set were used for the nationwide SAR performance calculations in this chapter.

5.3.2. Parameter values taken from other databases

Nationwide information on pH, alkalinity, and arsenic speciation is not available for Bangladesh. The background speciation of As for all simulations of this study was assumed to contain 80% As(III) and 20% As(V), similar to the speciation reported from their study sites by Rahman et al. [2014] (Chapter 3). Similar results on As speciation were also reported by Freitas et al. [2014] and Van Halem et al. [2010a]. The values of pH and alkalinity used for this study are 6.85 and 231.8 (mg/L), respectively, which are the mean values published by Aziz Hasan et al. [2009]. The data set published by Aziz Hasan et al. [2009] consists of 160 wells from six upazilas, namely Daudkandi, Chandina, Muradnagar, Debidwar, Burichang, and Comilla Sadar of Comilla district, covering an area of approximately 1500 km^2 with locations of wells selected to have even spatial coverage

with a sampling density of 1 per 10 km^2. This region is one of the most hydrogeochemically diverse areas of Bangladesh [Aziz Hasan et al., 2009]. The region includes severely As affected upazilas where 60–90% of the domestic wells are pumping water with As above the Bangladesh guideline [BGS and DPHE, 2001]. This region also includes intermediate to low As affected upazilas such as Burichang and Comilla Sadar. None of the locations from this data set were used for SAR simulation in this chapter because two SAR wells from the same area namely SAR well A2 and A3 were simulated in Chapter 4. Spatial geochemical data are not available for Bangladesh. Only a few data points on HFO content are available for Bangladesh [Stollenwerk et al., 2007; von Brömssen et al., 2008]. The measured values reported in Chapter 4 for HFO (0.71 mol/L) and $CaCO_3$ (0.39 mol/L) content and the calculated value in Chapter 4 for CEC (0.095 mol/L) were used for all simulations in this chapter.

5.4. Sensitivity Analysis

5.4.1. Sensitivity of SAR Performance to Key Hydrogeochemical Parameters

A sensitivity analysis was performed in order to determine the effect of variations in background levels of As, Fe, P, Si, pH, alkalinity, HFO, and CEC on SAR performance. The above parameters were identified as key controlling parameters for As removal in Chapter 4. The PHREEQC model discussed in Chapter 4 was used with the modification discussed in Sections 5.2.1 to 5.2.3 to develop a base case model. The median values of the locations with As concentrations higher than 10 μg/L from the BGS/DPHE data set were used as background groundwater composition for the base case model. Note that the dissolved oxygen concentration was assumed as 0 mg/L in the groundwater since the shallow Holocene aquifers in Bangladesh are commonly found to be anoxic[Ravenscroft et al., 2009]. The base case model parameters are presented in Table 5.2.

The levels of As, Fe, P, and Si were varied separately using the 5, 10, 25, 75, 90, 95th percentiles of the measured values of the locations with As concentration higher than 10 μg/L from the BGS/DPHE data set (Table 5.3). The data distribution and background concentrations of As, Fe, P, and Si are shown using a cumulative distribution function in Fig. 5.6. This graph plots the proportion of samples which are equal to or less than a given concentration. The curve rises from 0% at the minimum concentration to 100% at the maximum value measured in the sample set. The number of log-cycles on the horizontal axes of the plots in Fig. 5.6 indicate that the concentrations of the parameters are highly variable. The graphs indicate the 10, 25, 50, 75, and 90th percentiles with dotted vertical lines. The median values of other hydrochemical parameters used in the sensitivity analysis are presented in Table 5.4. Only one parameter was varied at

Table 5.2: Hydrogeochemical parameters used for the base case model.

Parameter	Value
As(total) (μg/L)	68.6
As(III) (μg/L)	54.8
As(V) (μg/L)	13.7
Fe (mg/L)	3.8
P (mg/L)	0.90
Si (mg/L)	19.5
Ca (mg/L)	49.55
Mg (mg/L)	23.3
Na (mg/L)	30.4
K (mg/L)	4.3
Mn (mg/L)	0.31
SO_4 (mg/L)	0.5
Alkalinity (mg/L)	231.8
pH	6.85
O	0
HFO (mol/L)	0.71
CEC (eq/L)	0.095

a time while all other parameters of the model were kept at the value of the base case model. This approach is similar as the approach followed by Van Breukelen and Rolle [2012]. Six PHREEQC models were run for each parameters to quantify its effect on SAR performance. In total, 25 PHREEQC models, including the base case model, were run to quantify the effect of As, Fe, P, and Si on SAR performance.

Sensitivity analysis was also performed for different background levels of HFO, CEC, pH, and alkalinity but not according to the Bangladesh statistical distribution since nationwide data for these parameters are not available. The same base case model was used. The HFO and CEC values were varied by using 0.25, 0.5, 2.0, and 4.0 times the background value of the base case model. The background pH and alkalinity levels were varied by taking the maximum and minimum pH (maximum and minimum pH values are 7.66 and 5.85, respectively) and alkalinity values (maximum and minimum alkalinity values are 716.14 and 58.6 mg/L, respectively) from Aziz Hasan et al. [2009]. The data distribution and background concentrations of pH and alkalinity used for sensitivity analysis are presented in Fig. 5.7.

Peak SAR performance was calculated for each model using the same Python script used for SAR simulation based on the highest extracted volume of water with As concentration below 50 μg/L.

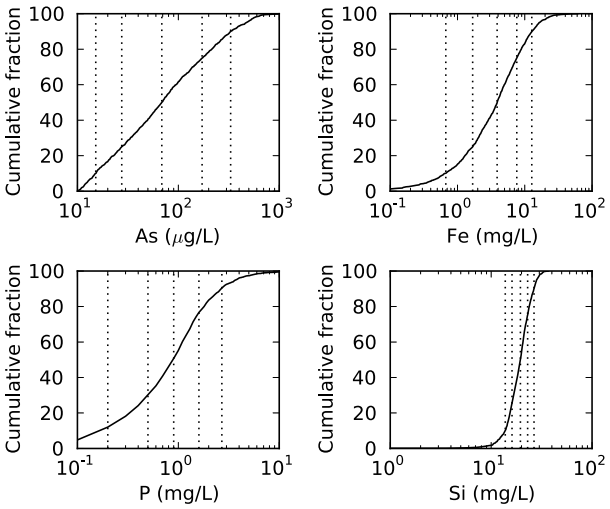

Figure 5.6: Relative cumulative fraction of As, Fe, P, and Si. The vertical dotted lines represent the concentrations of the 10, 25, 50, 75, 90th percentiles (from left to right in each subplot) n = 1470.

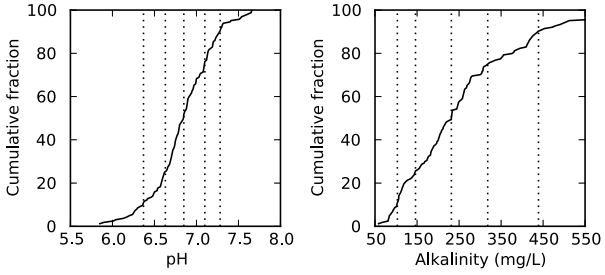

Figure 5.7: Relative cumulative fraction of pH and alkalinity reported by Aziz Hasan et al. [2009]. The vertical dotted lines represent the concentrations of the 10, 25, 50, 75, 90th percentiles (from left to right in each subplot). n = 160

5.4.2. Effect of Key Hydrochemical Parameters on SAR performance

The effect of different background levels of As, Fe, P, Si, pH, alkalinity, HFO, and CEC on peak SAR performance is presented in Fig. 5.8. Note that SAR performance increases to peak level with successive cycles due to gradual buildup of HFO acting as sorbent for As. SAR performance starts to decline after reaching the peak due to pH buffering by HFO in the subsurface, which lowers the pH of the injection water and thereby decreases the potential for As sorption onto HFO. It is important to mention that for different parameter, a different number of cycles was required to reach peak SAR performance (see Table 5.5).

Table 5.3: Percentiles values of different water quality parameters [BGS and DPHE, 2001] used for sensitivity analysis.

Parameter	percentile						
	5^{th}	10^{th}	25^{th}	Median	75^{th}	90^{th}	95^{th}
As(total) (μg/L)	12.6	15.2	27.5	68.6	172.0	330.0	471.5
As(III) (μg/L)	10.1	12.2	22.0	54.8	137.6	264.0	377.2
As(V) (μg/L)	2.5	3.0	5.5	13.7	34.4	66.0	94.3
Fe (mg/L)	0.4	0.7	1.6	3.8	7.6	12.7	16.4
P (mg/L)	0.20	0.20	0.50	0.90	1.60	2.70	3.76
Si (mg/L)	11.9	13.8	16.1	19.5	23.0	26.6	28.2

Table 5.4: Median value of other water quality parameters [BGS and DPHE, 2001] used for sensitivity analysis.

Parameter	Median (mg/L)
Ca	49.5
Mg	23.3
Na	30.4
K	4.3
Mn	0.3
SO_4	0.5

SAR performance decreases with increasing background levels of As. Note that groundwater with background levels of As below 50 μg/L (5, 10, and 25th percentile) will have SAR performance of infinity at base case as As will never exceed the standard (50 μg/L) considered here for SAR performance calculation. Therefore, the group just above the standard (50th percentile) of course has the highest performance at base case. The 75^{th}, 90^{th}, and 95^{th} percentile of As resulted in SAR performance of zero, which means that As levels never drop below 50 μg/L at base case (Fig. 5.8a). These results indicate that SAR will not work when background groundwater As level is above the 75^{th} percentile and all other parameters are equal to the base case. The relationship between background groundwater As levels and SAR performance is discussed in details later in this chapter.

SAR performance is fairly constant for increasing levels of background P and Si till the median value and then start to decrease with increasing background levels of P and Si. SAR performance is fairly constant for increasing levels of background Fe till the median value and then start to increase with increasing background levels of Fe (Fig. 5.8a). SAR performance is higher for higher background levels of alkalinity (Fig. 5.8b) and CEC (Fig. 5.8c). The effect of background groundwater pH on SAR performance varies. SAR performance is highest for the background pH used in the base case model and lowest for the maximum background pH. For the minimum background pH value, SAR per-

Table 5.5: Cycles required to reach peak SAR performance for various values of different water quality parameters [BGS and DPHE, 2001]. Cycle numbers for 5, 10, and 25 percentiles values of As were not calculated as background As levels were below the Bangladesh guideline. Cycle number for 75, 90, 95 percentile values of As and for maximum pH value was not calculated as SAR performance was always 0.

Parameter	Cycles to reach peak P_S						
	5^{th}	10^{th}	25^{th}	Median	75^{th}	90^{th}	95^{th}
As	-	-	-	7	-	-	-
Fe	4	4	5	7	9	200	20
P	14	14	8	7	6	3	3
Si	7	5	6	7	8	8	9
	Min	Base model	Max				
pH	20	7	-				
Alkalinity	2	7	5				
	0.25X	0.5X	Base model	2X	4X		
HFO	6	7	7	10	8		
CEC	7	7	7	9	8		

formance is slightly lower compared to the background pH value used in the base case model (Fig. 5.8b). SAR performance is higher for higher levels of background HFO till twice as much of the base case model value. Peak SAR performance is lower when the HFO value is equal to four times the base case model.(Fig. 5.8c). The above results are discussed separately in the following sections.

5.4.3. Effect of background Arsenic on SAR performance

The effect of As on SAR performance was assessed with varying background levels of As. The results show, not surprisingly, that SAR performance is lower for higher background levels of As (Fig. 5.8a). The levels of pH, As, and Fe in the extracted water and the amount of sorbed As in the aquifer for different background levels of As are presented in Fig. 5.9. The results show that SAR performance is lower for higher levels of background groundwater As (Fig.5.9c). The absolute As removal is considerably higher at higher levels of background groundwater As than at lower levels of background As (Fig.5.9d) even though for water with As levels just above the drinking water standard (50 μg/L), a much higher volume of water with As below 50 μg/L can be extracted. These results indicate that a much higher amount of As can be removed from groundwater with very high levels of As compared to groundwater with relatively lower levels of As using SAR even if the extracted water does not meet the drinking water standard for As.

The concentration of dissolved Fe in the extracted water is a little bit higher for higher background levels of As (Fig. 5.9b) due to increased sorption of As on to HFO (Fig. 5.9e).

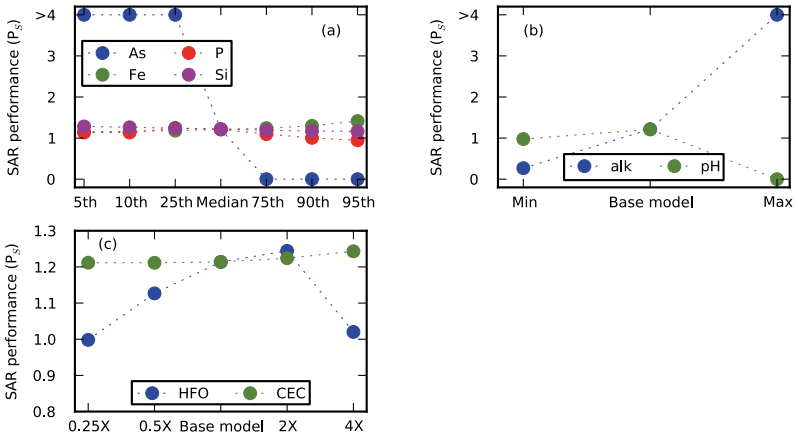

Figure 5.8: (a) Peak P_s for different background levels of As, Fe, P, and Si according to the statistical distribution of Bangladesh (5-10-25-75-90-95th percentiles), (b) Peak P_s for different background levels of pH and alkalinity according to the minimum, mean, and maximum values reported by Aziz Hasan et al. [2009], and (c) Peak P_s for different background levels of HFO and CEC according to the 0.25, 0.5, 2.0, and 4.0 times the background value of the base case model.

The increased As adsorption on HFO induces desorption of Fe and thus the concentration of dissolved Fe in the extracted water increases.

5.4.4. Effect of background Iron on SAR performance

Background levels of Fe in groundwater has influence on As removal during SAR operation as dissolved Fe in the water precipitates to form HFO during the injection phase. The precipitated HFO provides surface sites for As to be adsorbed [Sharma, 2001; Appelo and de Vet, 2003]. The effect of different background levels of Fe on SAR performance was assessed and the results are shown in Fig. 5.10. The concentration of dissolved As in the extracted water is lower for higher background Fe concentration during the entire extraction phase (Fig. 5.10c, d, e), due to higher sorption capacity for higher background Fe concentration. The sorption capacity is higher for higher background Fe concentration due to significantly higher the content of precipitated HFO in the aquifer (Fig. 5.10f). This is why As removal is also slightly higher for higher background levels of Fe at the base case (Fig. 5.8a). The amount of sorbed Fe and As (Fig. 5.10g and h, respectively) also suggests that due to higher content of precipitated HFO for higher background levels of Fe, the concentrations of dissolved As in the extracted water is lower (Fig. 5.10c, d, e). During the injection and storage phase, more Fe oxidizes when the background Fe concentration is higher. Fe oxidation in the subsurface results in the production of

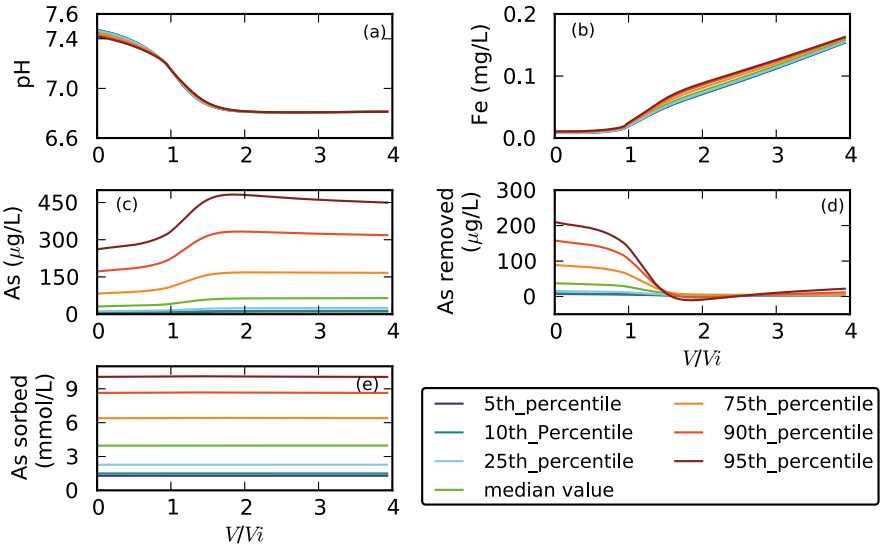

Figure 5.9: Effect of different background levels of As on levels of As, Fe, and pH in extracted water and sorbed As in the aquifer near the well on SAR performance. The figure shows the results of the final cycle when peak SAR performance is achieved.

H^+ during the formation of $Fe(OH)_3$ following the reaction Equation 3.2. Consequently, the more oxidation of Fe occurs in the subsurface the larger the pH drop. The pH levels in the extracted water for different background levels of Fe corroborate the reaction Equation 3.2 (Fig. 5.10a).

5.4.5. Effect of Background Phosphorus on SAR performance

PO_4 is one of the main competitors of As for sorption sites [Stollenwerk et al., 2007; Van Halem et al., 2010a] . That means high levels of background P may have negative impact on SAR performance. Fig. 5.11 shows the effect of different background levels of P on SAR performance. The sorbed amount of Fe and As are lower for higher background levels of P levels (Fig. 5.11i and j), because higher background levels of dissolved P lead to higher background amounts of sorbed P which in turn results in lower background amounts of sorbed Fe and As due to ion competition for sorption sites [Dixit and Hering, 2003; Guan et al., 2009; Hug et al., 2008; Meng et al., 2000; Sharma, 2001; Stollenwerk et al., 2007; Su and Puls, 2001; Van Halem et al., 2010a] . The lower dissolved concentration of Fe in the extracted water for higher background levels of P limits the oxidation of Fe during the injection phase and thus lower content of HFO is formed for higher background P (Fig. 5.11h). The concentration of dissolved As in the extracted wa-

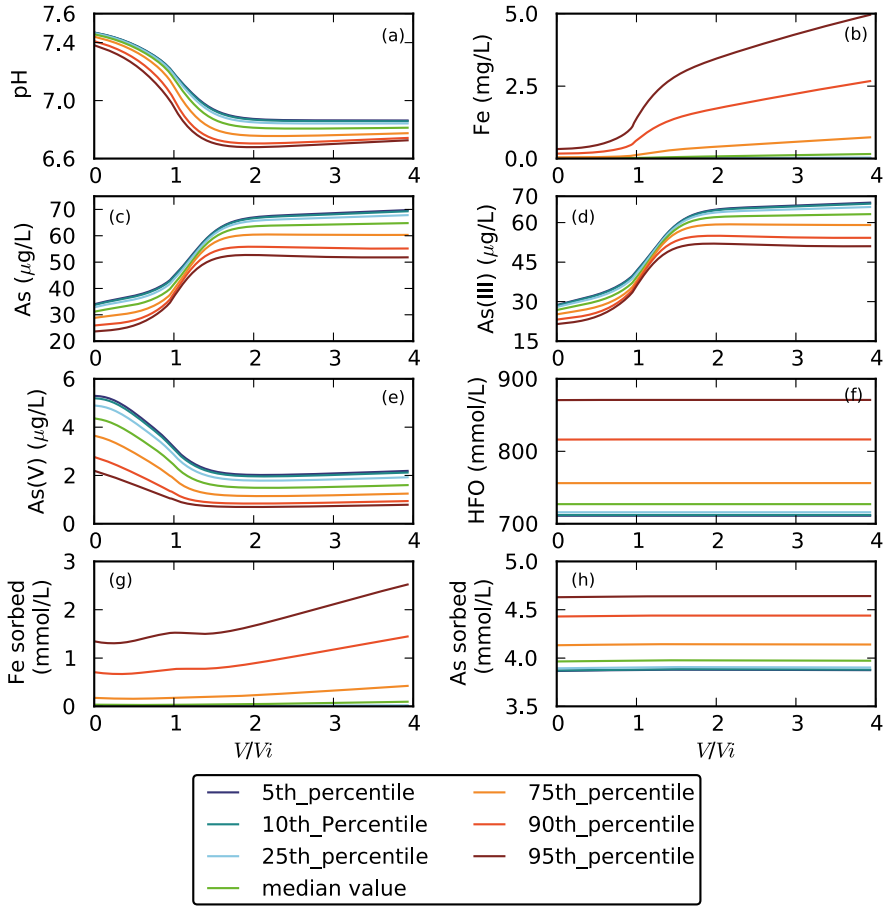

Figure 5.10: Effect of different background levels of Fe on levels of As, Fe, and pH in extracted water and sorbed As, Fe, and the content of HFO in the aquifer near the well on SAR performance. The figure shows the results of the final cycle when peak SAR performance is achieved.

ter is higher for higher background P concentrations during the entire extraction phase (Fig. 5.11c) because of higher P sorption (Fig. 5.11g). The higher P sorption for higher background levels of P decreased the sorption of As due to ion competition for sorption sites in the aquifer (Fig. 5.11j). The lower content of HFO in the aquifer (Fig. 5.11h) for higher background levels of P limits the sorption of As in the subsurface and thus also results in higher dissolved levels of As in the extracted water. The dissolved concentration of As(III) in the extracted water is higher for higher background P concentration (Fig. 5.11d). Similar results were reported for As(III) by Dixit and Hering [2003] and Hug et al. [2008].

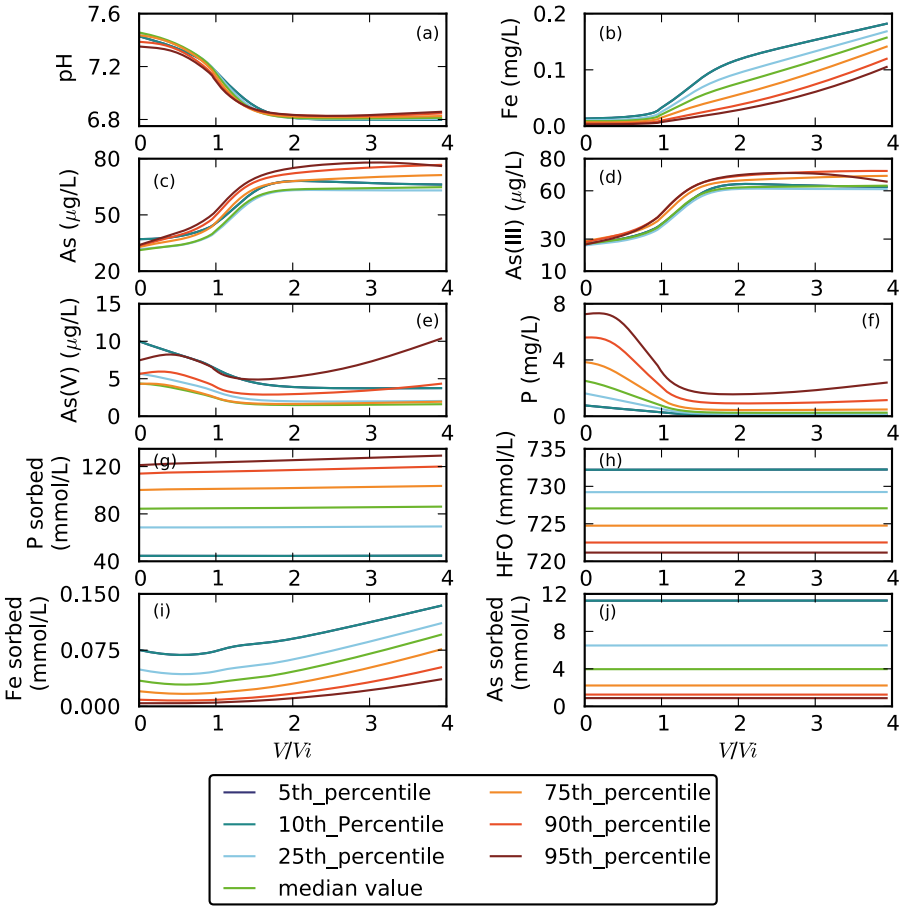

Figure 5.11: Effect of different background levels of P on levels of As, Fe, P, and pH in extracted water and sorbed As, Fe, P, and the content of HFO in the aquifer near the well on SAR performance. The figure shows the results of the final cycle when peak SAR performance is achieved.

5.4.6. Effect of Background Silicon on SAR performance

Si is another competitor of As for sorption sites [Meng et al., 2001; Su and Puls, 2001]. The effect of Si on As removal was assessed with varying background levels of Si. The results show that SAR performance is slightly lower for higher background levels of Si (Fig. 5.8a). The levels of pH, As, Fe, and Si in the extracted water and the amount of sorbed Si, Fe, and As in the aquifer for different background levels of P are plotted in Fig. 5.12. Total dissolved As concentrations is only slightly higher in the extracted water (Fig. 5.12c, d, e) and the sorption of As in the aquifer is lower (Fig. 5.12i) for higher background concentrations of Si. These higher dissolved As and lower As sorption for

higher background Si concentrations are due to competitive sorption between As and Si. The competitive sorption between As and Si is also reported by Hug et al. [2008]; Meng et al. [2000, 2001]; Rahman et al. [2014]; Stollenwerk et al. [2007]. The effect of background Si is generally negligible on Fe (Fig. 5.12b and h). The results show that the effect of Si on As removal is very small whereas the results in Chapters 3 and 4 showed that Si is an important competitor of As for sorption sites on HFO. Thus one could expect a stronger impact of Si on As removal than simulated results presented in this chapter.

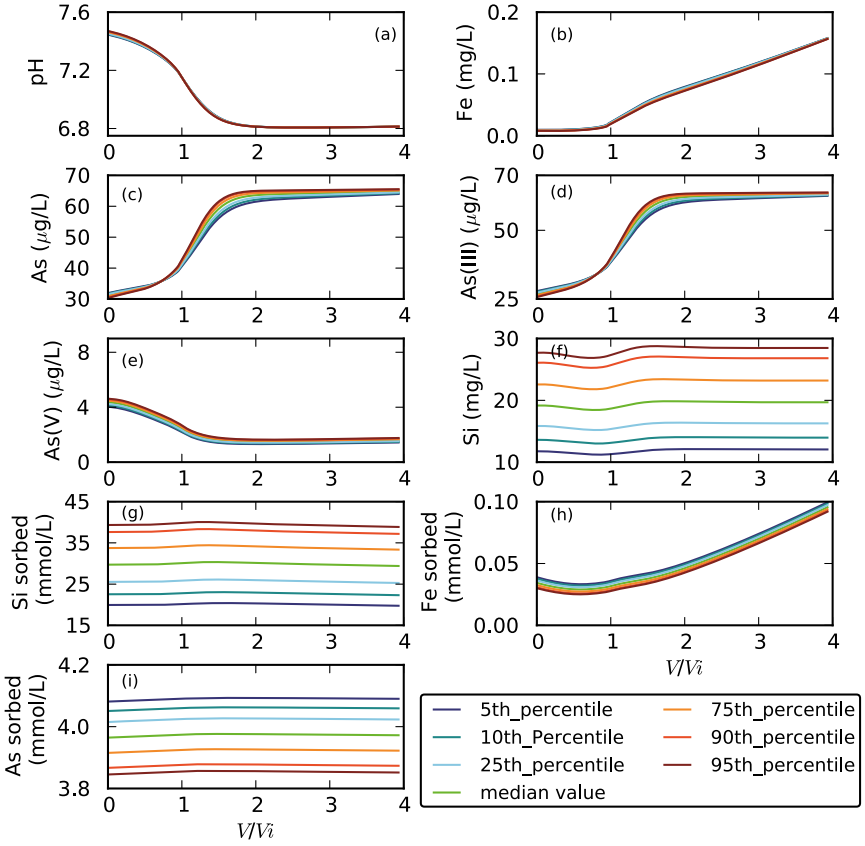

Figure 5.12: Effect of different background levels of Si on levels of As, Fe, Si, and pH in extracted water and sorbed As, Fe, and Si in the aquifer near the well on SAR performance. The figure shows the results of the final cycle when peak SAR performance is achieved.

5.4.7. Effect of Background HFO Content on SAR performance

The gradual builup of HFO in the sediment has a large impact on the sorption of As, Fe, Mn, P, and Si [Antoniou et al., 2013; Appelo and de Vet, 2003; Rahman et al., 2015]. The effect of HFO on SAR performance was also tested with varying background contents of HFO. The results show that SAR performance is higher for higher content of background HFO except for the highest content of background HFO (Fig. 5.8c). Background HFO shows significant effects on the pH of the extracted water from the beginning of extraction phase till $V/V_i \approx 1$ during SAR operation. The pH of the extracted water is much lower for higher background HFO content from the beginning of the extraction phase till $V/V_i \approx 1$ (Fig. 5.13a). This is possibly because of the oxidation of dissolved and sorbed Fe^{2+} on HFO during the injection phase. The lower pH in the extracted water for higher background HFO may also be related to the pH buffering of injection water due to desorption of H^+ from the HFO. Higher background HFO levels mean higher levels of adsorbed Fe, As, and P in the aquifer. The availability of Fe in the aquifer is thus higher and potentially more HFO can be formed. Aqueous and sorbed Fe^{2+} levels remain high during the entire extraction phase for the highest background HFO content. Higher availability of Fe^{2+} implies more Fe^{2+} oxidation and new HFO formation (see Equation 3.2) and as a result a decline in pH. Therefore, the higher the oxidation of Fe^{2+} the larger the pH drop. HFO also (de)sorbs H^+ and may tend to buffer the pH. Thus with higher background HFO the pH of the injection water is stronger buffered by H^+ exchange on the HFO and results in a further reduction in the pH of the injection water. The pH decline is inversely related to an As increase (compare Fig. 5.13a and c) illustrating the pH-dependent sorption behavior of As. Although SAR performance increased with higher background HFO levels except for the highest one, the reduction in the As level until around V/Vi = 1 is higher for the lower the background HFO level. The lower desorption of P due to lower pH in the extracted water for higher background content of HFO resulted in higher desorption of As due to ion competition for sorption sites [Hug et al., 2008; Meng et al., 2000; Rahman et al., 2015; Stollenwerk et al., 2007]. The higher desorption of As due to lower P desorption for higher background HFO content increased the dissolved As levels in the extracted water from the beginning of the extraction phase till $V/V_i \approx 1$. After $V/V_i \approx 1$, pH levels in the extracted water is higher for higher background HFO (Fig. 5.13a) which induced higher P desorption and higher As adsorption. Higher background contents of HFO also have a similar effect on dissolved Fe as As (Fig. 5.13b). The amount of sorbed Fe and As is higher for higher background HFO content (Fig. 5.13g and h respectively) due to the availability of more sorption sites for higher background content of HFO. The effect of goethite on As removal during SAR operation is negligible [Rahman et al., 2015] (Chapter 4) and thus not discussed in this chapter.

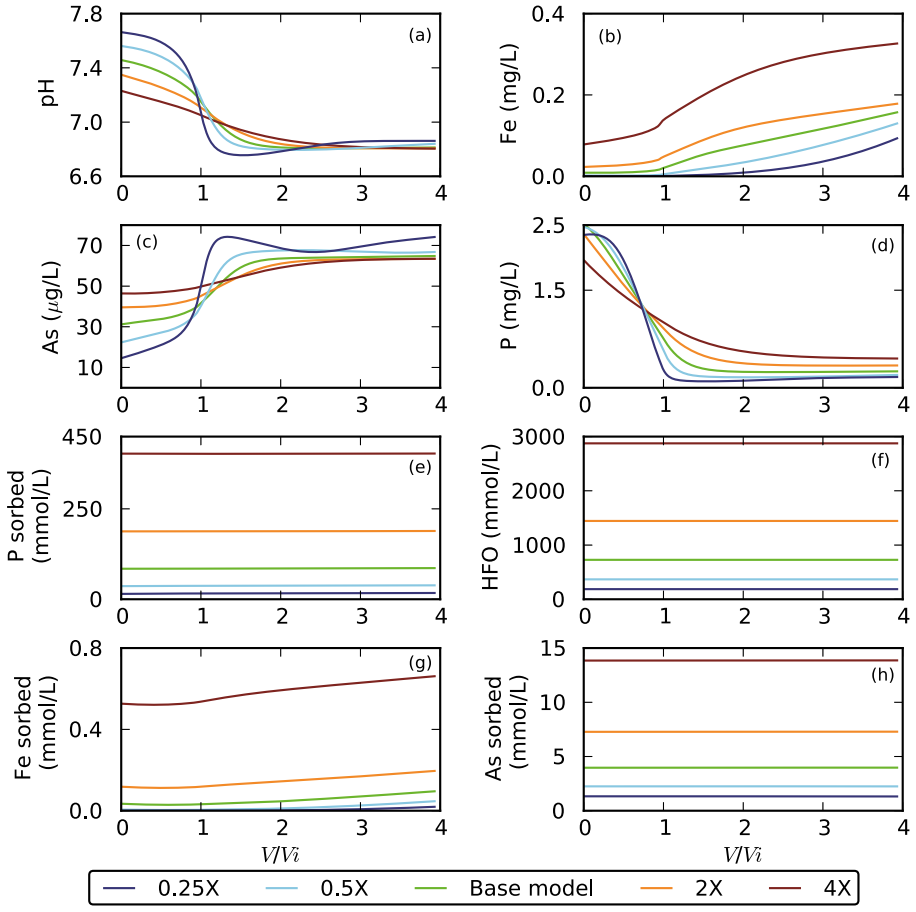

Figure 5.13: Effect of different background contents of HFO on concentrations of As, Fe, P, and pH in extracted water and sorbed As, Fe, P, and content of HFO in the aquifer near the well on SAR performance. The figure shows the results of the final cycle when peak SAR performance is achieved.

5.4.8. Effect of Background Cation Exchange Capacity (CEC) on SAR performance

CEC can influence SAR performance, because high CEC in the aquifer may result in high amounts of exchanged Fe. During injection this exchanged Fe will oxidize and produce higher content of HFO which in turn increases the As sorption. The results however show that SAR performance is only minimally higher for higher background levels of CEC (Fig. 5.8c). The levels of pH, As, and Fe in the extracted water and the content of exchanged Fe, sorbed As and Fe in the aquifer for different background levels of CEC are plotted in Fig. 5.14. The lower dissolved As concentrations in the extracted water for higher

background CEC (Fig. 5.14c, d, and e) is due to slightly higher contents of precipitated HFO in the subsurface. The slightly higher content of HFO for higher background CEC increases the opportunity for As to be adsorbed. The content of HFO is significantly higher for higher background CEC (Fig. 5.14g) due to oxidation of exchanged Fe during injection phase. The result also show not surprisingly that exchanged Fe is considerably higher for higher background CEC (Fig. 5.14f).

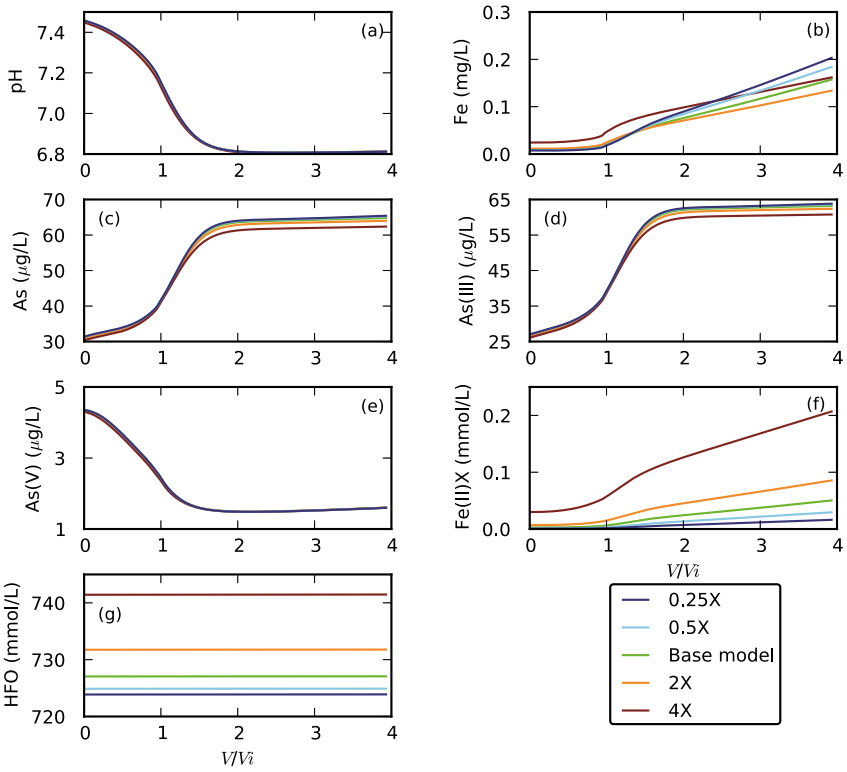

Figure 5.14: Effect of different background levels of CEC on levels of As, Fe, and pH in extracted water and exchanged Fe(II), and content of HFO in the aquifer near the well on SAR performance. The figure shows the results of the final cycle when peak SAR performance is achieved.

5.4.9. Effect of Background pH on SAR performance

Sorption of As and P is pH sensitive [Dixit and Hering, 2003; Kartinen Jr. and Martin, 1995; Stollenwerk et al., 2007] . The effect of background groundwater pH on SAR performance was tested with varying background pH levels. The results show that SAR performance is highest for the base case model background pH and lowest for the maximum background pH (Fig. 5.8b). The pH of the extracted water for the highest background groundwater pH does not increase above the background level at the beginning of the extraction phase till $V/V_i \approx 1$ (Fig. 5.15a). This is because, at the highest background pH there will be less dissolved CO_2 in the background groundwater and thus there will be less CO_2 stripping from the injection water during aeration. Therefore pH of the injection water does not increase above the background level. The background pH levels have a significant effect on the total dissolved As concentrations during SAR operation (Fig. 5.15c). At the beginning of the extraction phase with maximum background pH, the As concentration is highest and surprisingly largely exceeds the background As level. This is possibly due to the lower P concentration in the extracted water (Fig. 5.15d). The lower P desorption should have caused lower P concentrations and higher As concentrations in the extracted water for the highest background pH from the beginning of the extraction phase till $V/V_i \approx 1$ but the sorbed As and P content do not corroborate this (Fig. 5.15e and f). After $V/V_i \approx 1$ the dissolved As concentration in the extracted water continues to increase and surprisingly largely exceeds the background As level with increasing extracted volume (Fig. 5.15c). At the beginning of the extraction phase with minimum background pH level, P concentration in the extracted water is higher compared to the other background pH levels (Fig. 5.15d). The higher P concentration leads to lower dissolved As till $V/V_i \approx 1$ due to competitive sorption (Fig. 5.15c) but again the sorbed As and P content in the aquifer near the SAR well do not support this (Fig. 5.15e and f). After $V/V_i \approx 1$, the concentration of dissolved As continues to increase with increasing extracted volume due to the extraction of more acidic water (Fig. 5.15c). Extraction of water with minimum background pH level also has higher levels of dissolved Fe compared to the other background pH levels (Fig. 5.15b). It is unclear how the dissolved As concentration in the extracted water exceeds beyond the background level for highest background groundwater pH instead of a reduction towards a lower level. Therefore further exploration is required to understand the processes that produced the results discussed in this section.

5.4.10. Effect of Background Alkalinity on SAR performance

The effect of alkalinity on SAR performance was tested with varying background levels of alkalinity. The results show that SAR performance is higher for higher background al-

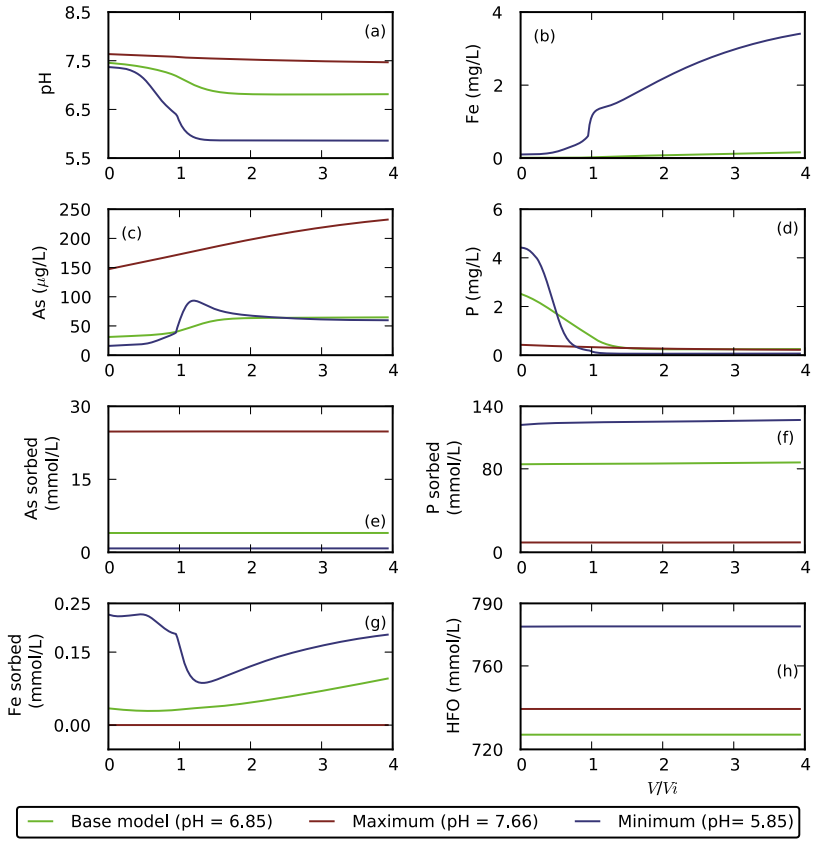

Figure 5.15: Effect of different background levels of pH on levels of As, Fe, P, and pH in extracted water and content of sorbed As, P and Fe and HFO in the aquifer near the well on SAR performance. The figure shows the results of the final cycle when peak SAR performance is achieved.

kalinity (Fig. 5.8b). The pH of the extracted water is significantly higher for higher levels of background alkalinity from the beginning of the extraction phase till $V/V_i \approx 1$ (Fig. 5.16a). This is due to higher CO_2 stripping from water for higher background levels of alkalinity during aeration. The water with higher background levels of alkalinity contains more dissolved CO_2 as the pH is assumed constant. During aeration more CO_2 is stripped out of the water and as a result the pH of the injection water becomes higher for higher background levels of alkalinity. Similar effect was also reported by Safari et al. [2014]. The higher pH in the extracted water from the beginning of the extraction phase till $V/V_i \approx 1$ leads to stronger sorption of Fe, Mn, and As which resulted in lower concentrations of dissolved Fe, Mn, and As in the extracted water for higher levels of background alkalinity (Fig. 5.16c, d, and e respectively).

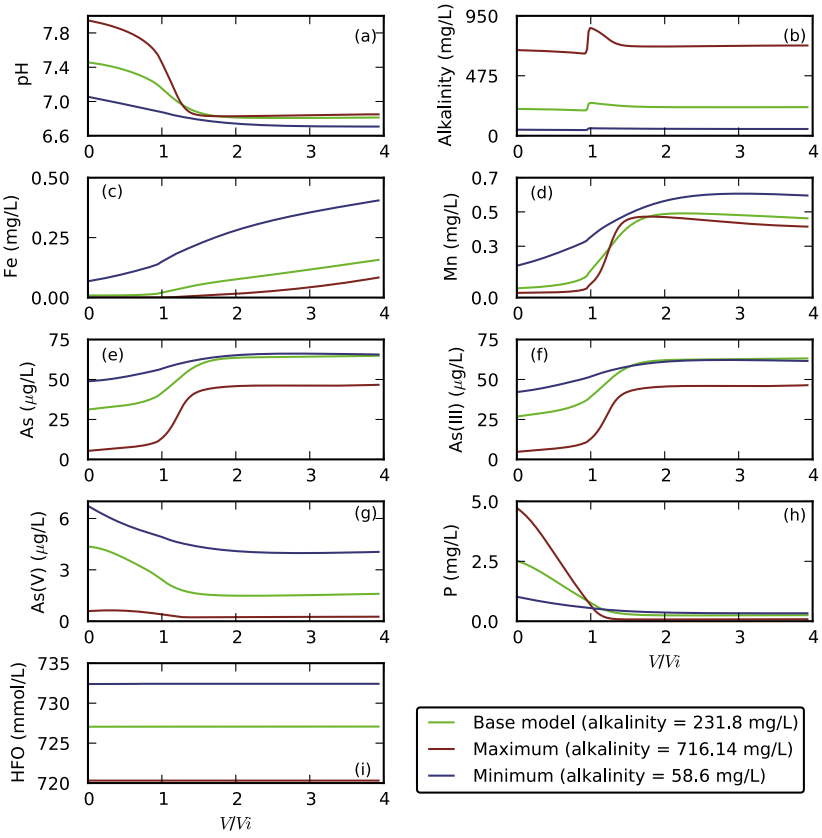

Figure 5.16: Effect of different background levels of alkalinity on levels of As, Fe, Mn, P, pH, and alkalinity in extracted water and content of HFO in the aquifer near the well on SAR performance. The figure shows the results of the final cycle when peak SAR performance is achieved.

5.4.11. Summary of sensitivity analysis

The effect of different background levels of As, Fe, P, Si, pH, alkalinity, HFO, and CEC on SAR performance was investigated using the modified RTM. The results show that SAR performance is lower for higher background levels of As, P, and Si. SAR performance is higher for higher background levels of Fe, alkalinity, and CEC. SAR performance is significantly higher for higher background contents of HFO except for highest background content of HFO. SAR performance is highest for background pH of the base case model and lowest for maximum background pH. SAR performance is slightly lower for minimum background pH compared to the background pH of the base case model. SAR performance is lower for higher background levels of As but the absolute As removal is

significantly higher for higher background levels of As which indicate that a significant amount of As can be removed with SAR technology even if the drinking water standard could not be achieved during SAR operation. The results of sensitivity analysis indicate that As is by far the most important background parameter that controls SAR performance. Other key background parameters that control SAR performance include HFO, alkalinity, and pH. The parameters that have minor impact of SAR performance include Fe, P, Si, and CEC. It is important to note that only one parameter was varied at a time in the sensitivity analysis while some parameters like As, Fe, and P may be correlated but these effects were not studied in the sensitivity analysis.

5.5. Nationwide SAR Performance Calculation

The BGS/DPHE data set was used to select different locations in Bangladesh to calculate SAR performance with the RTM. The locations for SAR performance calculation were selected in such a way that their spatial distribution covers the entire country. Note, all the selected locations for nationwide SAR performance calculation contains As level more than 50 μg/L. A total of 184 locations in Bangladesh were selected covering the range of parameter variation. As mentioned earlier, sixteen additional sites with As concentrations above 50 μg/L were selected from the BWDB data set. SAR was simulated for 200 locations and peak SAR performance was calculated for each location. Maps of peak SAR performance and its relation to key parameters were created for all 200 locations (Fig. 5.17).

Table 5.6: SAR performance assessment for Bangladesh groundwater.

P_s	Number of locations
0	97 (48.5%)
0 - 1	48 (24%)
1 - 2	35 (17.5%)
2 - 3	3 (1.5%)
3 - 4	17 (8.5%)

5.5.1. Assessment of SAR performance for Bangladesh groundwater

Assessment SAR performance for Bangladesh groundwater is summarized in Tables 5.6 and 5.7. The results show that 27.5% of the studied locations resulted in peak SAR performance greater than 1 and 24% of the studied locations resulted in peak SAR performance ranging between above 0 to 1 (Table 5.6). The results of SAR performance calculation show that SAR works better for background groundwater As levels ranging from above 50

to 150 μg/L (Table 5.7 and Fig. 5.17a). About 22% and 5% of the locations showed peak SAR performance above zero with background As concentrations ranging from 150-200 μg/L and more than 200 μg/L respectively (Table 5.7). The above results indicate that SAR technology has a great potential for locations with background groundwater As concentrations ranging between 50 and 150 μg/L but SAR might be useful for locations with background groundwater As levels of above 200 μg/L as well.

Table 5.7: SAR performance and its relation to background groundwater As.

Groundwater As (μg/L)	n sites	sites with $P_s > 0$	sites with $P_s > 1$
50 - 100	46 (23%)	97%	93%
100 - 150	56 (28%)	82%	38%
150 - 200	37 (19%)	22%	0%
>200	61 (30%)	5%	0%

Peak SAR performance and number of cycles required to achieve peak performance is computed with the RTM at 200 locations in Bangladesh. Results and their relation with background groundwater As concentrations are presented in Fig. 5.17. Peak performance is shown in Fig. 5.17a. The number of cycles to reach peak performance is shown in Fig. 5.17b. There is no distinct spatial pattern in SAR performance except that areas with high As level show low performance and vice versa (Fig. 5.17a). There are some locations for each range of background groundwater As level shown in Fig. 5.17a where As levels below 50 μg/L cannot be achieved with SAR. These locations are referred to as zero SAR performance. The percentage of locations with zero SAR performance is lower for lower levels of background groundwater As (Fig. 5.17a). For most of the locations with more than 200 μg/L of background As concentrations, SAR performance is zero. For locations with background As concentrations ranging between 150-200 μg/L, peak SAR performance is slightly higher (0-1) with fewer locations with zero performance. Peak SAR performance is considerably higher (ranging between 1-2) for most locations when background As concentrations ranges from 100-150 μg/L. The number of locations with zero performance is considerably lower when background As concentrations ranges from 100-150 μg/L. Peak SAR performance is best (between 2-4) and the number of zero performance locations is smallest for background As concentrations ranging from 50-100 μg/L (Fig. 5.17a).

SAR performance increases with successive cycles due to gradual buildup of HFO in the subsurface [Rahman et al., 2015] (Chapter 4). It is important to determine how many cycles it takes to reach peak SAR performance at each location. The number of cycles required to reach peak SAR performance is presented in Fig. 5.17b. For the locations of the BGS/DPHE data set (circles) the number of cycles required to reach peak SAR per-

formance varies over the full range of 2 to 500, while only a small number of locations required more than 250 cycles. For the locations of the BWDB data set (squares), 2 cycles were required for most sites to reach peak SAR performance while only two locations required 20 to 60 cycles to reach peak SAR performance. In general, a smaller number of cycles was required to reach peak performance when peak performance was relatively small.

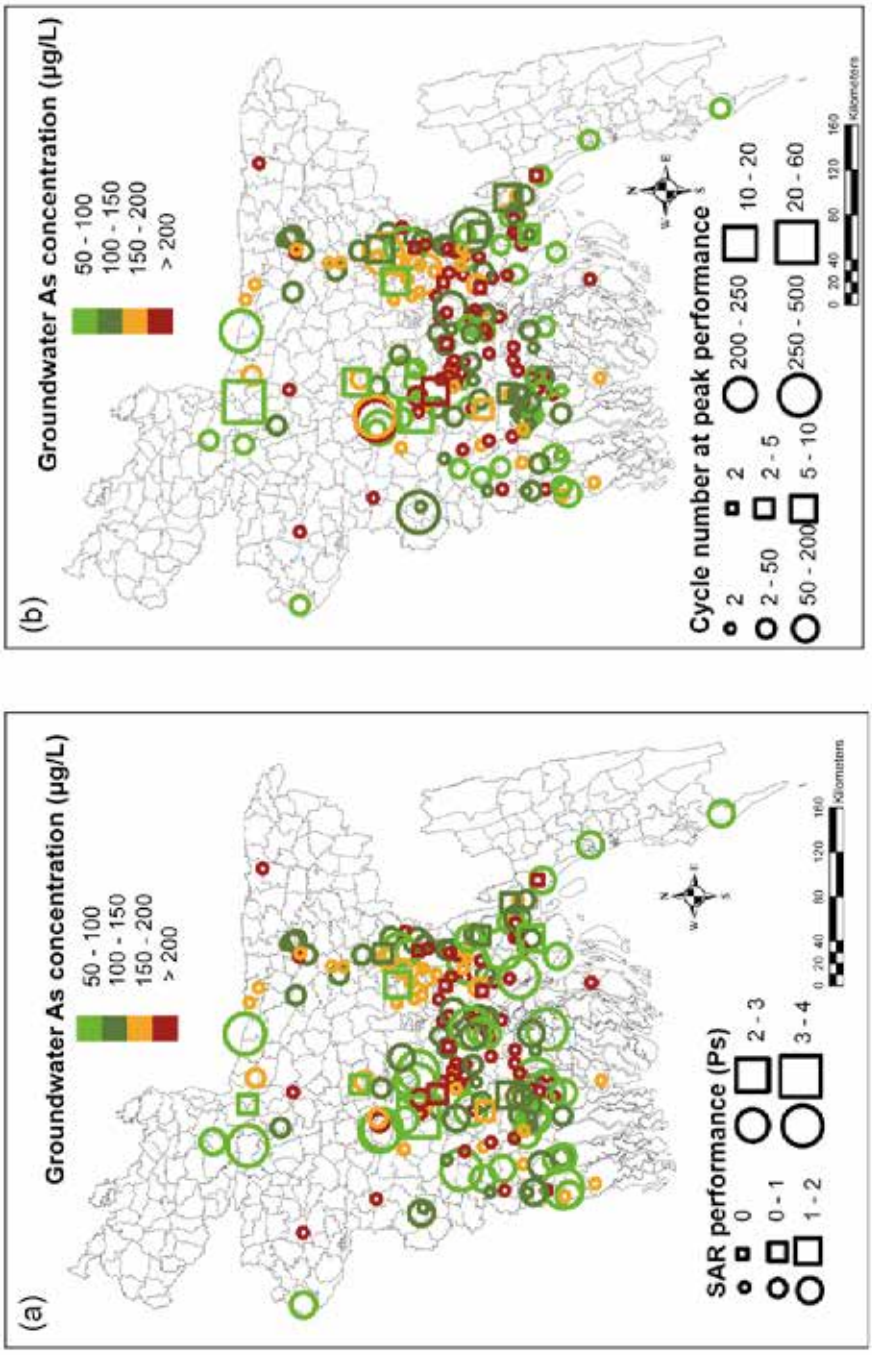

Figure 5.17: Peak SAR performances at different locations in Bangladesh and their relationship with dissolved As (a). Numbers of cycles required to reach peak SAR performance at different locations are plotted in 5.17(b). Circles and squares in the legends of panel a and b represents BGS/DPHE and BWDB survey data set respectively as reported in BGS and DPHE [2001]. The color represents the background groundwater As concentrations. The symbol size represents peak SAR performance in panel a. The symbol size in panel b represent cycle number. The circle represents SAR performance (panel a) or cycle number (panel b) for BGS/DPHE data set and the square represents SAR performance (panel a) or cycle number (panel b) for BWDB data set.

5.5.2. Relation between peak SAR performance and different background water quality parameters

A simple linear regression analysis was performed in order to determine the correlation between peak SAR performance computed at 200 locations in Bangladesh and background groundwater As, P, and Fe levels, as well as the ratio of background groundwater Fe over As concentrations (Fig. 5.18). The results of the regression analysis are summarized in Table 5.8. From Fig. 5.18a it is clear that peak SAR performance is inversely related to background groundwater As concentrations. There is a slight positive correlation between Peak SAR performance and the ratio of background groundwater Fe over As concentrations (Fig. 5.18d). Background groundwater Fe and P levels do not show any significant correlation with peak SAR performance ((Fig. 5.18b and c).

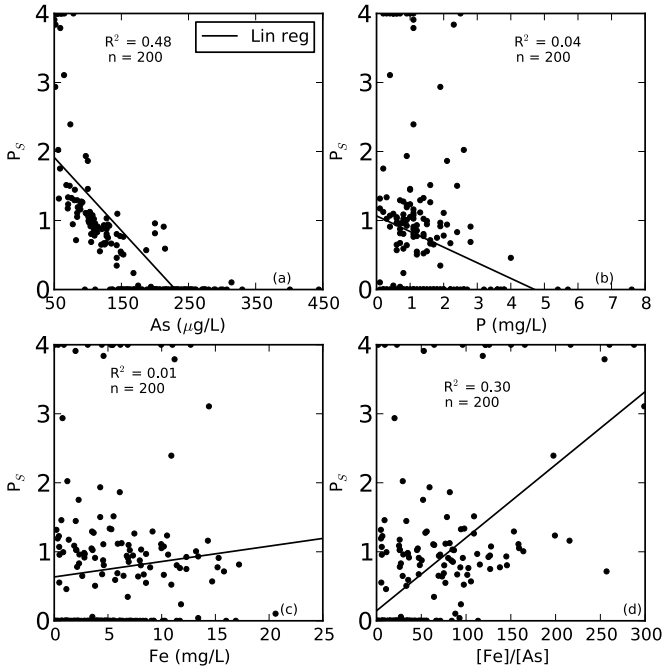

Figure 5.18: Relationship between SAR performance and As (a), SAR performance and P, (b), SAR performance and Fe (c), and SAR performance and molar ratio of Fe and As (d).

Linear regression analysis shows a moderately strong and statistically significant relationship (R^2 = 0.48, p < 0.001) between As and SAR performance corresponding to a decrease in SAR performance with higher levels of background groundwater As. For

Table 5.8: Regression Analysis of SAR performance as a Function of Different parameters (P_s = aX + C) for As, P, Fe, [Fe]/[As].

X	a	C	R^2	p
As	-0.01	2.44 ± 0.69	0.48	<0.001
P	-0.22	1.66 ± 0.21	0.043	<0.001
Fe	0.02	0.63 ± 0.08	0.01	<0.01
$[Fe]/[As]$	0.01	0.14 ± 0.54	0.30	<0.001

[Fe]/[As], the linear regression shows a weak but statistically significant relationship (R^2 = 0.30 with p value of less than 0.001) corresponding to an increase in SAR performance with higher [Fe]/[As] values. For background groundwater P and Fe the linear regression shows no significant relationship (R^2 = 0.043 and 0.01 respectively with p values of < 0.001 and < 0.01 respectively). Meng et al. [2001] reported that in order to lower As levels using a household filter with through co-precipitation and filtration system to below 50 μg/L, typically a [Fe]/[As] ratio of >40 (mg/mg) or 53 (M/M) is required but the results presented in Fig. 5.18d and Table 5.8 do not entirely corroborate the finding of Meng et al. [2001]. The results of linear regression analysis indicate that it is very difficult to predict SAR performance on the basis of a single parameter except background groundwater As.

5.5.3. Lifetime of potential SAR systems in Bangladesh

SAR performance initially increases with the gradual built up of HFO acting as sorbant for As. However, with prolonged built up of HFO in the subsurface, the HFO starts to act as a pH buffer lowering the pH of the injection water and thereby decreasing the potential of As for sorption to HFO. The pH buffering of the injection water by HFO therefore causes a slow decline of the SAR performance after reaching peak performance. It is important to determine the lifetime of SAR locations simulated in this study. Model simulations were continued to determine how many cycles are required for SAR performance to decrease 50% of peak performance for each location. Model simulations were stopped when SAR performance declined to 50% of peak performance or after completion of the 500^{th} cycle, whichever occurred first. The decline to 50% of peak performance was only computed for locations with peak performance above zero. Results of SAR performance and cycle numbers are presented in Figs. 5.19a and b. A large number of cycles (200 to 500) is required for SAR performance to decline below 50% of peak performance for most of the locations and for both data sets. There are a few locations which took only between 3 to 50 cycles to decline below 50% of peak SAR performance (Fig. 5.19b). These results indicate that the life time of SAR systems can be considerable at most of the studied locations.

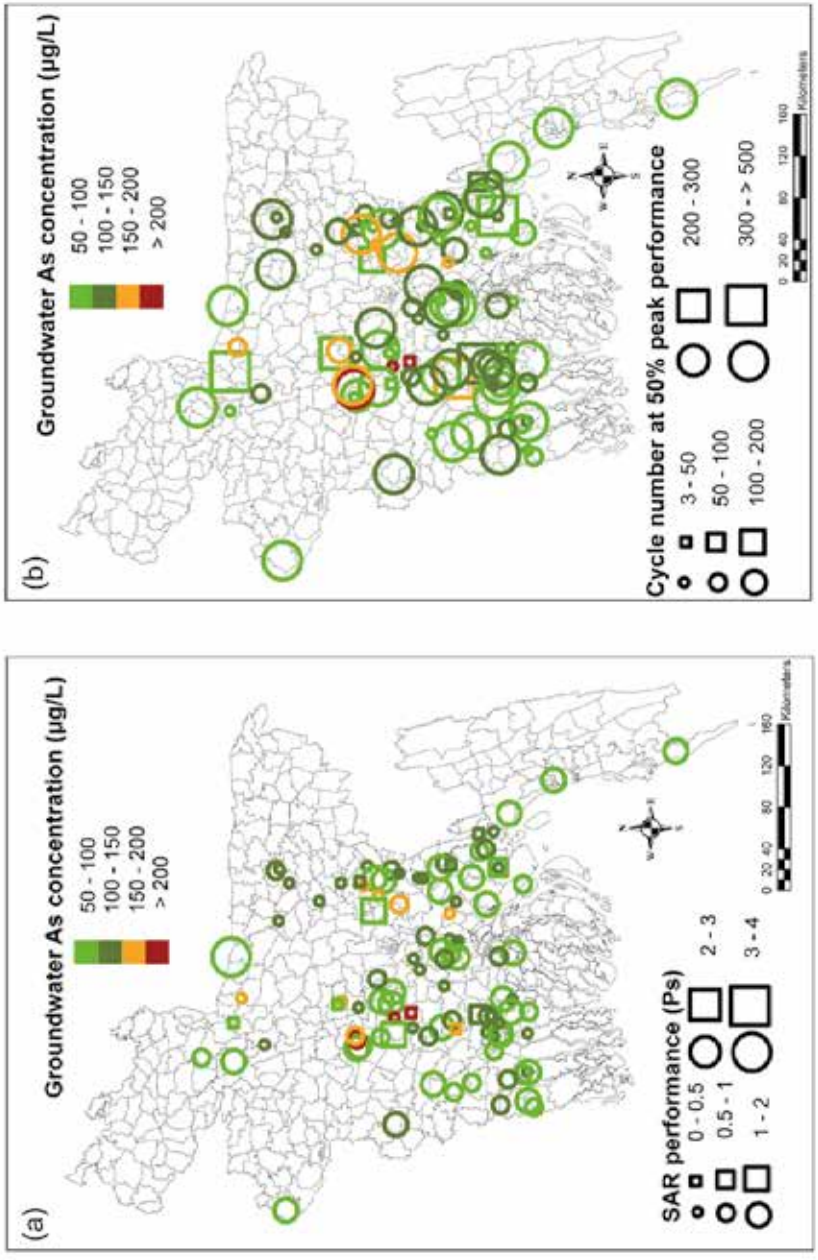

Figure 5.19: SAR Performances at different locations in Bangladesh after slow declination down to 50% of the peak performance and their relationship with dissolved As (a). Numbers of cycles required for declination down to 50% of peak SAR performance at different locations (b). Circles and squares in the legends of panel a and b represents BGS/DPHE and BWDB survey data set respectively as reported in BGS and DPHE [2001]. The color represents the background groundwater As concentrations. The symbol size represents SAR performance at different locations in Bangladesh after slow declination down to 50% of the peak performance in panel a. The symbol size in panel b represent number of cycles required for declination down to 50% of peak performance. The circle represents SAR performance (a) or cycle number (b) for BGS/DPHE data set and the square represents SAR performance (a) or cycle number (b) for BWDB data set. Locations with zero SAR performance are not included in Fig. 5.19 (a and b).

5.5.4. LIMITATIONS OF THIS MODELING STUDY

The model used in this chapter was calibrated at one SAR well and the transferability of the model was tested at two other sites but still the range in hydrogeochemistry was considerably smaller than the variability that is present across Bangladesh. For locations with very low or high values of background hydrogeochemical parameters, the model prediction may be less reliable. The results produced by the model for the sensitivity analysis with high background groundwater pH are not reliable and further research is needed to understand SAR and model SAR in aquifers with high background pH. There are some other limitations to this modeling study mainly because of the lack of data on background pH, alkalinity, As speciation, HFO, CEC, SOM, $CaCO_3$ content, and $FeCO_3$ content. The model used the same pH, alkalinity, HFO, and CEC content for all locations in this study, and the As speciation was 80% As(III) and 20% As(V) for all locations. In reality, there will be some variability of these parameters, but this was not taken into account.

The SAR performance calculations with the RTM reported in this study did not consider the potential impact of SOM and pyrite oxidation processes and $FeCO_3$ dissolution process, as these processes were not relevant for the SAR study sites considered in Chapter 4. The nationwide data for these parameters is not available as well. The oxidation process of SOM may be relevant for locations with very high SOM content. For locations with high SOM content, the SOM oxidation process could consume a large amount of injected O_2 [Antoniou et al., 2013] resulting in a reduction of O_2 available for Fe(II) and As(III) oxidation. The pyrite oxidation process could also consume a large amount of O_2, [Antoniou et al., 2013] and can even release As into the system [Wallis et al., 2010, 2011]. As concentrations in the extracted water could eventually increase due to the release of As caused by pyrite oxidation. The overall impact of $FeCO_3$ dissolution on oxygen consumption is negligible as reported by Antoniou et al. [2013] but location with high content of $FeCO_3$ might have impact on overall oxygen consumption process. An extension including SOM and pyrite oxidation and $FeCO_3$ dissolution processes to the current model is recommended in order to estimate SAR performance for locations with high SOM, pyrite, $FeCO_3$ content.

5.6. SUMMARY AND CONCLUSIONS

In this chapter, the potential for SAR application was investigated across Bangladesh. The reactive transport model of Chapter 4 was combined with a new aeration model to quantify the effects of variation on concentrations of As, Fe, P, Si, pH, alkalinity, and contents HFO, and CEC on SAR performance. The results of the new combined model for SAR well B was compared to the results of the RTM of Chapter 4. Data from BGS and

DPHE [2001], BWDB, and Hasan et al. [2009] was used for background hydrochemistry of the model simulated in this study. For background geochemistry, measured values of HFO, Goethite, and CEC were taken from Chapter 4 and used in the model for this study. All simulation in this study were run upto a maximum of 500 cycles even if peak performance was not achieved. It is also important to note that SAR performance slowly declines after reaching peak performance. Therefore, model simulations were continued to determine how many cycles are required to go down to 50% of peak performance for each location. Model simulations were stopped when SAR performance declined to 50% of peak performance or 500 cycles whichever came first.

The SAR performances was calculated at 200 locations in Bangladesh and a preliminary map of potential SAR performance was generated. SAR performance of the studied locations in Bangladesh ranges from 0 to 4 and 28% had SAR performance above 1. The results of the nationwide SAR performance calculation indicate that SAR technology might be useful for locations with background groundwater As concentrations ranging from 50 to 150 μg/L. The results also indicate that the potential for SAR application in Bangladesh is substantial as 27.5% percent of the studied locations resulted in SAR performance above 1 and 48.5% of the studied locations resulted in SAR performance above 0.5. Note that SAR performance of 0.5 means that injection of 5,000 L of water results in 2,500 L of As safe water, which is enough drinking water for 143 families per day assuming five members per family and 3.5 L/day/capita drinking water [Milton et al., 2006].

The results of the SAR simulation suggest that SAR performance is lower for higher background levels of As and it is by far the most important controlling parameter for successful SAR application. According to the results, absolute As removal is significantly higher for higher background levels of As. The background levels of Fe, P, Si, and CEC have minor impact on SAR performance. SAR performance is higher for higher background levels of alkalinity and [Fe]/[As]. SAR performance is highest for the background pH of the base case model and lowest for the maximum background pH considered. SAR performance is slightly lower for the minimum background pH compared to the background pH of base case model. Peak SAR performance is higher for higher levels of background HFO except for the highest background HFO content. The results of sensitivity analysis and the regression analyses indicate that SAR performance is influenced simultaneously by a combination of parameters. So in order to identify a suitable location for SAR operation in Bangladesh, background levels of As, Fe, P, pH, alkalinity, CEC, and HFO need to be considered and SAR performance should be assessed with the RTM discussed in this chapter before field application of the technology.

According to the results of this modeling study, the lifetime of SAR systems for most of the locations in Bangladesh can potentially be significant but sometimes SAR units may become nonfunctional before the expected lifetime due to broken parts. The modeling

results reported in Chapter 4 and in this chapter show that the model calculations tend to underestimate SAR performance. The model is expected to be useful to give a lower bound on expected SAR performance for most locations.

The estimates on SAR performance for particular location can be useful for the local users. Users of SAR system cannot, in practice, measure As concentrations. A feasible operation procedure is as follows: The users can store a preset volume of water based on the estimates during the extraction phase of a SAR cycle for drinking purpose. After storing the drinking water, people can use another preset volume of water for other daily household purposes and finally the injection tank can be refilled, aerated, and injected into the aquifer for the next SAR cycle. The modeled SAR performance can also be useful to identify locations where SAR performance is expected to be better compared to alternative As mitigation options.

6

SYNTHESIS

The overall objective of this research is to asses the potential applicability of subsurface arsenic removal (SAR) technology in Bangladesh. Specifically, the following objectives are considered in this research: 1) To determine the effect of operational parameters on SAR performance. 2) To develop a reactive transport model in order to understand the processes that control the (im)mobilization of As during SAR operation in Bangladesh. 3) To determine the sensitivity of subsurface arsenic removal to different key hydrogeochemical parameters. 4) To quantify and map the potential performance of SAR system under different hydrogeochemical settings in Bangladesh with a developed reactive transport model. Field experiments were conducted and a reactive transport model was developed through simulation of the SAR experiments reported in Chapter 3 and applied in order to achieve the objectives of this research.

In this chapter, a synthesis of the research is presented. The implications for process-based SAR performance calculation are highlighted and future research directions for SAR application in other parts of the world are discussed.

6.1. Effects of operational parameters on SAR (Objective 1

Four SAR exploratory experiments were carried out at two wells (As in groundwater = 200 μg/L) in Bangladesh. The aim of these experiments was to determine the effects of operational parameters on SAR performance to asses the potential of applicability of SAR technology in Bangladesh (chapter 3). Each experiment investigated a different approach to increase the opportunity for subsurface As immobilization by adsorption on hydrous ferric oxide (HFO) surfaces. SAR performance was quantified with the extraction efficiency (Q_E) (Eq 3.1).

The effect of larger and smaller injection volumes with saturated levels of dissolved oxygen on As removal was investigated with the first experiment. SAR operation with larger injection volume was more favorable for As and Fe removal in the subsurface than smaller injection volume with extraction efficiency (Q_E) of 0.1 and 0.5 for As with smaller and larger injection volume respectively. The Q_E for Fe with smaller and larger injection volumes are 1.7 and 2.5 respectively.

The effect of repeated injection-extraction-injection cycles of an equal (extraction=injection) volume (of water) followed by extraction of a larger volume than was injected on SAR was investigated with the second experiment. Repeated injection-extraction cycles of an equal volume resulted in higher As removal (Q_E = 1.6) compared to regular cycles (Q_E = 0.9). Repeated injection-extraction cycles of an equal volume likely increased the ion sorption capacity in the subsurface due to the precipitation of more HFO sorption sites compared to regular operation and resulted in higher As removal in the subsurface.

The effect of pumping rates on SAR during the extraction phase was investigated with the third experiment. Higher As removal was observed during extraction phase with a reduced pumping rate with maximum observed Q_E of 0.5 and 0.75 for higher and lower pumping rates respectively.

Finally, the effect of intermittent pumping rather than continuous pumping on SAR was investigated with the fourth experiment. Similarly, SAR operation with intermittent pumping resulted in higher As removal ($Q_E \geq 2$) than cycles with continuous pumping ($Q_E \approx 1.4$). Better As removal with a larger injection volume, reduced pumping rate and intermittent pumping indicate that the sorption of As on iron hydroxides is kinetically limited.

Experiments with repeated injection-extraction-injection cycles of an equal volume, reduced pumping rates, and intermittent pumping are referred to as alternative operations. All three alternative operations resulted in better As removal than regular operation. The highest Q_E during regular operation was 0.5. Cycles with intermittent pumping resulted in the highest extraction efficiency ($Q_E \geq 2$) and cycles with reduced pumping resulted in the lowest extraction efficiency ($Q_E = 0.75$) of all the alternative operations performed in this study. A combination of all three alternative operations is recommended for SAR application in rural Bangladesh. The WHO guideline (10 μg/L) was never achieved with any of the SAR experiments performed in Bangladesh during this study but the Bangladesh guideline (50 μg/L) was achieved with all the experiments performed in this study with a maximum $Q_E \geq 2$. The estimated number of families that can be supported by a SAR unit is 114 when 1000 L of As safe water is produced. The approximate cost for a SAR unit installation with an injection capacity of 1 m^3 is around US$925.00 or a little more than US$8.00 per family and the maintenance cost for one SAR unit with a 1 m^3 injection capacity per family is US$13.00/year. The price of a SONO filter (a household As removal system) is US$45.00 to 50.00 with an average lifetime of 1 year [Shafiquzzaman et al., 2009]. The yearly cost for a SAR unit per family with a 1 m^3 injection capacity is almost half of the cost for an unit of SONO arsenic removal filter.

6.2. Reactive transport modeling of SAR operation in Bangladesh (Objective 2)

In Chapter 4, development and results of a reactive transport model for a strongly reducing shallow Holocene aquifer were discussed. The one-dimensional radially symmetric reactive transport model was developed with PHREEQC (version 2.17) to model key hydrogeochemical reactions during SAR operation. Oxidation of Fe(II) to Fe(III) and As(III) to As(V) was modeled using kinetic-rate expressions. Cation exchange, precipitation of HFO, and surface complexation were modeled as equilibrium processes whereas the re-

sults of SAR field experiments reported in Chapter 3 indicate that the sorption of As is kinetically limited (discussed later). The reasonable model fit with the measured concentrations of As, Fe(II), Mn(II), Si, Mg, Na, and K in the extracted water at the SAR well indicates that the key processes taking place in the subsurface during SAR operation were simulated reasonably well by the model. The sorption of As is significantly influenced by the pH of the groundwater in the SAR system during injection, storage, and extraction phases. Particularly, the high pH of injection water facilitated As sorption. During SAR operation As(III) oxidizes to As(V) which is preferentially removed from the water and thereby As(III) dominates in the end. These processes increase the overall As sorption. The increased sorption capacity due to gradual buildup of HFO facilitates As removal during SAR operation. The surface complexation modeling suggests that simultaneous sorption of H_4SiO_4 is an important factor that limits As removal during SAR operation. The simulated content of freshly precipitated HFO is such that aquifer clogging does not seem to be a problem.

The model was applied to two additional SAR sites in Bangladesh to assess its transferability. The model is able to reproduce the observations reasonably well for most of the parameters discussed in Chapter 4. This is an important finding, as reactive transport models are not commonly transferred from one site to another site.

As sorption is kinetically limited as indicated by Rahman et al. [2014] (Chapter 3). The modeled SAR performance was generally underestimated compared to the observed performance at the SAR wells even though the equilibrium sorption was simulated with a set of surface complexation parameters adopted from the literature. Kinetic sorption with the same set of surface complexation parameters may be expected to result in a further reduction of As removal simulated by the model. Therefore, a kinetically-controlled simulation will require increased constants for sorption reactions of As(III) and As(V) to produce a reasonable model fit and it may give a better fit than was obtained now, because the sorption of As on HFO is kinetically limited (Chapter 3). For the sake of model simplicity, the surface complexation reactions were simulated in thermodynamic equilibrium (see Chapter 4). Considering the overall results it is concluded that the model may be useful to give a lower bound on expected SAR performance for specific locations and may be used to assess potential SAR performance at other locations in Bangladesh with similar aquifer characteristics based on local hydrogeochemical conditions.

6.3. Assessment of the potentials of SAR technology in rural Bangladesh (Objectives 3 and 4

The reactive transport model discussed in Chapter 4 was coupled with a new aeration model using a Python script to quantify the effects of As, Fe, P, Si, pH, alkalinity, HFO,

and CEC on SAR performance in Chapter 5. Data from BGS and DPHE [2001], BWDB, and Hasan et al. [2009] were used for background hydrochemistry used in the model. For background geochemistry, measured values of HFO, Goethite, and CEC were taken from the RTM discussed in Chapter 4. The combination of the aeration model and reactive transport model (RTM) model performed almost as good as the RTM of Chapter 4 that used the measured injection water composition of each phase.

All simulations discussed in Chapter 5 were run upto a maximum of 500 cycles even if peak performance was not achieved. It is important to note that SAR performance slowly declines after reaching peak performance. Therefore, model simulations were continued to determine how many cycles are required to go down to 50% of peak performance for each location. Model simulations were stopped when SAR performance declined to 50% of peak performance or 500 cycles were reached, whichever came first.

SAR performance was calculated at 200 locations in Bangladesh and a preliminary map of suitable locations for SAR application was generated. The results suggest that SAR performance is lower for higher background levels of As, P, and Si. SAR performance is higher for higher background levels of Fe, alkalinity, CEC, HFO (except for the highest background HFO due to higher oxidation of sorbed Fe^{2+} onto HFO during injection phase for the highest background HFO), and molar ratio of Fe over As. The effect of background groundwater pH on SAR performance varies. SAR performance is highest for the base model background groundwater pH (6.85) and lowest for the maximum background groundwater pH (7.66). For the minimum background groundwater pH (5.85) value , SAR performance is slightly lower compared to the base model background pH.

SAR performance is lower for higher levels of background groundwater As but it is important to realized that the absolute amount of As removal is considerably higher at higher levels of background groundwater As than at lower levels of background As (see Chapter 5). These results indicate that a significant amount of As can be removed from groundwater with very high levels of As compared to groundwater with relatively lower levels of As using SAR even though the targeted drinking water standard could not be reached. A high volume of water (≈ 3 V_i) that meets the Bangladesh standard for Fe (1 mg/L) can be extracted during SAR operation (Chapters 3, 4, and 5). Although the extracted water does not meet the drinking water standard for As, it meets the standard for Fe which means it can be useful for various other household purposes including washing and bathing and possibly irrigation.

SAR technology may be useful for locations with background groundwater As concentrations ranging from 50 to 150 μg/L as indicated by the nationwide SAR performance calculations. SAR technology has a small potential for locations with background groundwater As concentrations larger than 150 μg/L (Chapters 3 and 5). 27.5% of the studied locations resulted in SAR performance above 1 and 48.5% of the studied loca-

tions resulted in SAR performance above 0.5, which indicates that the potential for SAR application in Bangladesh is substantial. Note that SAR performance of 0.5 means that injection of 5,000 L of water results in 2,500 L of As safe water, which is enough drinking water for 143 families per day assuming five members per family and 3.5 L/day/capita drinking water [Milton et al., 2006]. The results of this modeling study showed that the lifetime of SAR systems for most of the locations in Bangladesh where SAR performance is above 0.5 can be significant as the average is more than 300 cycles.

6.4. Implications for process-based SAR performance calculations

The results presented in Chapter 5 indicate that it is difficult to predict SAR performance based solely on background groundwater composition. Assessment of SAR performance based on process-based reactive transport modeling is better than based solely on background groundwater composition and is considered to be a novel approach. Therefore, the sole use of the background groundwater composition may not be useful to predict SAR performance. In SAR operation, background groundwater is aerated before injection, hence the composition is changed. The composition of the injection water is therefore not comparable to the background groundwater composition which makes it difficult to predict SAR performance based on background groundwater composition alone. The estimation of SAR performance based on process-based reactive transport modeling may be useful to determine the site-specific applicability of SAR technology for aquifers under strongly reducing condition with different hydrogeochemical settings.

The Sector Development Plan (FY 2011-25): Water Supply and Sanitation Sector in Bangladesh [GoB, 2011] includes a section on SAR and recommends field trials of SAR to determine the technical feasibility and optimum conditions for As removal, optimization of costs, and operational procedures for implementation of SAR by GOs or NGOs. The results of the SAR field studies (2011 to 2014) with different hydrogeochemical settings (Chapters 3 and 4) and cost estimation (see Section 3.4.5 and 6.1) and the preliminary map with potential locations for SAR application (Chapter 5) presented in this thesis can provide useful information for future As mitigation in Bangladesh.

6.5. Directions for future research

The approach of predicting SAR performance using a reactive transport model may be applicable to other deltaic regions with elevated arsenic concentrations and similar hydrogeochemical properties. The Mekong and the Red river delta may be two potential regions for SAR application because geologically these regions are very similar to

Bangladesh [Hug et al., 2008]. The aquifers of these regions are under strongly reducing conditions [Smedley and Kinniburgh, 2002]. The average groundwater composition of the Red river and Mekong delta are more or less similar to Bangladesh [Hug et al., 2008] and may be suitable for SAR application. Geochemical properties such as HFO content (0.2 to 2.5 mol/L) in the Mekong and the Red River delta [Eiche et al., 2008; Postma et al., 2007] is also similar to the Bangladesh range (0.08 to 1.7 mol/L) [Hasan et al., 2007; von Brömssen et al., 2008].

Table 6.1: Assessment of potential for SAR performance for the average groundwater composition of Red River delta (Vietnam), Mekong Delta (Vietnam), and Mekong Delta (Cambodia) as reported in Hug et al. [2008]. P_S was not calculated for Red River delta at 60 (µg/L) of As and for Mekong delta (Vietnam) P_S was not calculated at 30, 50, and 60 (µg/L) of As.

SAR performance	Red River delta	Mekong delta Vietnam	Mekong delta Cambodia
P_S((std = 10 (µg/L))	0	0	0
P_S((std = 15 (µg/L))	0	0.3	0
P_S((std = 20 (µg/L))	0	0.9	0
P_S((std = 30 (µg/L))	0.2	-	0
P_S((std = 50 (µg/L))	1.5	-	0
P_S((std = 60 (µg/L))	-	-	0.1
Groundwater composition	**Red River delta**	**Mekong delta Vietnam**	**Mekong delta Cambodia**
pH	7	6.8	6.9
Alkalinity (mg/L)	512.5	231.8	335.6
Ca (mg/L)	76.1	68.1	44.1
Mg (mg/L)	21.8	63.2	24.3
Si (mg/L)	17.0	20.0	20.0
Fe (mg/L)	13.7	2.6	2.2
P (mg/L)	0.8	0.3	0.5
Mn (mg/L)	0.6	3.4	0.7
As (µg/L)	159.0	39.0	150.0
Standard for As (µg/L)	10	10	50

Arsenic removal using sand filters has been the main mitigation option in Vietnam [Berg et al., 2006]. The dissolved Fe(II) in the precipitates to form HFO when comes in contact with the atmosphere. The dissolved As in the water partly co-precipitates along with Fe(II) during the formation of HFO and partly sorbed onto the newly formed HFO. The sand filters are used to removed the precipitated HFO with sorbed As through filtration or by settling [Hug et al., 2008]. So far there is no effective As mitigation option in use in Cambodia [Chiew et al., 2009]. SAR performance for an average (representative) groundwater composition of the Red river (Vietnam), and Mekong delta (Vietnam and Cambodia) were calculated using the same model discussed in Chapter 5 to obtain

preliminary assessment of the potential of SAR technology for these delta regions. SAR performance was calculated for different drinking water standards. For Vietnam, the guideline for As is 10 µg/L [Sampson et al., 2008], whereas for Cambodia, the guideline for As is 50 µg/L [Agusa et al., 2014]. SAR performance for the red river and Mekong delta are presented in Table 6.1. According to the results the target drinking water standard was not achieved with SAR simulations for the average groundwater composition of the Red river and Mekong delta used in the model. The reasons for not reaching the drinking water standard may be that the average As concentration at the Red River delta is very high to reach the low drinking water standard of 10 µg/L (Table 6.1) but the performance is 1.5 for a standard of 50 µg/L (as used in Bangladesh and Cambodia). For the Mekong delta (Vietnam and Cambodia), the average background Fe concentrations are too low to achieve the drinking water standard (Table 6.1).

Despite the fact that the targeted drinking water standard was not achieved for the three deltas discussed here, a significant amount of water can be extracted with much lower As concentrations compared to the background groundwater As concentration (Table 6.1). Approximately 0.2 V_i (V_i is the volume of injected water) and 1.5 V_i of water can be extracted with As concentration below 30 µg/L and 50 µg/L respectively for the average groundwater composition of Red river delta even after 150 cycles. For the Vietnamese part of the Mekong delta it is 0.3 V_i and 0.9 V_i with As concentrations below 15 µg/L and 20 µg/L, respectively, after 200 cycles. For the Mekong delta of Cambodia, it is 0.1 V_i and 0.5 V_i with As concentration below 60 µg/L and 80 µg/L, respectively, after 47 cycles.

The presence of high levels of natural iron in the groundwater of the Red river delta (Table 6.1) facilitates arsenic removal [Hug et al., 2008]. People in the Vietnamese villages use sand filters to remove dissolved Fe from water. The sand filters remove considerable amount of dissolved arsenic from water during the precipitation of the iron on the surface of the sand. Berg et al. [2006], reported that more than 90% of the tested sand filters were able to reduce the arsenic concentration below 50 µg/L and 40% were able to reduce the concentration below the WHO guideline of 10 µg/L. So, there is a great potential for SAR technology to achieve the drinking water standard for locations in the Red river delta of Vietnam where the dissolved As, P, and Si levels are lower compared to the average value and dissolved Fe is high or within the range of the reported average value (Table 6.1). SAR could be considered as a better As removal option compared to the sand filters in Vietnam (Red river delta) if the drinking water standard of 10 µg/L is achieved, because it can be operated with negligible waste generation compared to the sand filters. The targeted drinking water standard may possibly be achieved for other locations of the Vietnamese and Cambodian part of the Mekong delta where dissolved background Fe levels are higher, and As, P, and Si levels are lower or near the average

values given in Table 6.1. In conclusion, estimation of SAR performance using process-based reactive transport model and field trials of SAR for other deltaic regions similar to Bangladesh deserves further exploration.

Subsurface manganese removal was beyond the scope of this thesis, but elevated manganese concentrations have been reported in Bangladesh groundwater over the past years [BGS and DPHE, 2001; Hasan et al., 2007; Aziz Hasan et al., 2009]. Chronic exposure to manganese through drinking water above the WHO guideline of 0.4 mg/L [WHO, 2006] may have neurological effects. Subsurface manganese removal has been successfully operated in several European countries [Hallberg and Martinell, 1976; Van Beek, 1983] and in Egypt [Olsthoorn, 2000]. Subsurface removal of Mn along with SAR may also be feasible in Bangladesh as indicated by the results presented in Section 4.4.1 of Chapter 4. The results of the RTM also show a reasonable fit with the observed values of Mn in the extracted water. The model fit for the observed values of Mn may be improved by extending and calibrating the model. The process of kinetic oxidation of Mn(II) for the formation of Mn oxides may be included in the model as Mn(II) oxidizes during the aeration phase. The exchange coefficients for Mn may be calibrated for better simulation of Mn sorption on the exchanger. The surface complexation constants for Mn may be calibrated and Mn oxide may be included as a separate surface in the model. Estimation of Mn removal with field experimentation and RTM are an interesting future research topic to asses the potential of subsurface Mn removal along with SAR in Bangladesh.

6.6. Overall Conclusion

Field experiments were conducted at several locations with different hydrogeochemical conditions to assess the potential for subsurface arsenic removal (SAR) technology in Bangladesh. A reactive transport model (RTM) was developed and applied to understand the processes that control the (im)mobilization of arsenic (As) in the shallow aquifer during SAR operation in Bangladesh. The RTM was coupled with a new aeration model with a Python script and used to determine the sensitivity of SAR to different key hydrogeochemical parameters and to quantify and map the potential performance of SAR under different hydrogeochemical settings in Bangladesh. The ultimate goal was to investigate whether the WHO standard of 10 µg/L for As can be reached with SAR technology. The results of this thesis show that the WHO guideline was never achieved with any of the conducted SAR experiments and simulations, but the Bangladesh standard of 50 µg/L for As was achieved at several locations in Bangladesh. The results also show that the potential of SAR technology in Bangladesh is substantial as significant amounts of water that meet the Bangladesh drinking water standard can be extracted at 27.5% of the studied locations. A significant amount of As was removed from the groundwater at

sites where the Bangladesh standard could not be reached. A large volume of water that meets the standard for Fe can be extracted during SAR operation, So that the water can be used for other household purposes besides drinking. Overall, the preliminary map of suitable locations for SAR application presented in this thesis can form the basis for future exploration of the possibilities of SAR in Bangladesh.

REFERENCES

Acharyya, S. K., Chakraborty, P., Lahiri, S., Raymahashay, B. C., Guha, S., and Bhowmik, A.: Arsenic poisoning in the Ganges delta, Nature, 401, 545–547, URL http://www.scopus.com/inward/record.url?eid=2-s2.0-0033533682&partnerID=40&md5=fe29dd64518e38128e7eaf6fc11a6714, 1999.

Agusa, T., Trang, P., Lan, V., Anh, D., Tanabe, S., Viet, P., and Berg, M.: Human exposure to arsenic from drinking water in Vietnam, Science of the Total Environment, 488-489, 562–569, doi:10.1016/j.scitotenv.2013.10.039, 2014.

Ahmed, K., Bhattacharya, P., Hasan, M., Akhter, S., Alam, S., Bhuyian, M., Imam, M., Khan, A., and Sracek, O.: Arsenic enrichment in groundwater of the alluvial aquifers in Bangladesh: An overview, Applied Geochemistry, 19, 181–200, doi:10.1016/j.apgeochem.2003.09.006, 2004.

Akai, J., Izumi, K., Fukuhara, H., Masuda, H., Nakano, S., Yoshimura, T., Ohfuji, H., Md Anawar, H., and Akai, K.: Mineralogical and geomicrobiological investigations on groundwater arsenic enrichment in Bangladesh, Applied Geochemistry, 19, 215–230, doi:10.1016/j.apgeochem.2003.09.008, URL http://www.sciencedirect.com/science/article/pii/S088329270300177X, 2004.

Alam, M. and Sattar, M.: Assessment of arsenic contamination in soils and waters in some areas of Bangladesh, 42, 185–193, 2000.

Alam, M., Hasan, A., Khan, M., and Whitney, J.: Geological map of Bangladesh, Tech. rep., Geological Survey of Bangladesh, Dhaka, 1990.

Ali, M. A., Badruzzaman, A. B. M., Jalil, M. A., Hossain, M. D., Ahmed, M. F., Masud, A. A., Kamruzzaman, M., and Rahman, M. A.: Arsenic in plant-soil environment in Bangladesh, in: Fate of arsenic in the environment. Dhaka: Bangladesh University of Engineering and Technology, pp. 85–112, URL http://www.bvsde.ops-oms.org/bvsacd/arsenico/arsenic/ali2.pdf, 2003.

Allison, J.D., Brown, D.S., and Novo-Gradac, K.J.: MINTEQA2/PRODEFA2–A geochemical assessment model for environmental systems–version 3.0 user's manual: Environmental Research Laboratory, Office of Research and Development, U.S. Environmental Protection Agency, Athens, Georgia, 1990.

Amirbahman, A., Kent, D. B., Curtis, G. P., and Davis, J. A.: Kinetics of sorption and abiotic oxidation of arsenic(III) by aquifer materials, Geochimica et Cosmochimica Acta, 70, 533–547, doi:10.1016/j.gca.2005.10.036, URL http://www.sciencedirect.com/science/article/pii/S0016703705009592, 2006.

Antoniou, E. A., Stuyfzand, P. J., and van Breukelen, B. M.: Reactive transport modeling of an aquifer storage and recovery (ASR) pilot to assess long-term water quality improvements and potential solutions, Applied Geochemistry, 35, 173–186, doi:10.1016/j.apgeochem.2013.04.009, URL http://www.sciencedirect.com/science/article/pii/S0883292713001030, 2013.

Appelo, C., Van Der Weiden, M., Tournassat, C., and Charlet, L.: Surface complexation of ferrous iron and carbonate on ferrihydrite and the mobilization of arsenic, Environmental Science and Technology, 36, 3096–3103, doi:10.1021/es010130n, 2002.

Appelo, C. a. J. and de Vet, W. W. J. M.: Modeling in situ iron removal from groundwater with trace elements such as As, in: Arsenic in Ground Water, edited by Welch, A. H. and Stollenwerk, K. G., pp. 381–401, Springer US, URL http://link.springer.com/chapter/10.1007/0-306-47956-7_14, 2003.

Appelo, C. A. J. and Postma, D.: Geochemistry, Groundwater and Pollution, Second Edition, CRC Press, 2005.

Aziz, Z.: Hydrology and Arsenic Distribution in Shallow Aquifers of Bangladesh, Ph.D. thesis, 2010.

Aziz Hasan, M., Bhattacharya, P., Sracek, O., Ahmed, K., von Brömssen, M., and Jacks, G.: Geological controls on groundwater chemistry and arsenic mobilization: Hydrogeochemical study along an E-W transect in the Meghna basin, Bangladesh, Journal of Hydrology, 378, 105–118, doi:10.1016/j.jhydrol.2009.09.016, 2009.

Bakr, M.: Quaternary Geomorphic Evolution of the Brahmanbaria–Noakhali Area, Comilla and Noakhali District, Bangladesh., Tech. rep., Records of the Geological Survey of Bangladesh., 1977.

Berg, M., Luzi, S., Trang, P., Viet, P., Giger, W., and Stüben, D.: Arsenic removal from groundwater by household sand filters: Comparative field study, model calculations, and health benefits, Environmental Science and Technology, 40, 5567–5573, doi:10.1021/es060144z, 2006.

BGS and DPHE: Final Report. Arsenic contamination of groundwater in Bangladesh, vol. 2. In: Kinniburgh, D.G., Smedley, P.L. (Eds.), Brit. Geol. Surv. (BGS) Technical Report WC/00/19, Tech. rep., British Geological Survey, Keyworth., 2001.

Bhattacharya, P., Chatterjee, D., and Jacks, G.: Occurrence of arsenic-contaminated groundwater in alluvial aquifers from delta plains, eastern India: options for safe drinking water supply, Water Resources Development, 13, 79–92, doi:10.1080/07900629749944, 1997.

Bhattacharya, P., Frisbie, S. H., Smith, E., Naidu, R., Jacks, G., and Sarkar, B.: Arsenic in the environment: a global perspective, in: Heavy Metals in the Environment (Sarkar B, ed). New York: Marcel Dekker Inc, pp. 147–215, 2002a.

Bhattacharya, P., Jacks, G., Ahmed, K., Routh, J., and Khan, A.: Arsenic in groundwater of the Bengal Delta Plain aquifers in Bangladesh, Bulletin of Environmental Contamination and Toxicology, 69, 538–545, doi:10.1007/s00128-002-0095-5, 2002b.

Bhattacharya, P., Ahmed, K. M., Hasan, M. A., Broms, S., Fogelström, J., Jacks, G., Sracek, O., von Brömssen, M., and Routh, J.: Mobility of arsenic in groundwater in a part of Brahmanbaria district, NE Bangladesh, Managing Arsenic in the Environment: From Soil to Human Health. CSIRO Publishing, Melbourne, Australia, pp. 95–115, URL http://books.google.nl/books?hl=en&lr=&id=izVjtgwO_8kC&oi=fnd&pg=PA95&dq=Mobility+of+arsenic+in+groundwater+in+a+part+of+Brahmanbaria+district,+NE+Bangladesh.&ots=8TdB0lBeA8&sig=LV1s_PqVdvYf6c_zqOp0zZL52nc, 2006.

Buschmann, J. and Berg, M.: Impact of sulfate reduction on the scale of arsenic contamination in groundwater of the Mekong, Bengal and Red River deltas, Applied Geochemistry, 24, 1278–1286, doi:10.1016/j.apgeochem.2009.04.002, 2009.

Chakraborti, D., Sengupta, M., Rahman, M., Ahamed, S., Chowdhury, U., Hossain, M., Mukherjee, S., Pati, S., Saha, K., Dutta, R., and Quamruzzaman, Q.: Groundwater arsenic contamination and its health effects in the Ganga-Meghna-Brahmaputra plain., Journal of environmental monitoring : JEM, 6, 74N–83N, 2004.

Chen, C.-J., Chiou, H.-Y., Chiang, M.-H., Lin, L.-J., and Tai, T.-Y.: Dose-response relationship between ischemic heart disease mortality and long-term arsenic exposure, Arteriosclerosis, Thrombosis, and Vascular Biology, 16, 504–510, 1996.

Chen, Y. and Ahsan, H.: Cancer Burden from Arsenic in Drinking Water in Bangladesh, American Journal of Public Health, 94, 741–744, 2004.

Chiew, H., Sampson, M., Huch, S., Ken, S., and Bostick, B.: Effect of groundwater iron and phosphate on the efficacy of arsenic removal by iron-amended bios and filters, Environmental Science and Technology, 43, 6295–6300, doi:10.1021/es803444t, 2009.

Chowdhury, U. K., Biswas, B. K., Chowdhury, T. R., Samanta, G., Mandal, B. K., Basu, G. C., Chanda, C. R., Lodh, D., Saha, K. C., Mukherjee, S. K., Roy, S., Kabir, S., Quamruzzaman, Q., and Chakraborti, D.: Groundwater arsenic contamination in Bangladesh and West Bengal, India., Environmental Health Perspectives, 108, 393–397, URL http://www.ncbi.nlm.nih.gov/pmc/articles/PMC1638054/, 2000.

Clifford, D., Ceber, L., and Chow, S.: Arsenic(III)/arsenic(V) separation by chloride-form ion exchange resins. XI. AWWA Water Qual. Tech. Conf., Norfolk, VA., 1983.

Darland, J. and Inskeep, W.: Effects of pore water velocity on the transport of arsenate, Environmental Science and Technology, 31, 704–709, doi:10.1021/es960247p, 1997.

De Vitre, R., Belzile, N., and Tessier, A.: Speciation and adsorption of arsenic on diagenetic iron oxyhydroxides, Limnology & Oceanography, 36, 1480–1485, 1991.

Descourvieres, C., Prommer, H., Oldham, C., Greskowiak, J., and Hartog, N.: Kinetic reaction modeling framework for identifying and quantifying reductant reactivity in heterogeneous aquifer sediments, Environmental Science and Technology, 44, 6698–6705, doi:10.1021/es101661u, 2010.

Dixit, S. and Hering, J.: Comparison of arsenic(V) and arsenic(III) sorption onto iron oxide minerals: Implications for arsenic mobility, Environmental Science and Technology, 37, 4182–4189, doi:10.1021/es030309t, 2003.

Dowling, C., Poreda, R., Basu, A., Peters, S., and Aggarwal, P.: Geochemical study of arsenic release mechanisms in the Bengal Basin groundwater, Water Resources Research, 38, 121–1218, 2002.

Driehaus, W., Seith, R., and Jekel, M.: Oxidation of arsenate(III) with manganese oxides in water treatment, Water Research, 29, 297–305, doi:10.1016/0043-1354(94)E0089-O, URL http://www.sciencedirect.com/science/article/pii/0043135494E0089O, 1995.

Dzombak, D. A. and Morel, F. M. M.: Surface Complexation Modeling: Hydrous Ferric Oxide, John Wiley & Sons, 1990.

Eiche, E., Neumann, T., Berg, M., Weinman, B., van Geen, A., Norra, S., Berner, Z., Trang, P., Viet, P., and Stüben, D.: Geochemical processes underlying a sharp contrast in groundwater arsenic concentrations in a village on the Red River delta, Vietnam, Applied Geochemistry, 23, 3143–3154, doi:10.1016/j.apgeochem.2008.06.023, 2008.

Freitas, S., Van Halem, D., Rahman, M., Verberk, J., Badruzzaman, A., and Van Der Meer, W.: Hand-pump subsurface arsenic removal: The effect of groundwater conditions and intermittent operation, 14, 2014.

GoB: Sector Development Plan (FY 2011-25): Water Supply and Sanitation Sector in Bangladesh. Local Government Division, Ministry of Local government, Rural Development and Cooperatives, Government of Bangladesh., Tech. rep., 2011.

GRG and HG: The status of arsenic transport in the deep wells at Manikganj district town. Final Report for Research and Development. DPHE, Water and Environmental Sanitation Section, UCICEF, Bangladesh, Tech. rep., 2002.

Guan, X., Ma, J., Dong, H., and Jiang, L.: Removal of arsenic from water: Effect of calcium ions on As(III) removal in the KMnO4-Fe(II) process, Water Research, 43, 5119–5128, URL http://www.scopus.com/inward/record.url?eid=2-s2.0-70649100406&partnerID=40&md5=a874a3168f8da2a845fb7ba0dcbd857b, 2009.

Hallberg, R. O. and Martinell, R.: Vyredox — In Situ Purification of Ground Water, Ground Water, 14, 88–93, doi:10.1111/j.1745-6584.1976.tb03638.x, URL http://onlinelibrary.wiley.com/doi/10.1111/j.1745-6584.1976.tb03638.x/abstract, 1976.

Harvey, C., Swartz, C., Badruzzaman, A., Keon-Blute, N., Yu, W., Ali, M., Jay, J., Beckie, R., Niedan, V., Brabander, D., Oates, P., Ashfaque, K., Islam, S., Hemond, H., and Ahmed, M.: Arsenic mobility and groundwater extraction in Bangladesh, Science, 298, 1602–1606, doi:10.1126/science.1076978, 2002.

Harvey, C., Ashfaque, K., Yu, W., Badruzzaman, A., Ali, M., Oates, P., Michael, H., Neumann, R., Beckie, R., Islam, S., and Ahmed, M.: Groundwater dynamics and arsenic contamination in Bangladesh, Chemical Geology, 228, 112–136, doi:10.1016/j.chemgeo.2005.11.025, 2006.

Hasan, M., Ahmed, K., Sracek, O., Bhattacharya, P., Brömssen, M., Broms, S., Fogelström, J., Mazumder, M., and Jacks, G.: Arsenic in shallow groundwater of Bangladesh: Investigations from three different physiographic settings, Hydrogeology Journal, 15, 1507–1522, doi:10.1007/s10040-007-0203-z, 2007.

Hasan, M. A., Brömssen, M. v., Bhattacharya, P., Ahmed, K. M., Sikder, A. M., Jacks, G., and Sracek, O.: Geochemistry and mineralogy of shallow alluvial aquifers in Daudkandi upazila in the Meghna flood plain, Bangladesh, Environmental Geology, 57, 499–511, doi:10.1007/s00254-008-1319-8, URL http://link.springer.com/article/10.1007/s00254-008-1319-8, 2009.

Hassan, Z., Sultana, M., van Breukelen, B. M., Khan, S. I., and Röling, W. F. M.: Diverse arsenic- and iron-cycling microbial communities in arsenic-contaminated aquifers used for drinking water in Bangladesh, FEMS microbiology ecology, doi:10.1093/femsec/fiv026, 2015.

Heikens, A., Panaullah, G. M., and Meharg, A. A.: Arsenic behaviour from groundwater and soil to crops: impacts on agriculture and food safety, Reviews of Environmental Contamination and Toxicology, 189, 43–87, 2007.

Hossain, M., Jahiruddin, M., Panaullah, G., Loeppert, R., Islam, M., and Duxbury, J.: Spatial variability of arsenic concentration in soils and plants, and its relationship with iron, manganese and phosphorus, Environmental Pollution, 156, 739–744, doi:10.1016/j.envpol.2008.06.015, 2008.

Hug, S., Leupin, O., and Berg, M.: Bangladesh and Vietnam: Different groundwater compositions require different approaches to arsenic mitigation, Environmental Science and Technology, 42, 6318–6323, doi:10.1021/es7028284, 2008.

Hug, S. J. and Leupin, O.: Iron-Catalyzed Oxidation of Arsenic(III) by Oxygen and by Hydrogen Peroxide: pH Dependent Formation of Oxidants in the Fenton Reaction, Environmental Science & Technology, 37, 2734–2742, doi:10.1021/es026208x, URL http://dx.doi.org/10.1021/es026208x, 2003.

Huq, S. I., Rahman, A., Sultana, N., and Naidu, R.: Extent and severity of arsenic contamination in soils of Bangladesh, Fate of arsenic in the environment. Dhaka: Bangladesh University of Engineering and Technology, pp. 69–84, URL http://www.researchgate.net/publication/237281636_Extent_and_Severity_of_Arsenic_Contamination_in_Soils_of_Bangladesh/file/60b7d52cbdfa457096.pdf, 2003.

Islam, F., Gault, A., Boothman, C., Polya, D., Chamok, J., Chatterjee, D., and Lloyd, J.: Role of metal-reducing bacteria in arsenic release from Bengal delta sediments, Nature, 430, 68–71, doi:10.1038/nature02638, 2004.

Itai, T., Takahashi, Y., Seddique, A., Maruoka, T., and Mitamura, M.: Variations in the redox state of As and Fe measured by X-ray absorption spectroscopy in aquifers of Bangladesh and their effect on As adsorption, Applied Geochemistry, 25, 34–47, doi:10.1016/j.apgeochem.2009.09.026, 2010.

Jakariya, M., Rahman, M., Chowdhury, A., Rahman, M., Yunus, M., Bhiuya, A., Wahed, M., Bhattacharya, P., Jacks, G., Vahter, M., and Persson, L.-.: Sustainable safe water

options in Bangladesh: Experiences from the Arsenic Project at Matlab (AsMat), pp. 319–330, 2005.

Jakariya, M., Von Brömssen, M., Jacks, G., Chowdhury, A., Ahmed, K., and Bhattacharya, P.: Searching for a sustainable arsenic mitigation strategy in Bangladesh: Experience from two upazilas, International Journal of Environment and Pollution, 31, 415–430, doi:10.1504/IJEP.2007.016506, 2007.

Jessen, S., Postma, D., Larsen, F., Nhan, P., Hoa, L., Trang, P., Long, T., Viet, P., and Jakobsen, R.: Surface complexation modeling of groundwater arsenic mobility: Results of a forced gradient experiment in a Red River flood plain aquifer, Vietnam, Geochimica et Cosmochimica Acta, 98, 186–201, doi:10.1016/j.gca.2012.07.014, 2012.

JICA and DPHE: Situation analysis of arsenic mitigation, Tech. rep., Japan international cooperation agency and Department of public health and engineering, 2009.

Johnston, R., Heijnen, H., and Wurzel, P.: Chapter 6: Safe water technology, United Nations Synthesis Report on Arsenic in Drinking-Water, 2001.

Johnston, R., Hanchett, S., and Khan, M.: The socio-economics of arsenic removal, Nature Geoscience, 3, 2–3, doi:10.1038/ngeo735, 2010.

Kartinen Jr., E. and Martin, C.: An overview of arsenic removal processes, Desalination, 103, 79–88, 1995.

Khan, M., Islam, M., Panaullah, G., Duxbury, J., Jahiruddin, M., and Loeppert, R.: Fate of irrigation-water arsenic in rice soils of Bangladesh, Plant and Soil, 322, 263–277, doi:10.1007/s11104-009-9914-3, 2009.

Kirk, M., Holm, T., Park, J., Jin, Q., Sanford, R., Fouke, B., and Bethke, C.: Bacterial sulfate reduction limits natural arsenic contamination in groundwater, Geology, 32, 953–956, doi:10.1130/G20842.1, 2004.

Kocar, B., Polizzotto, M., Benner, S., Ying, S., Ung, M., Ouch, K., Samreth, S., Suy, B., Phan, K., Sampson, M., and Fendorf, S.: Integrated biogeochemical and hydrologic processes driving arsenic release from shallow sediments to groundwaters of the Mekong delta, Applied Geochemistry, 23, 3059–3071, doi:10.1016/j.apgeochem.2008.06.026, 2008.

Koerth-Baker, M.: Presidents Before Trump Have Meddled With The EPA — It Didn't Go Well, URL https://fivethirtyeight.com/features/presidents-before-trump-have-meddled-with-the-epa-it-didnt-go-well/, 2017.

Konert, M. and Vandenberghe, J.: Comparison of laser grain size analysis with pipette and sieve analysis: A solution for the underestimation of the clay fraction, Sedimentology, 44, 523–535, 1997.

Kundu, D., Gupta, A., Mol, A., and Nasreen, M.: Understanding social acceptability of arsenic-safe technologies in rural Bangladesh: A user-oriented analysis, Water Policy, 18, 318–334, doi:10.2166/wp.2015.026, 2016a.

Kundu, D., Mola, A., and Gupta, A.: Failing arsenic mitigation technology in rural Bangladesh: Explaining stagnation in niche formation of the Sono filter, Water Policy, 18, 1490–1507, doi:10.2166/wp.2016.014, 2016b.

Liger, E., Charlet, L., and Van Cappellen, P.: Surface catalysis of uranium(VI) reduction by iron(II), Geochimica et Cosmochimica Acta, 63, 2939–2955, doi:10.1016/S0016-7037(99)00265-3, 1999.

Lowers, H., Breit, G., Foster, A., Whitney, J., Yount, J., Uddin, M., and Muneem, A.: Arsenic incorporation into authigenic pyrite, Bengal Basin sediment, Bangladesh>, Geochimica et Cosmochimica Acta, 71, 2699–2717, doi:10.1016/j.gca.2007.03.022, 2007.

Manning, B., Hunt, M., Amrhein, C., and Yarmoff, J.: Arsenic(III) and arsenic(V) reactions with zerovalent iron corrosion products, Environmental Science and Technology, 36, 5455–5461, doi:10.1021/es0206846, 2002a.

Manning, B. A., Fendorf, S. E., Bostick, B., and Suarez, D. L.: Arsenic(III) Oxidation and Arsenic(V) Adsorption Reactions on Synthetic Birnessite, Environmental Science & Technology, 36, 976–981, doi:10.1021/es0110170, URL http://dx.doi.org/10.1021/es0110170, 2002b.

McArthur, J., Ravenscroft, P., Safiulla, S., and Thirlwall, M.: Arsenic in groundwater: Testing pollution mechanisms for sedimentary aquifers in Bangladesh, Water Resources Research, 37, 109–117, doi:10.1029/2000WR900270, 2001.

McArthur, J., Banerjee, D., Hudson-Edwards, K., Mishra, R., Purohit, R., Ravenscroft, P., Cronin, A., Howarth, R., Chatterjee, A., Talukder, T., Lowry, D., Houghton, S., and Chadha, D.: Natural organic matter in sedimentary basins and its relation to arsenic in anoxic ground water: The example of West Bengal and its worldwide implications, Applied Geochemistry, 19, 1255–1293, doi:10.1016/j.apgeochem.2004.02.001, 2004.

Meharg, A. and Rahman, M.: Arsenic contamination of Bangladesh paddy field soils: Implications for rice contribution to arsenic consumption, Environmental Science and Technology, 37, 229–234, doi:10.1021/es0259842, 2003.

Meharg, A., Scrimgeour, C., Hossain, S., Fuller, K., Cruickshank, K., Williams, P., and Kinniburgh, D.: Codeposition of organic carbon and arsenic in Bengal Delta aquifers, Environmental Science and Technology, 40, 4928–4935, doi:10.1021/es060722b, 2006.

Meng, X., Bang, S., and Korfiatis, G.: Effects of silicate, sulfate, and carbonate on arsenic removal by ferric chloride, Water Research, 34, 1255–1261, doi:10.1016/S0043-1354(99)00272-9, 2000.

Meng, X., Korfiatis, G., Bang, S., and Bang, K.: Combined effects of anions on arsenic removal by iron hydroxides, Toxicology Letters, 133, 103–111, doi:10.1016/S0378-4274(02)00080-2, 2002.

Meng, Z. G., Korfiatis, G. P., Christodoulatos, C., and Bang, S.: Treatment of arsenic in Bangladesh well water using a household coprecipitation and filtration system., Water Res., pp. 2805–2810, 2001.

Meyerhoff, R.: Planning and application of in situ iron and manganese treatment of groundwater: Ber. Siedlungswasserbau, v. 139, University of Stuttgart, Germany. (in German)., 139, 1996.

Milton, A., Smith, W., Rahman, H., Shrestha, R., and Dear, K.: Water consumption patterns in rural Bangladesh: are we underestimating total arsenic load?, URL http://www.iwaponline.com/jwh/004/jwh0040431.htm, 2006.

Morgan, J. P. and McINTIRE, W. G.: Quaternary Geology of the Bengal Basin, East Pakistan and India, Geological Society of America Bulletin, 70, 319–342, doi:10.1130/0016-7606(1959)70[319:QGOTBB]2.0.CO;2, URL http://gsabulletin.gsapubs.org/content/70/3/319, 1959.

Mukherjee, A., Bhattacharya, P., Shi, F., Fryar, A. E., Mukherjee, A. B., Xie, Z. M., Jacks, G., and Bundschuh, J.: Chemical evolution in the high arsenic groundwater of the Huhhot basin (Inner Mongolia, PR China) and its difference from the western Bengal basin (India), Applied Geochemistry, 24, 1835–1851, doi:10.1016/j.apgeochem.2009.06.005, URL http://www.sciencedirect.com/science/article/pii/S0883292709001851, 2009.

Neumann, R., Ashfaque, K., Badruzzaman, A., Ashraf Ali, M., Shoemaker, J., and Harvey, C.: Anthropogenic influences on groundwater arsenic concentrations in Bangladesh, Nature Geoscience, 3, 46–52, doi:10.1038/ngeo685, 2010.

Nickson, R., McArthur, J., Burgess, W., Matin Ahmed, K., Ravenscroft, P., and Rahman, M.: Arsenic poisoning of Bangladesh groundwater, Nature, 395, 338, doi:10.1038/26387, 1998.

Nickson, R., Mcarthur, J., Ravenscroft, P., Burgess, W., and Ahmed, K.: Mechanism of arsenic release to groundwater, Bangladesh and West Bengal, Applied Geochemistry, 15, 403–413, doi:10.1016/S0883-2927(99)00086-4, 2000.

Nordstrom, D.: Worldwide occurrences of arsenic in ground water, Science, 296, 2002.

Norra, S., Berner, Z., Agarwala, P., Wagner, F., Chandrasekharam, D., and Stüben, D.: Impact of irrigation with As rich groundwater on soil and crops: A geochemical case study in West Bengal Delta Plain, India, Applied Geochemistry, 20, 1890–1906, doi:10.1016/j.apgeochem.2005.04.019, 2005.

Nriagu, J., Bhattacharya, P., Mukherjee, A., Bundschuh, J., Zevenhoven, R., and Loeppert, R.: Arsenic in soil and groundwater: an overview, vol. 9 of *Trace Metals and other Contaminants in the Environment*, 2007.

O'Day, P., Vlassopoulos, D., Root, R., and Rivera, N.: The influence of sulfur and iron on dissolved arsenic concentrations in the shallow subsurface under changing redox conditions, Proceedings of the National Academy of Sciences of the United States of America, 101, 13 703–13 708, doi:10.1073/pnas.0402775101, 2004.

Olsthoorn, T. N.: Background of subsurface iron and manganese removal. Amsterdam Water Supply Research and Development, Hydrology Department., 2000.

Oremland, R. and Stolz, J.: The ecology of arsenic, Science, 300, 939–944, doi:10.1126/science.1081903, 2003.

Oscarson, D. W., Huang, P. M., Defosse, C., and Herbillon, A.: Oxidative power of Mn(IV) and Fe(III) oxides with respect to As(III) in terrestrial and aquatic environments, Nature, 291, 50–51, doi:10.1038/291050a0, URL http://www.nature.com/nature/journal/v291/n5810/abs/291050a0.html#close, 1981.

Oscarson, D. W., Huang, P. M., Hammer, U. T., and Liaw, W. K.: Oxidation and sorption of arsenite by manganese dioxide as influenced by surface coatings of iron and aluminum oxides and calcium carbonate, Water, Air, and Soil Pollution, 20, 233–244, doi:10.1007/BF00279633, URL http://link.springer.com/article/10.1007/BF00279633, 1983a.

Oscarson, D. W., Huang, P. M., Liaw, W. K., and Hammer, U. T.: Kinetics of Oxidation of Arsenite by Various Manganese Dioxides1, Soil Science Society of America Journal, 47, 644, doi:10.2136/sssaj1983.03615995004700040007x, URL https://dl.sciencesocieties.org/publications/sssaj/abstracts/47/4/SS0470040644, 1983b.

Panaullah, G., Alam, T., Hossain, M., Loeppert, R., Lauren, J., Meisner, C., Ahmed, Z., and Duxbury, J.: Arsenic toxicity to rice (Oryza sativa L.) in Bangladesh, Plant and Soil, 317, 31–39, doi:10.1007/s11104-008-9786-y, 2009.

Parkhurst, D. L., Appelo, C. A. J., and others: User's guide to PHREEQC (Version 2): A computer program for speciation, batch-reaction, one-dimensional transport, and inverse geochemical calculations, URL ftp://ceres.udc.es/Master_en_Ingenieria_del_Agua/master%20antiguo_antes%20del%202012/Segundo_Curso/Modelos_de_Calidad_de_Aguas/Phreeqc%20Interactive%202.15.0/Doc/manual.pdf, 1999.

Patel, K., Shrivas, K., Brandt, R., Jakubowski, N., Corns, W., and Hoffmann, P.: Arsenic contamination in water, soil, sediment and rice of central India, Environmental Geochemistry and Health, 27, 131–145, doi:10.1007/s10653-005-0120-9, 2005.

Plummer, L., Wigley, T., and Parkhurst, D.: KINETICS OF CALCITE DISSOLUTION IN CO//2-WATER SYSTEMS AT 5 degree TO 60 degree C AND 0. 0 TO 1. 0 ATM CO//2., Am J Sci, 278, 179–216, 1978.

Polizzotto, M., Harvey, C., Li, G., Badruzzman, B., Ali, A., Newville, M., Sutton, S., and Fendorf, S.: Solid-phases and desorption processes of arsenic within Bangladesh sediments, Chemical Geology, 228, 97–111, doi:10.1016/j.chemgeo.2005.11.026, 2006.

Polizzotto, M., Kocar, B., Benner, S., Sampson, M., and Fendorf, S.: Near-surface wetland sediments as a source of arsenic release to ground water in Asia, Nature, 454, 505–508, doi:10.1038/nature07093, 2008.

Postma, D., Larsen, F., Minh Hue, N., Duc, M., Viet, P., Nhan, P., and Jessen, S.: Arsenic in groundwater of the Red River floodplain, Vietnam: Controlling geochemical processes and reactive transport modeling, Geochimica et Cosmochimica Acta, 71, 5054–5071, doi:10.1016/j.gca.2007.08.020, 2007.

Postma, D., Jessen, S., Hue, N., Duc, M., Koch, C., Viet, P., Nhan, P., and Larsen, F.: Mobilization of arsenic and iron from Red River floodplain sediments, Vietnam, Geochimica et Cosmochimica Acta, 74, 3367–3381, doi:10.1016/j.gca.2010.03.024, 2010.

Quicksall, A., Bostick, B., and Sampson, M.: Linking organic matter deposition and iron mineral transformations to groundwater arsenic levels in the Mekong delta, Cambodia, Applied Geochemistry, 23, 3088–3098, doi:10.1016/j.apgeochem.2008.06.027, 2008.

Radu, T., Subacz, J., Phillippi, J., and Barnett, M.: Effects of dissolved carbonate on arsenic adsorption and mobility, Environmental Science and Technology, 39, 7875–7882, doi:10.1021/es050481s, 2005.

Rahman, M., Bakker, M., Freitas, S., Van Halem, D., van Breukelen, B., Ahmed, K., and Badruzzaman, A.: Exploratory experiments to determine the effect of alternative operations on the efficiency of subsurface arsenic removal in rural Bangladesh, Hydrogeology Journal, 23, 19–34, doi:10.1007/s10040-014-1179-0, 2014.

Rahman, M., Bakker, M., Patty, C., Hassan, Z., Röling, W., Ahmed, K., and van Breukelen, B.: Reactive transport modeling of subsurface arsenic removal systems in rural Bangladesh, Science of the Total Environment, 537, 277–293, doi:10.1016/j.scitotenv.2015.07.140, 2015.

Ravenscroft, P., Burgess, W., Ahmed, K., Burren, M., and Perrin, J.: Arsenic in groundwater of the Bengal Basin, Bangladesh: Distribution, field relations, and hydrogeological setting, Hydrogeology Journal, 13, 727–751, doi:10.1007/s10040-003-0314-0, 2005.

Ravenscroft, P., Brammer, H., and Richards, K.: Arsenic Pollution: A Global Synthesis, John Wiley & Sons, 2009.

Robinson, C., Brömssen, M., Bhattacharya, P., Häller, S., Bivén, A., Hossain, M., Jacks, G., Ahmed, K., Hasan, M., and Thunvik, R.: Dynamics of arsenic adsorption in the targeted arsenic-safe aquifers in Matlab, south-eastern Bangladesh: Insight from experimental studies, Applied Geochemistry, 26, 624–635, doi:10.1016/j.apgeochem.2011.01.019, 2011.

Rott, U., Meyer, C., and Friedle, M.: Residue-free removal of arsenic, iron, manganese and ammonia from groundwater, vol. 2 of *Water Science and Technology: Water Supply*, 2002.

Safari, I., Hsieh, M.-K., Chien, S.-H., Walker, M. E., Vidic, R. D., Dzombak, D. A., and Abbasian, J.: Effect of CO2 stripping on pH in open-recirculating cooling water systems, Environmental Progress & Sustainable Energy, 33, 275–282, doi:10.1002/ep.11769, URL http://doi.wiley.com/10.1002/ep.11769, 2014.

Sampson, M., Bostick, B., Chiew, H., Hagan, J., and Shantz, A.: Arsenicosis in Cambodia: Case studies and policy response, Applied Geochemistry, 23, 2976–2985, doi:10.1016/j.apgeochem.2008.06.022, 2008.

Sarkar, A. R. and Rahman, O. T.: In-situ removal of arsenic -experiences of DPHE-Danida pilot project. Technologies for Arsenic Removal from Drinking Water. Bangladesh

University of Engineering and Technology and The United Nations University, Bangladesh., 2001.

Sen Gupta, B., Chatterjee, S., Rott, U., Kauffman, H., Bandopadhyay, A., DeGroot, W., Nag, N., Carbonell-Barrachina, A., and Mukherjee, S.: A simple chemical free arsenic removal method for community water supply - A case study from West Bengal, India, Environmental Pollution, 157, 3351–3353, doi:10.1016/j.envpol.2009.09.014, 2009.

Shafiquzzaman, M., Azam, M. S., Mishima, I., and Nakajima, J.: Technical and Social Evaluation of Arsenic Mitigation in Rural Bangladesh, Journal of Health, Population, and Nutrition, 27, 674–683, URL http://www.ncbi.nlm.nih.gov/pmc/articles/PMC2928078/, 2009.

Shamsudduha, M., Uddin, A., Saunders, J., and Lee, M.-K.: Quaternary stratigraphy, sediment characteristics and geochemistry of arsenic-contaminated alluvial aquifers in the Ganges-Brahmaputra floodplain in central Bangladesh, Journal of Contaminant Hydrology, 99, 112–136, doi:10.1016/j.jconhyd.2008.03.010, 2008.

Sharma, P., Rolle, M., Kocar, B., Fendorf, S., and Kappler, A.: Influence of natural organic matter on as transport and retention, Environmental Science and Technology, 45, 546–553, doi:10.1021/es1026008, 2011.

Sharma, S. K.: Adsorptive iron removal from groundwater. PhD Dissertation. Wageningen University., 2001.

Singer, P. and Stumm, W.: Acidic mine drainage: The rate-determining step, Science, 167, 1121–1123, 1970.

Smedley, P. and Kinniburgh, D.: A review of the source, behaviour and distribution of arsenic in natural waters, Applied Geochemistry, 17, 517–568, doi:10.1016/S0883-2927(02)00018-5, 2002.

Stollenwerk, K., Breit, G., Welch, A., Yount, J., Whitney, J., Foster, A., Uddin, M., Majumder, R., and Ahmed, N.: Arsenic attenuation by oxidized aquifer sediments in Bangladesh, Science of the Total Environment, 379, 133–150, doi:10.1016/j.scitotenv.2006.11.029, 2007.

Stumm, W. and Lee, G. F.: Oxygenation of Ferrous Iron, Industrial & Engineering Chemistry, 53, 143–146, doi:10.1021/ie50614a030, URL http://dx.doi.org/10.1021/ie50614a030, 1961.

Su, C. and Puls, R.: Arsenate and arsenite removal by zerovalent iron: Effects of phosphate, silicate, carbonate, borate, sulfate, chromate, molybdate, and nitrate, relative to chloride, Environmental Science and Technology, 35, 4562–4568, doi:10.1021/es010768z, 2001.

Sun, X. and Doner, H.: Adsorption and oxidation of arsenite on goethite, Soil Science, 163, 278–287, 1998.

Sutherland, D., Swash, P., Macqueen, A., McWilliam, L., Ross, D., and Wood, S.: A field based evaluation of household arsenic removal technologies for the treatment of drinking water, Environmental Technology, 23, 1385–1404, 2002.

Swartz, C., Blute, N., Badruzzman, B., Ali, A., Brabander, D., Jay, J., Besancon, J., Islam, S., Hemond, H., and Harvey, C.: Mobility of arsenic in a Bangladesh aquifer: Inferences from geochemical profiles, leaching data, and mineralogical characterization, Geochimica et Cosmochimica Acta, 68, 4539–4557, doi:10.1016/j.gca.2004.04.020, 2004.

Swedlund, P. and Webster, J.: Adsorption and polymerisation of silicic acid on ferrihydrite, and its effect on arsenic adsorption, Water Research, 33, 3413–3422, doi:10.1016/S0043-1354(99)00055-X, 1999.

Uddin, A. and Lundberg, N.: Cenozoic history of the Himalayan-Bengal system: Sand composition in the Bengal basin, Bangladesh, Geological Society of America Bulletin, 110, 497–511, doi:10.1130/0016-7606(1998)110<0497:CHOTHB>2.3.CO;2, URL http://gsabulletin.gsapubs.org/content/110/4/497, 1998.

Van Beek, C.: Ondergrondse ontijzering, een evaluatie van uitgevoerd onderzoek (in Dutch). KIWA mededeling 78., 1983.

Van Beek, C.: Experiences with underground water treatment in the Netherlands, Water Supply, 3, 1–11, 1985.

Van Breukelen, B. and Rolle, M.: Transverse hydrodynamic dispersion effects on isotope signals in groundwater chlorinated solvents plumes, Environmental Science and Technology, 46, 7700–7708, doi:10.1021/es301058z, 2012.

van Geen, A., Rose, J., Thoral, S., Garnier, J., Zheng, Y., and Bottero, J.: Decoupling of As and Fe release to Bangladesh groundwater under reducing conditions. Part II: Evidence from sediment incubations, Geochimica et Cosmochimica Acta, 68, 3475–3486, doi:10.1016/j.gca.2004.02.014, 2004.

van Geen, A., Zheng, Y., Cheng, Z., He, Y., Dhar, R., Garnier, J., Rose, J., Seddique, A., Hoque, M., and Ahmed, K.: Impact of irrigating rice paddies with groundwater containing arsenic in Bangladesh, Science of the Total Environment, 367, 769–777, doi:10.1016/j.scitotenv.2006.01.030, 2006.

Van Halem, D.: Subsurface Iron and Arsenic Removal for drinking water treatment in Bangladesh, Ph.D. thesis, 2011.

Van Halem, D., Heijman, S., Amy, G., and van Dijk, J.: Subsurface arsenic removal for small-scale application in developing countries, Desalination, 248, 241–248, doi:10.1016/j.desal.2008.05.061, 2009.

Van Halem, D., Heijman, S., Johnston, R., Huq, I., Ghosh, S., Verberk, J., Amy, G., and Van Dijk, J.: Subsurface iron and arsenic removal: Low-cost technology for community-based water supply in Bangladesh, Water Science and Technology, 62, 2702–2709, doi:10.2166/wst.2010.463, 2010a.

Van Halem, D., Olivero, S., de Vet, W., Verberk, J., Amy, G., and van Dijk, J.: Subsurface iron and arsenic removal for shallow tube well drinking water supply in rural Bangladesh, Water Research, 44, 5761–5769, doi:10.1016/j.watres.2010.05.049, 2010b.

Veling, E. and Maas, C.: Strategy for solving semi-analytically three-dimensional transient flow in a coupled N-layer aquifer system, Journal of Engineering Mathematics, 64, 145–161, doi:10.1007/s10665-008-9256-9, 2009.

von Brömssen, M., Häller Larsson, S., Bhattacharya, P., Hasan, M., Ahmed, K., Jakariya, M., Sikder, M., Sracek, O., Bivén, A., Doušová, B., Patriarca, C., Thunvik, R., and Jacks, G.: Geochemical characterisation of shallow aquifer sediments of Matlab Upazila, Southeastern Bangladesh - Implications for targeting low-As aquifers, Journal of Contaminant Hydrology, 99, 137–149, doi:10.1016/j.jconhyd.2008.05.005, 2008.

Wallis, I., Prommer, H., Simmons, C., Post, V., and Stuyfzand, P.: Evaluation of conceptual and numerical models for arsenic mobilization and attenuation during managed aquifer recharge, Environmental Science and Technology, 44, 5035–5041, doi:10.1021/es100463q, 2010.

Wallis, I., Prommer, H., Pichler, T., Post, V., B. Norton, S., Annable, M., and Simmons, C.: Process-based reactive transport model to quantify arsenic mobility during aquifer storage and recovery of potable water, Environmental Science and Technology, 45, 6924–6931, doi:10.1021/es201286c, 2011.

Waltham, C. and Eick, M.: Kinetics of arsenic adsorption on goethite in the presence of sorbed silicic acid, Soil Science Society of America Journal, 66, 818–825, 2002.

Wasserman, G., Liu, X., Parvez, F., Ahsan, H., Factor-Litvak, P., van Geen, A., Slavkovich, V., Lolacono, N., Cheng, Z., Hussain, I., Momotaj, H., and Graziano, J.: Water arsenic exposure and children's intellectual function in Araihazar, Bangladesh, Environmental Health Perspectives, 112, 1329–1333, doi:10.1289/ehp.6964, 2004.

WHO: Guidelines for Drinking-water Quality: First addendum to volume 1, Recommendations, World Health Organization, 2006.

WHO: Guidelines for Drinking-water Quality, World Health Organization, 2011.

Wilkie, J. A. and Hering, J. G.: Adsorption of arsenic onto hydrous ferric oxide: effects of adsorbate/adsorbent ratios and co-occurring solutes, Colloids and Surfaces A: Physicochemical and Engineering Aspects, 107, 97–110, doi:10.1016/0927-7757(95)03368-8, URL http://www.sciencedirect.com/science/article/pii/0927775795033688, 1996.

WRI: World resources 1998-99., 1998.

Yu, W., Harvey, C., and Harvey, C.: Arsenic in groundwater in Bangladesh: A geostatistical and epidemiological framework for evaluating health effects and potential remedies, Water Resources Research, 39, WES11–WES117, 2003.

Zheng, Y., Stute, M., Van Geen, A., Gavrieli, I., Dhar, R., Simpson, H., Schlosser, P., and Ahmed, K.: Redox control of arsenic mobilization in Bangladesh groundwater, Applied Geochemistry, 19, 201–214, doi:10.1016/j.apgeochem.2003.09.007, 2004.

ACKNOWLEDGMENT

I am extremely grateful to Almighty for enabling me to pursue my PhD degree. With the blessings of him I have successfully completed my PhD thesis, which was quite difficult some times, especially in the middle of my PhD endeavor.

I would like to acknowledge and thank many people for their help while conducting this PhD research.

First of all, I would like to express my greatest gratitude and heartfelt respect to my supervisor and promotor, Professor Mark Bakker, for giving me the opportunity to work as a PhD student under his supervision. I am extremely grateful to Mark for his immense contribution from the very beginning to the very end of my PhD research period. I learned a lot from Mark throughout the period of my research as a PhD student. I thank him from the bottom of my heart for his outstanding supervision through his scientific knowledge, superb guidance, enthusiasm to help, extreme tolerance and interest.

I express my sincere gratitude and thanks to my co-promotor, Dr. Boris M. van Breukelen for being with me during the entire period of my PhD research. I am grateful to Boris for his continuous support and valuable input regarding my PHREEQC model setup and, field experimental design. I am also highly thankful to Boris for his continuous support even when I was not in the Netherlands. Without his kind support and guidance it would have been impossible for me to finish my PhD. Moreover, it would not have been possible to submit the thesis to the committee members without his critical reviews and proper guidance.

Now I have the honor to express my earnest thanks and gratitude to the person who has been my mentor and guru since 2005, Professor Kazi Matin Uddin Ahmed, University of Dhaka for his interest and careful supervision and guidance right from the beginning of my thesis work and for providing necessary papers and references to conduct fieldwork in Bangladesh and finally for helping me to complete this research work successfully. This PhD thesis would not have been possible without his unconditional inputs. I am deeply in debt to Professor Kazi Matin Uddin Ahmed.

I am thankful to all the PhD supervisors and PhD students of the NWO WOTRO project: Dr. Doris van Halem (TU Delft), Dr. Wilfred F.M. Röling (VU Amsterdam) who tragically died in 2015, Prof. M. Nasreen (University of Dhaka), Prof. A.B.M. Badruzzaman (BUET), Prof. Sirajul Islam Khan (University of Dhaka), Dr. Aarti Gupta (Wageningen UR), Sandra (TU Delft), Debasish (Wageningen UR), and Dr. Zahid Hasan(VU

Amsterdam) for their cordial co-operation, and perceptive guidance throughout my PhD study.

I express my heartfelt gratitude to Mr. Dhiman Ranjan Mondal for his unconditional help to write the Python script for one of my chapters of the PhD thesis. I would not be able to run my model without Dhiman's enormous help in writing the Python script. I will always be grateful to Dhiman.

I am grateful to the Integrated Programme of WOTRO Science for Global Development of the Netherlands Organization for Scientific Research (NWO) for funding this research and for allowing me to pursue my PhD here in the Netherlands.

I would like to express my gratitude to all the committee members of my PhD thesis: Prof. Dr. P. J. Stuyfzand, Prof. dr. ir. T. J. Heimovaara, Prof. dr. ir.W. G. J. van derMeer, Dr. B. J. Mailloux for their valuable scientific inputs regarding my research.

I thank the Water Resources Section, Department of Water Management, Faculty of Civil Engineering and Geosciences, Delft University of Technology, the Netherlands for hosting me during my PhD research period. I would like to express my gratitude to Hanneke, Luz, Lydia, and Betty for all their help, taking care of many issues including secretarial and a load of paper work.

I thank all the teachers and staff of the Department of Geology, University of Dhaka, Bangladesh from the bottom of my heart for allowing me to conduct laboratory experiments, as well as for providing other logistic support during field sampling in Bangladesh.

I am thankful to the authority of North South University, Dhaka, Bangladesh for allowing me to pursue my dream. Special thanks go to all my colleagues at the Department of Environmental Science and Management, North South University for their good wishes and encouragements throughout my PhD endeavor. I am also thankful to all my friends here in the Netherlands for entertaining me during my stay in the Netherlands.

I would like to convey my immense love and gratitude to my beloved parents, parents-in-laws, my loving sisters, brothers, my friends and juniors for their endless love, encouragement and inspiration without which I find everything incomplete and barren.

Most importantly thanks from the inner core of my heart to my beloved wife Fatema Mostafa Rupa, who has taken all the burdens of my family whenever I was out of Bangladesh. She took care of our kids for the last six years. It would not have been possible for me to complete my PhD without her endless love, unconditional support, patience, and blessings. I feel deeply indebted to her for all the support. I am very grateful to my daughters, Marsiha and Munjerin, who missed me a lot, during my stay in The Netherlands but continued to support me.

CURRICULUM VITÆ

Mohammad Moshiur RAHMAN

31-08-1980 Born in Comilla, Bangladesh.

EDUCATION

1998–2002 Undergraduate in Geology
University of Dhaka, Bangladesh

2002–2003 Master in Geology
University of Dhaka, Bangladesh

2008–2010 Master in Applied Environmental Geosciences
Queens College,
City University of New York, USA

2011–2017 PhD. in Water Resources (Subsurface Arsenic Removal)
Delft University of Technology, the Netherlands
Thesis: Field Experiments and Reactive Transport Modeling of Subsurface Arsenic Removal in Bangladesh
Promotor: Prof. dr. Ir. Mark Bakker

EXPERIENCES

2005–2007 Research Associate in the Environmental Research Project
Health Hazard and Arsenic Mobilization
in Bangladesh Groundwater
Activities: Hydrogeological Investigation
Geophysical Investigation

2007–2008 Assistant Director
Geological Survey of Bangladesh
Activities: Geotechnical Investigation
Subsurface Modeling

2008–2010 Adjunct Lecturer
School of earth and Environmental Sciences,
Queens College, New York, USA
Activities: Teaching Environmental Science 111 Lab

2011–Present Lecturer
Department of Environmental Science and Management,
NSU, Bangladesh
Activities: Teaching Environmental Science ENV 107,
Geographical Information System (GIS) ENV 316,
Geology & Geomorphology ENV 311

2011–2017 PhD researcher
Delft University of Technology, the Netherlands
Activities: Development of a reactive transport model of the fate and transport of arsenic during subsurface arsenic removal.

LIST OF PUBLICATIONS

1. **M.M. Rahman**, M. Bakker, C.H.L. Patty, Z. Hassan, W.F.M. Röling, K.M. Ahmed, B.M. van Breukelen (2015), *Reactive transport modeling of subsurface arsenic removal systems in rural Bangladesh.*, Science of the Total Environment (537 (2015) 277–293).

2. **M.M. Rahman**, M. Bakker, S.C.B. Freitas, D. van Halem, B.M. van Breukelen, K.M. Ahmed, A.B.M. Badruzzaman (2014), *Exploratory experiments to determine the effect of alternative operations on the efficiency of subsurface arsenic removal in rural Bangladesh.*, Hydrogeolgy. Journal. (23, 19–34. doi:10.1007/s10040-014-1179-0).

3. **Freitas, S.C.B.**, Van Halem, D., **Rahman, M.M.**, Verberk, J.Q.J.C., Badruzzaman, A.B.M., Van Der Meer, W.G.J. (2014), *Hand-pump subsurface arsenic removal: The effect of groundwater conditions and intermittent operation.*, Water Science and Technology: Water Supply.

4. **Aziz, Z.**, Bostick, B.C., Zheng, Y., Huq, M.R., **Rahman, M.M.**, Ahmed, K.M., van Geen, A. (2017), *Evidence of decoupling between arsenic and phosphate in shallow groundwater of Bangladesh and potential implications.*, Applied Geochemistry (77, pp. 167-177).

5. **Radloff, K.A.**, Zheng, Y., Stute, M., Weinman, B., Bostick, B., Mihajlov, I., Bounds, M., **Rahman, M.M.**, Huq, M.R., Ahmed, K.M., Schlosser, P., van Geen, A. (2017), *Reversible adsorption and flushing of arsenic in a shallow, Holocene aquifer of Bangladesh.*, Applied Geochemistry (77, pp. 142-157).

6. **Jung, H.B**, Zheng, Y., Rahman, M.W.,**Rahman, M.M.**, Ahmed, K.M., (2015), *Redox zonation and oscillation in the hyporheic zone of the Ganges-Brahmaputra-Meghna Delta: Implications for the fate of groundwater arsenic during discharge.*, Appl. Geochem. (63, 647–660. doi:10.1016/j.apgeochem.2015.09.001.

7. **N. Mladenov**, Y. Zheng, B. Simone, T.M. Bilinski, D.M. McKnight, D.R. Nemergut, K.A. Radloff,**M. M. Rahman**, K.M.U. Ahmed, (2015), *Dissolved Organic Matter Quality in a Shallow Aquifer of Bangladesh: Implications for Arsenic Mobility.*, Environmental Science & Technology. (DOI: 10.1021/acs.est.5b01962.

8. **Legg, T.M.**, Zheng, V., Simone, B., Radloff, K.A., Mladenov, N., Gonzalez, A., Knights, D., Siu, H.C., **Rahman, M.M.**, Ahmed, K.M., McKnight, D.M., Nemergut, D.R. (2012), *Carbon, metals, and grain size correlate with bacterial community structure in sediments of a high arsenic aquifer.*, Frontiers in Microbiology. DOI: 10.3389/fmicb.2012.00082.

9. **Leber, J.**, **Rahman, M. M.**, Ahmed, K.M., Mailloux, B., Van Geen, A., (2011), *Contrasting Influence of Geology on E. coli and Arsenic in Aquifers of Bangladesh.*, Ground Water, 49 (1), pp. 111-123.

10. **Natalie mladenov**, Yan zheng, Matthew p. Miller, Diana R. Nemergut, Teresa legg, Bailey Simone,Clarrisa Hageman, **M. Mosiur Rahman**,K. Matin Ahmed, Diane M. Macknight, (2009), *Dissolved Organic Matter Sources and Consequences for Iron and Arsenic Mobilization in Bangladesh Aquifers.*, Environmental Science & Technology.

11. **Radloff, K.A.**,Manning, A.R., Mailloux, B., Zheng, Y.,**Moshiur Rahman, M.**,M., Rezaul Huq, M., Ahmed, K.M., Geen, A.V., (2008), *Considerations for conducting incubations to study the mechanisms of As release in reducing groundwater aquifers.*, Appl. Geochem **23 (11), pp. 3224-3235**.

12. **van Geen, A.**, Z. Cheng, Q. Jia, A. A. Seddique, M. W. Rahman,**M. M. Rahman**, K. M. Ahmed, (2007), *Monitoring 51 deep community wells in Araihazar , Bangladesh , for up to 5 years: Implications for arsenic mitigation.*, Journal of Environmental Science and Health **42, 1729-1740**.

The principle of Subsurface Arsenic (As) Removal (SAR) is to extract anoxic groundwater, aerate it and reinject it. Oxygen in the injected water reacts with iron in the resident groundwater to form hydrous ferric oxide (HFO). Dissolved As sorbs onto the HFO, which allows for the extraction of groundwater with lower As concentrations.